State of the Art- New achievements in Fetal MRI

Daniela Prayer
Division of Neuroradiology
And Musculoskeletal
Radiology

Medical University Vienna/ Austria

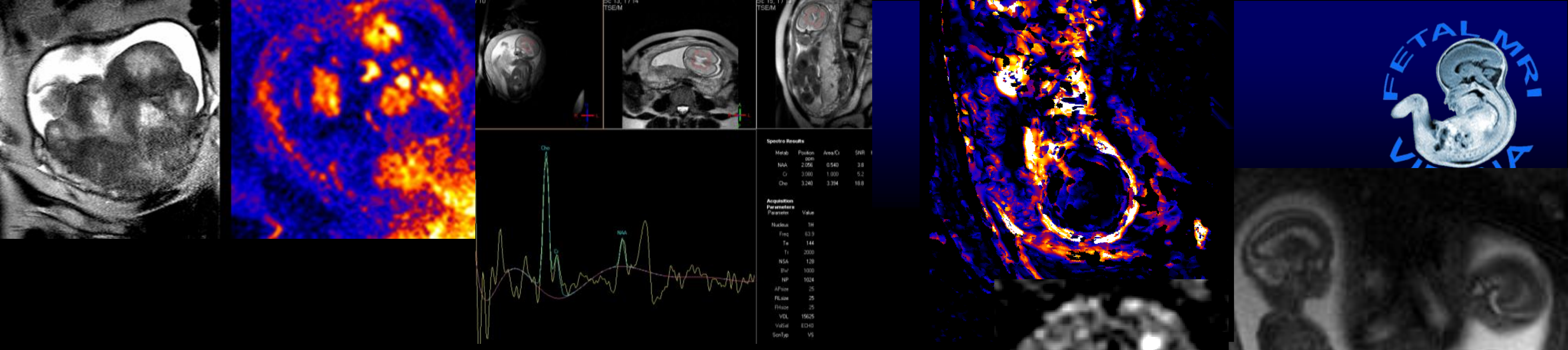

T2

T1
EPI
Angiography
FLAIR
Diffusion-
Thick slab
Dynamic
Metabolic
Perfusion-

f-MRI, 3D

information

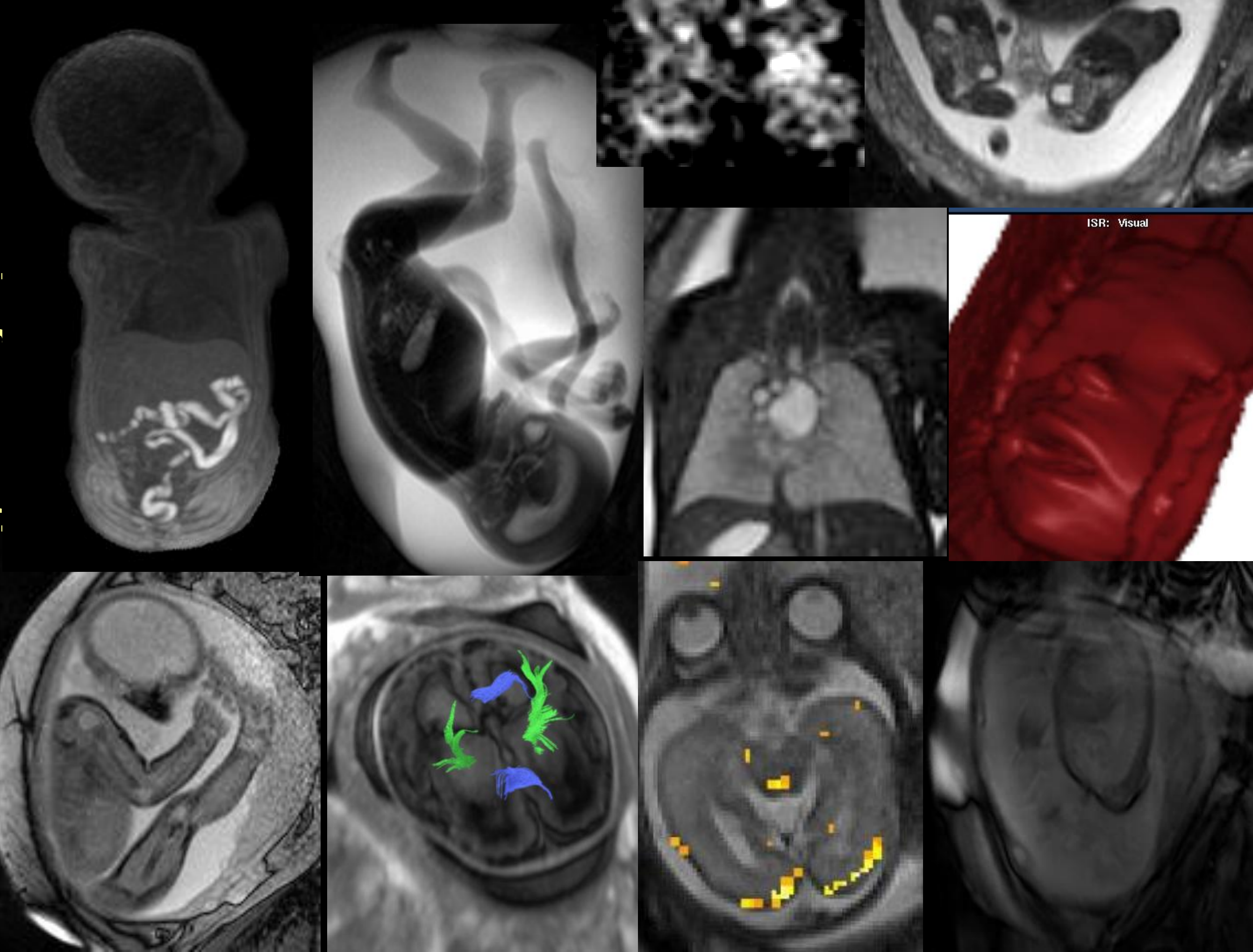

Advances in morphology

Higher resolution

3D techniques

2D and 3D developmental models

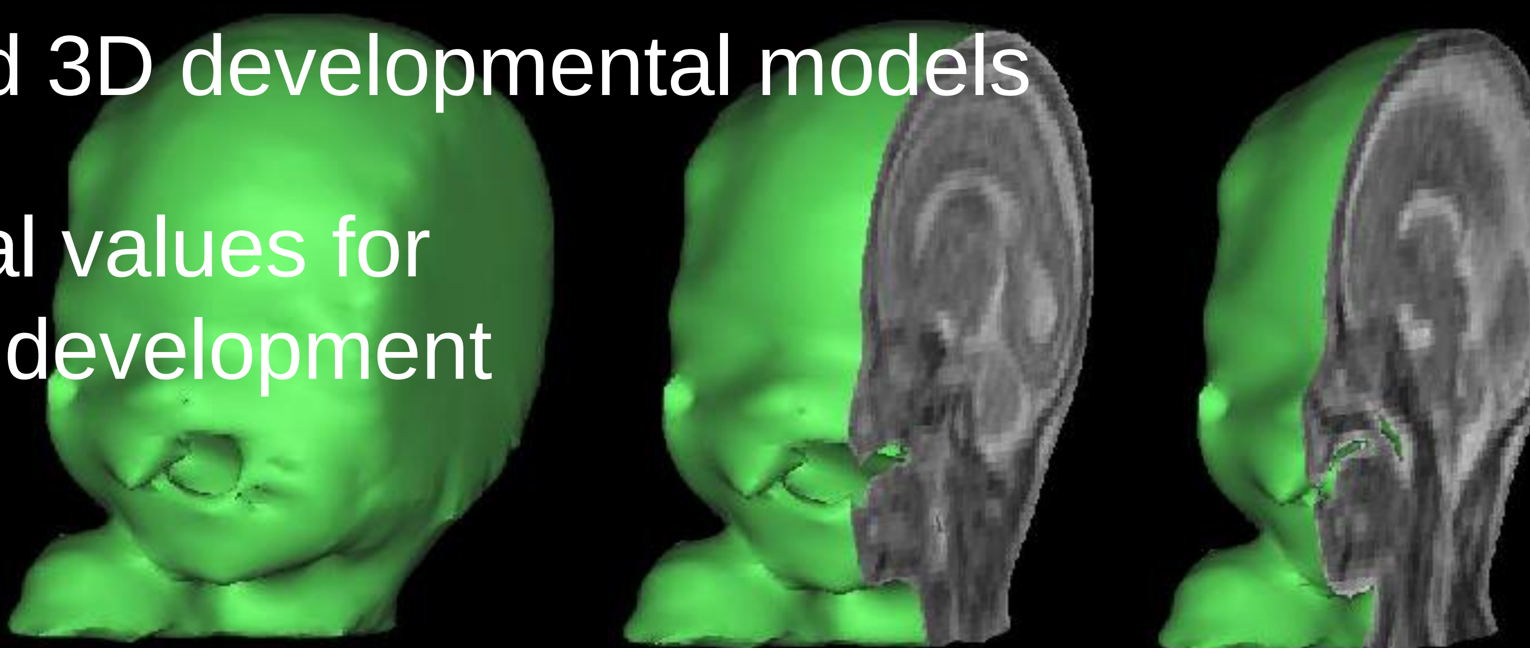

Normal values for
organ development

Advances beyond morphology ?

Tractography

Signal measurements

Spectroscopy

(intrinsic) movement patterns

fMRI

Perfusion

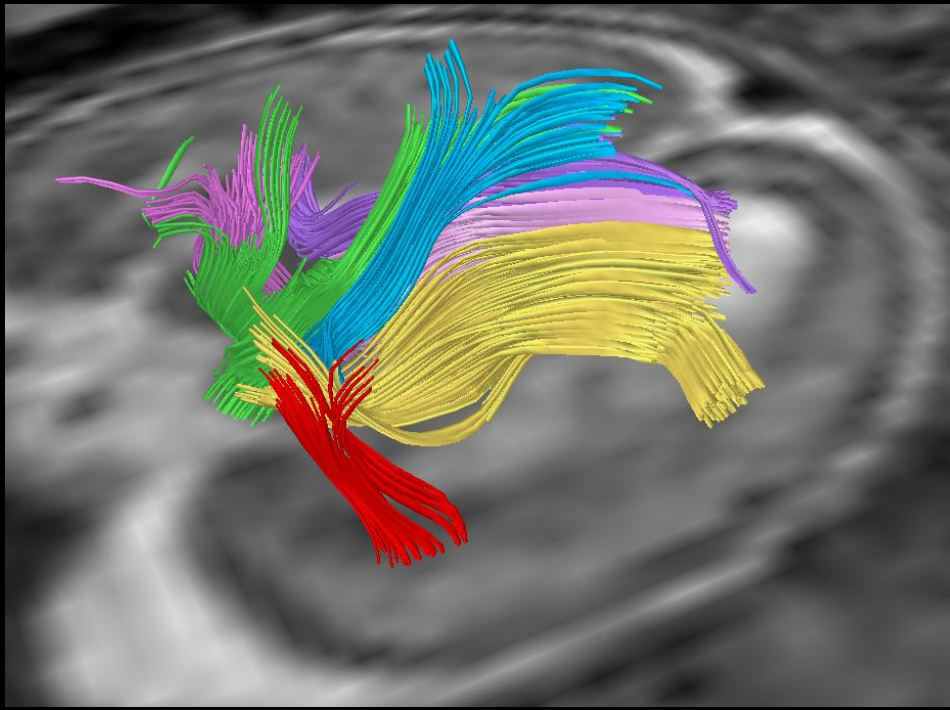

Learning

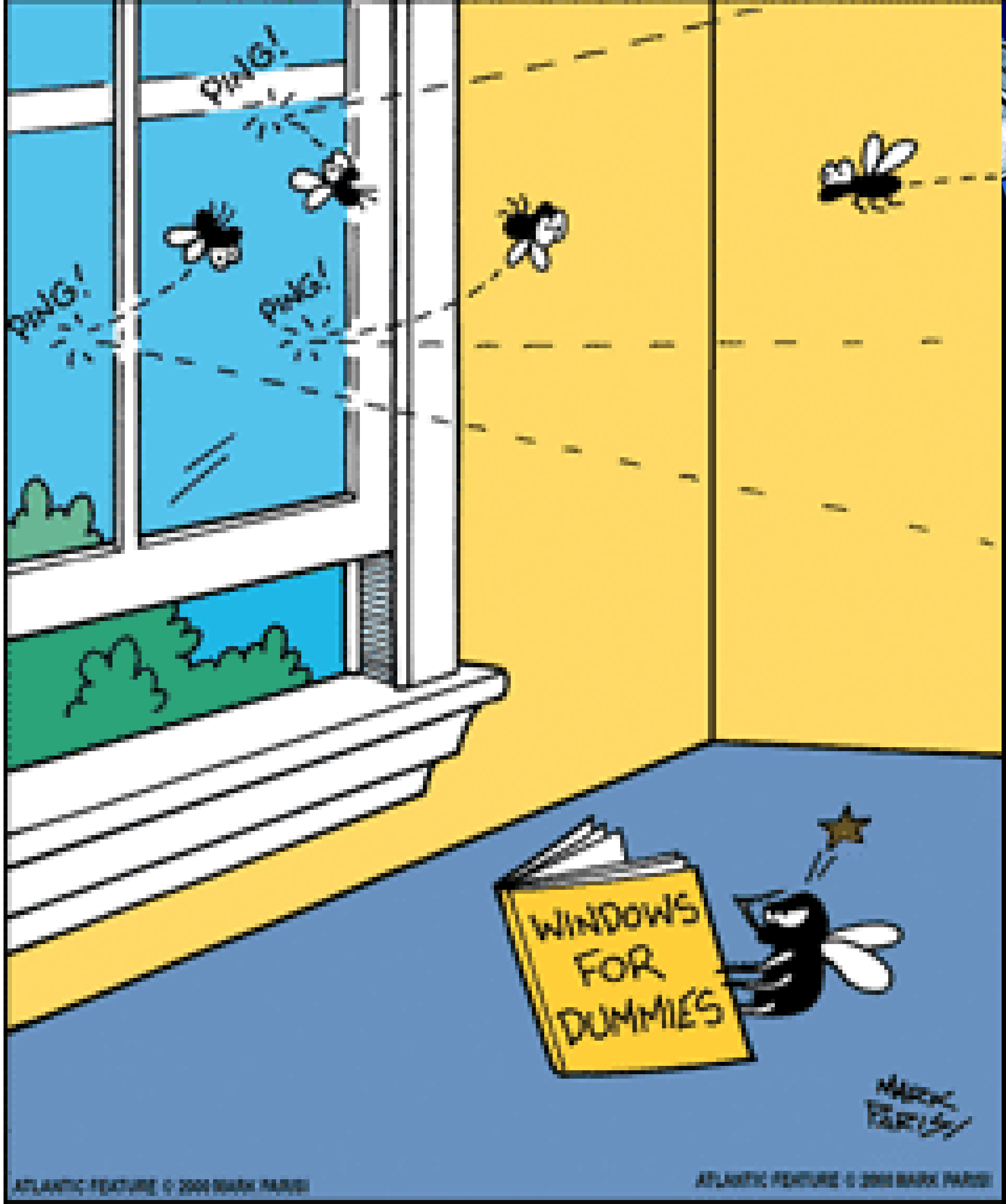

Indications

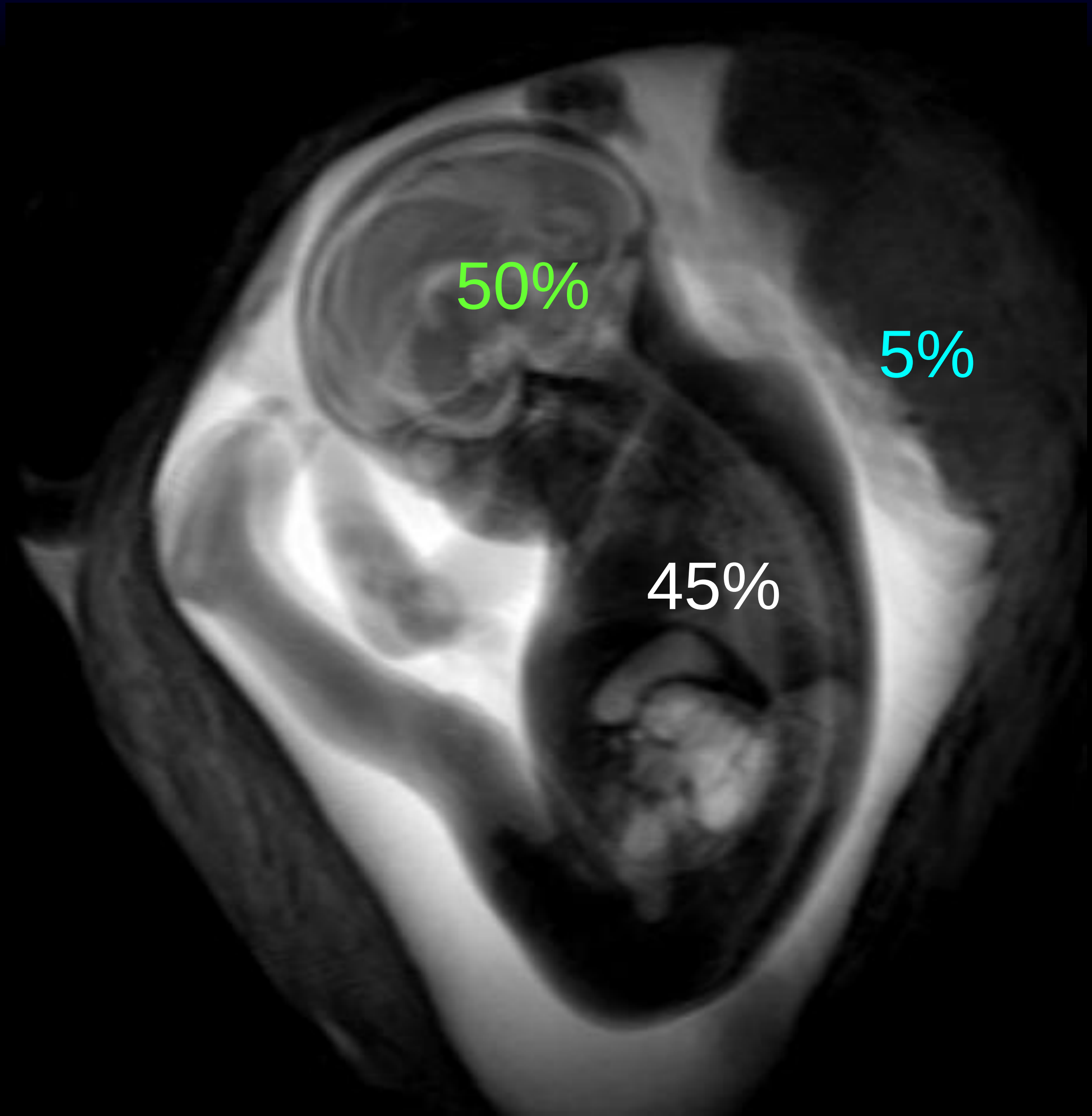

- Brain
- Face
- Skin
- Neck
- Thorax
- Gastrointestinal-system
- Urogenital-system
- Skeleton
- Placenta

Thorax: Lungs

Lung growth

⬇

Volumetry

MRI

Lung maturation

⬇

Signal intensities

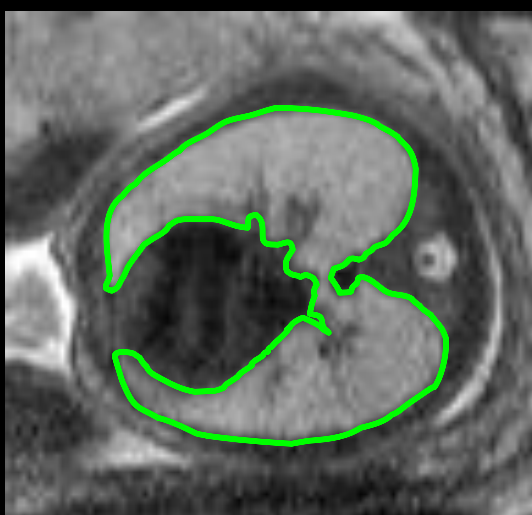

Normal fetal lung development

Thorax: Lungs

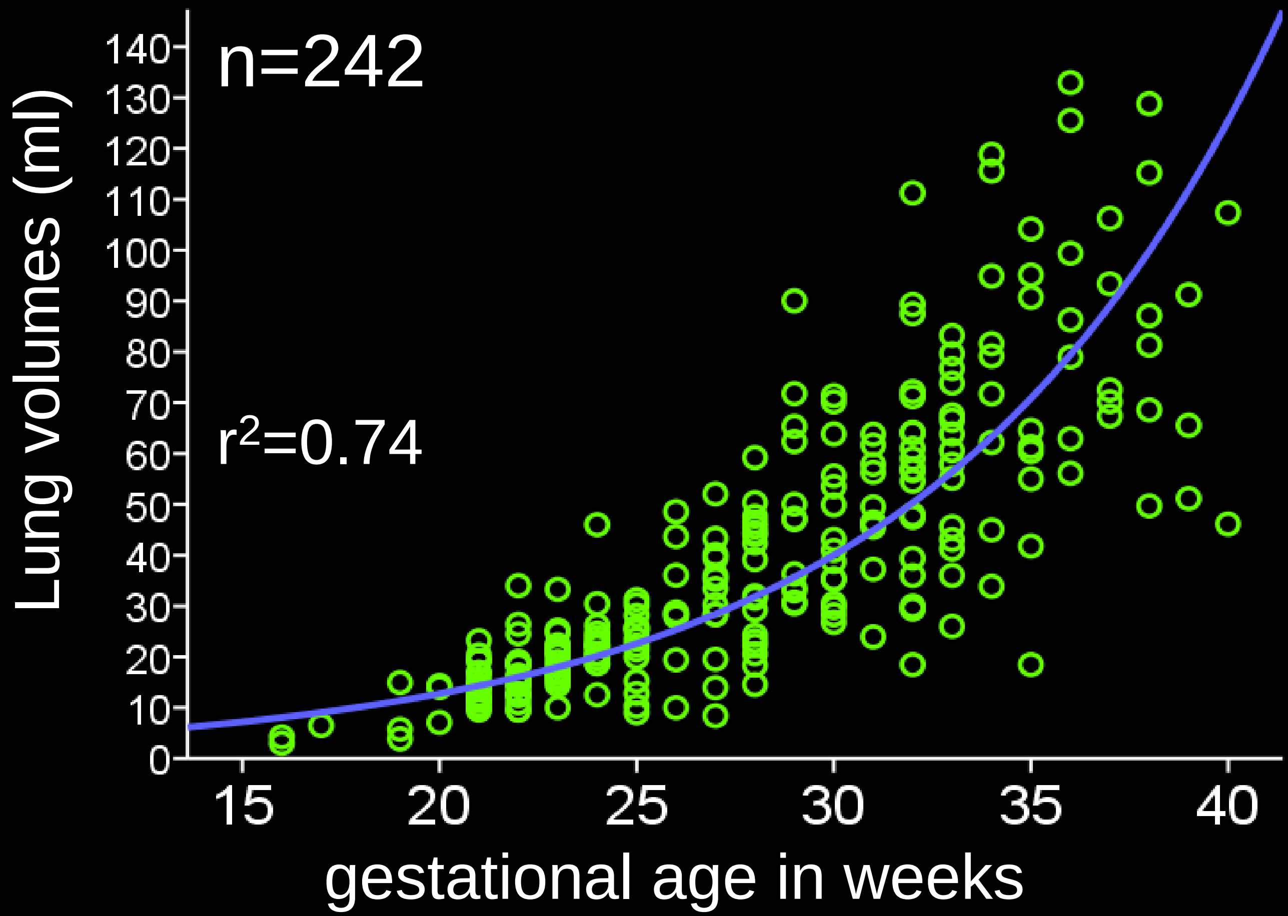

Gregor Kasprian EJR 2006.

Thorax: Lungs
Signal intensity-Physiology

Sequences (= choice of MR parameters that give different contrasts)

age

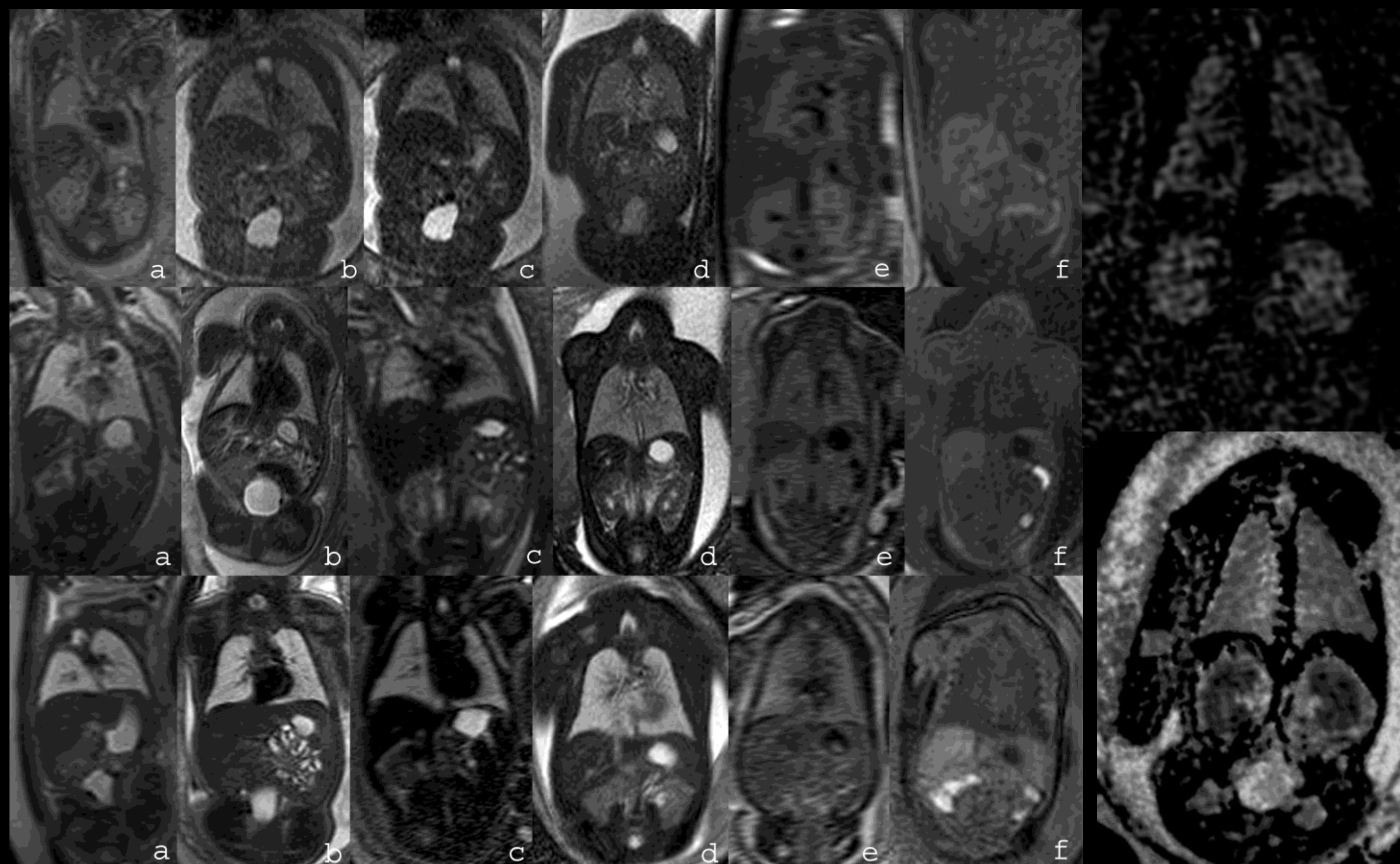

Balassy C. European Radiology 2007

SI before/ after lung maturation

GW 25+3

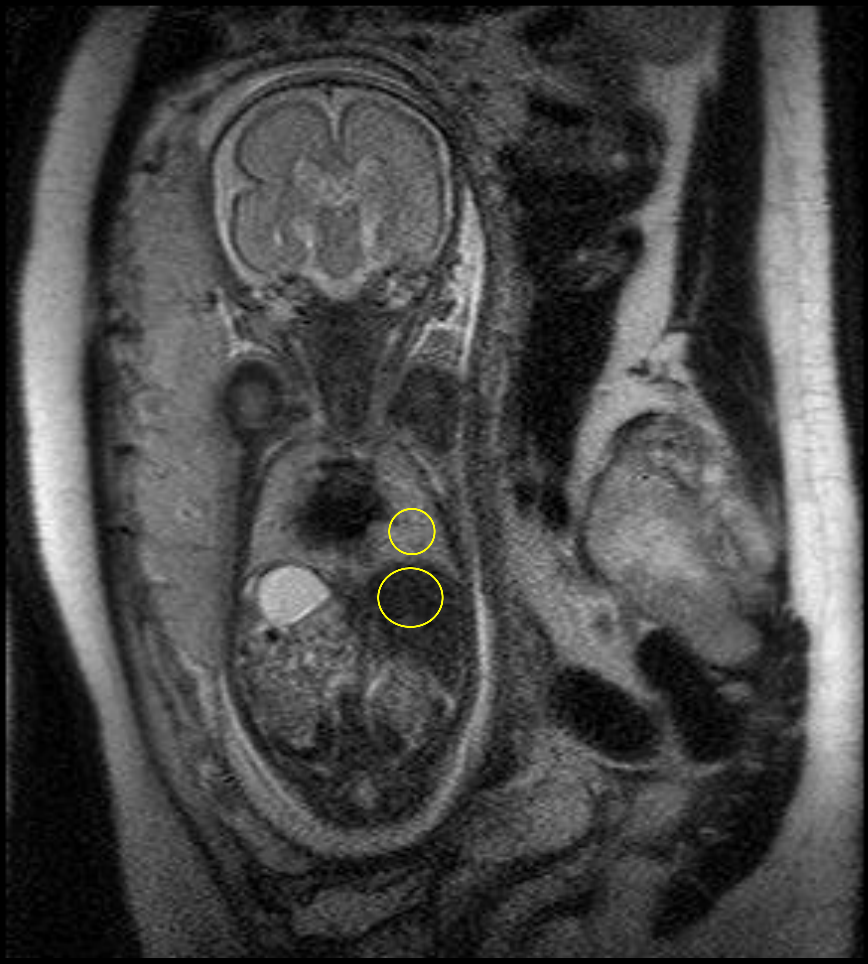

< 24 h

UOG 2011

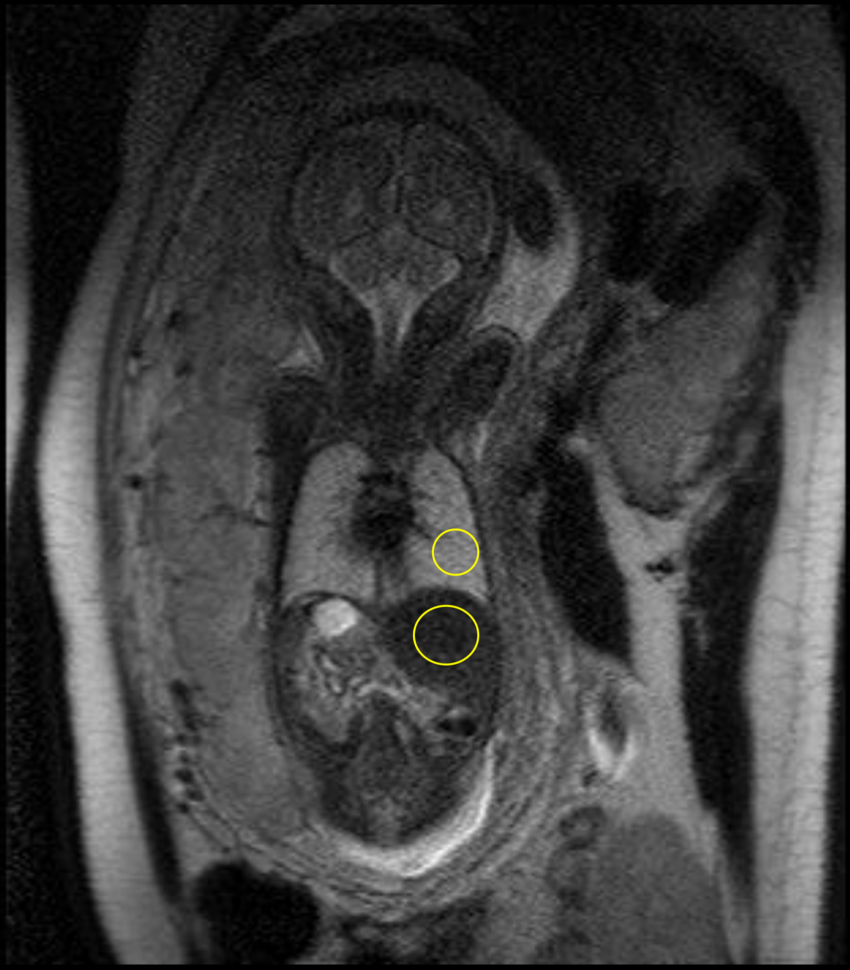

>72 h

Thorax: Lungs

Sequences

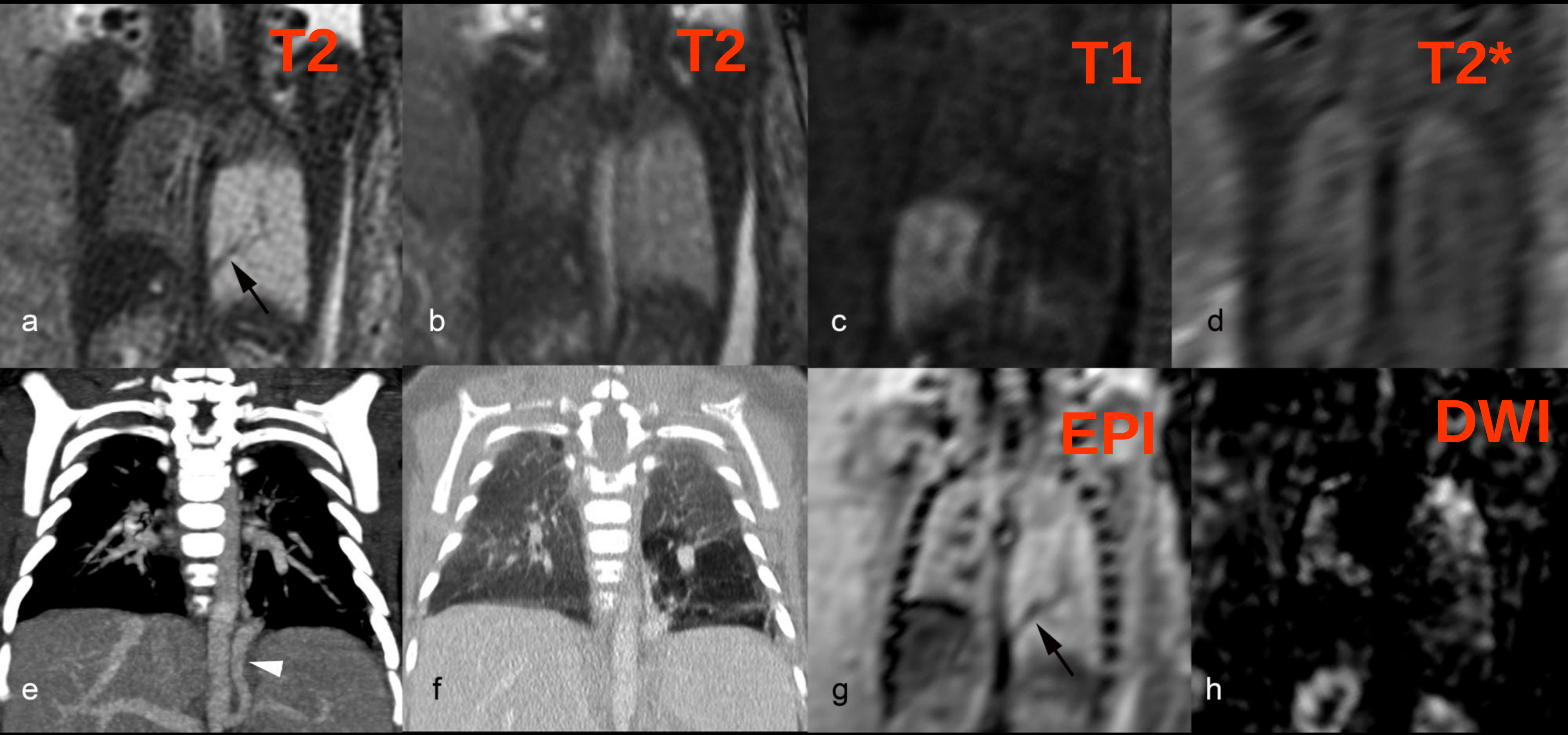

Lung sequestration GW 28

Brain

Ultrasound

Sulcation/ gyration

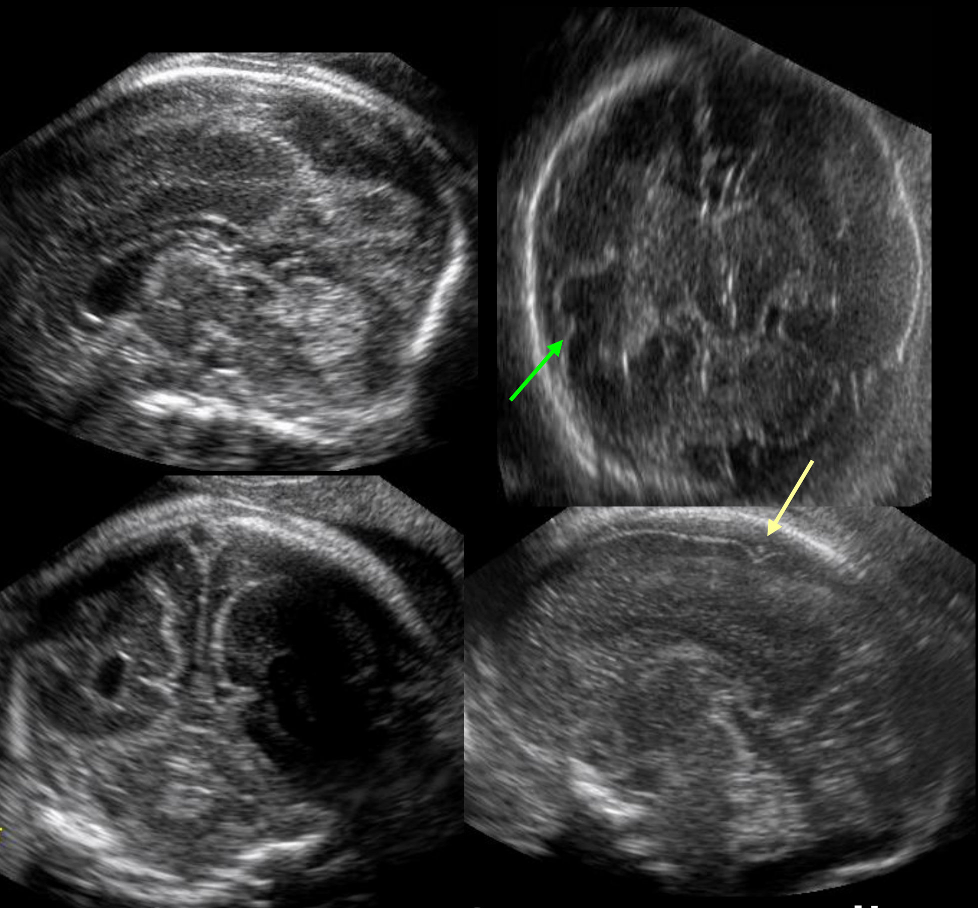

MRI

GW 26

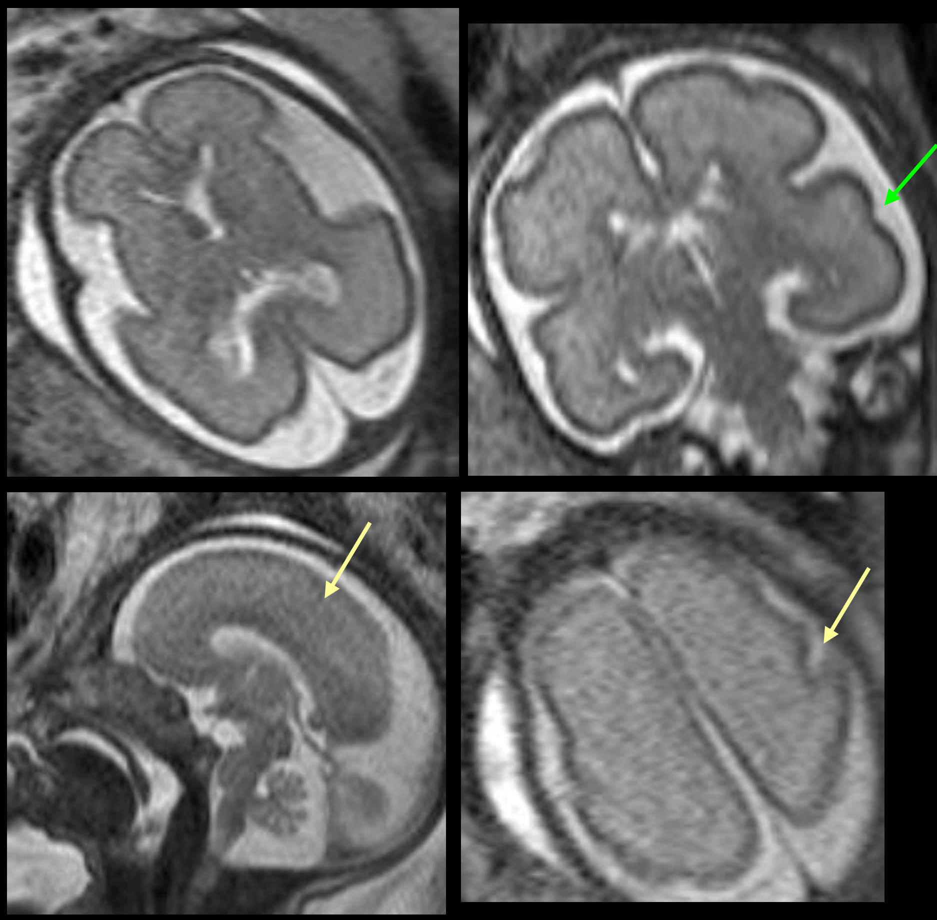

Courtesy Gustavo Malinger

18

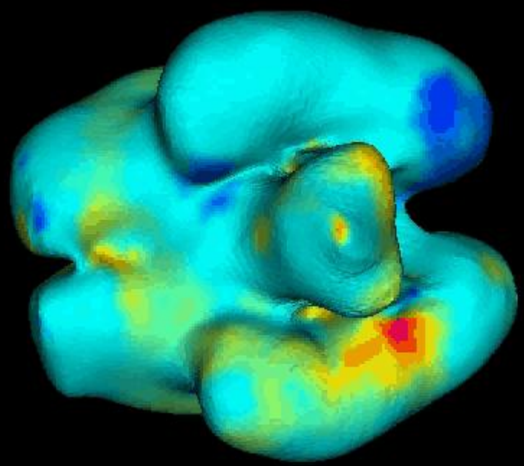

18

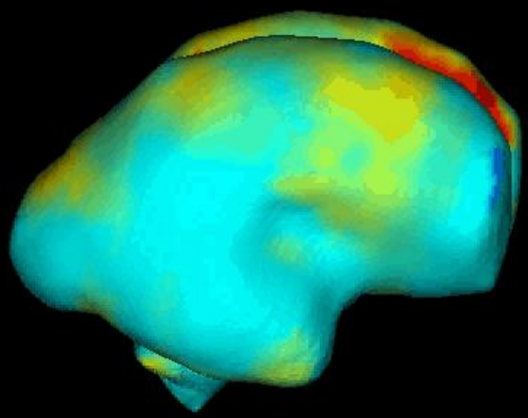

Spatiotemporal atlas of human brain maturation

(Draft)

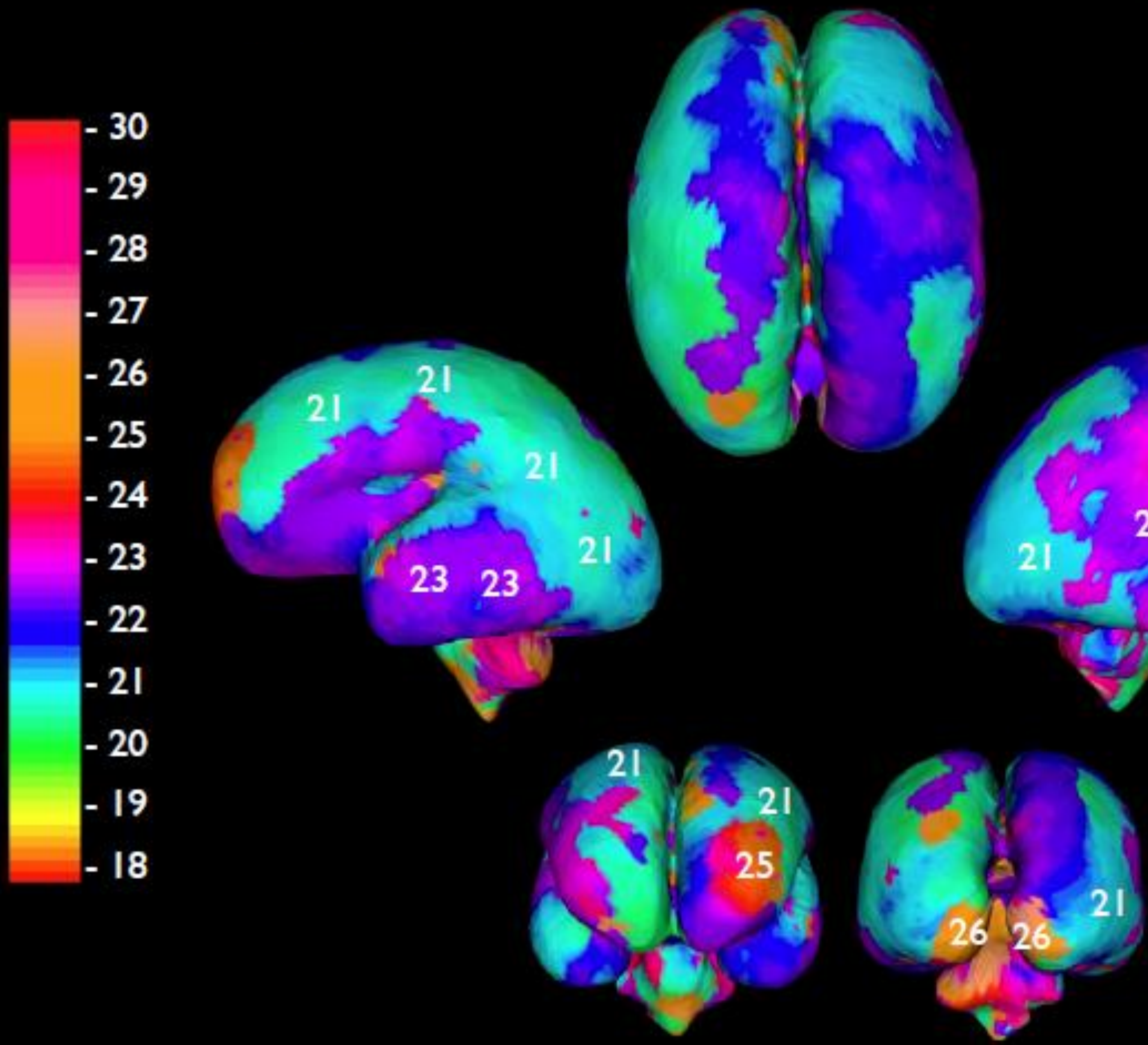

G Langs
G Kasprian
et al MIT/
Vienna

Surface of the fetal brain landmarks – superior temporal sulcus

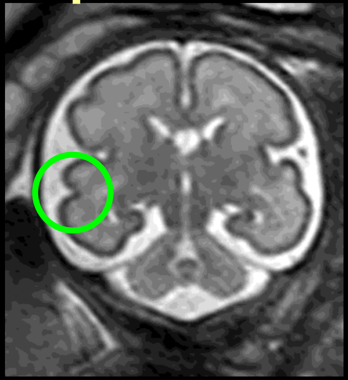

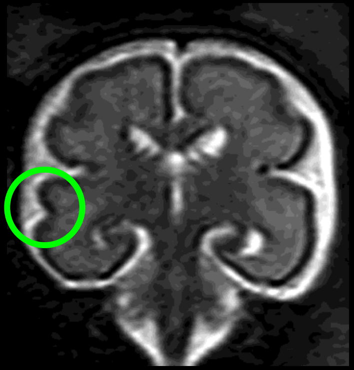

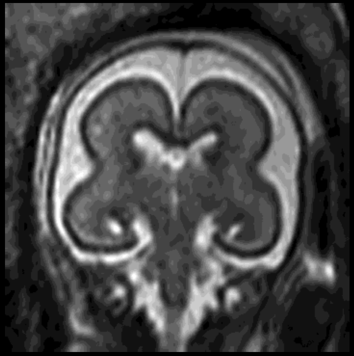

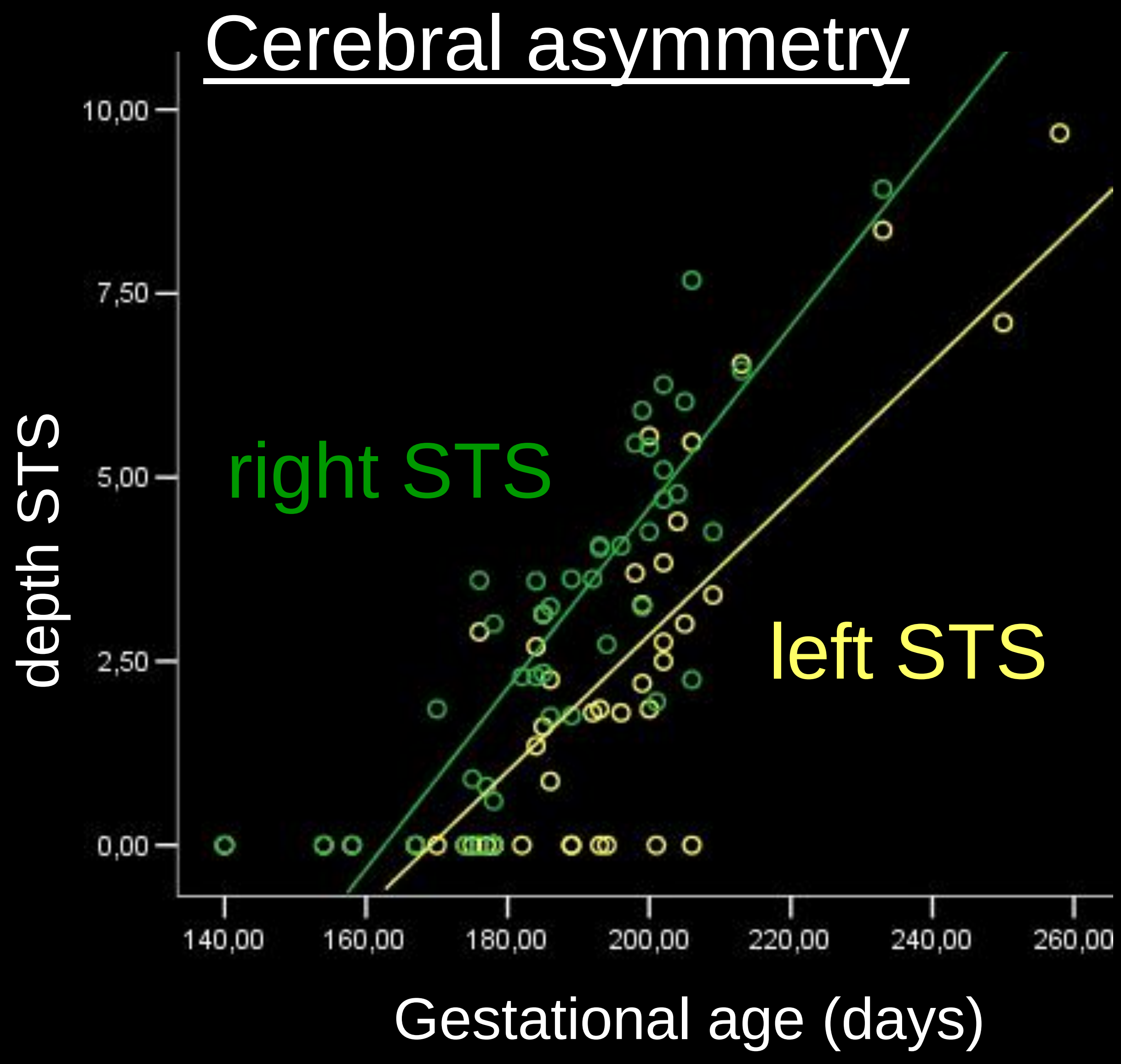

Methods – Morphometry

n=22, 23-30GW

- Cortical contour delineation[1]
- Corresponding positions defined by minimized description length[2]
- Modeling of shape[3] (multivariate Gaussian model)

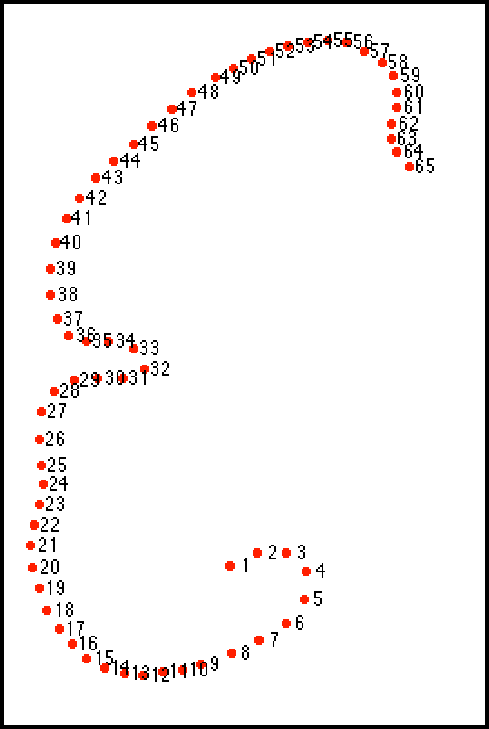

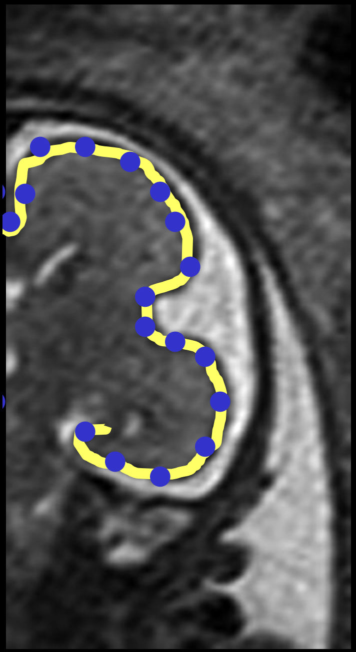

separated

[1]M. Kass, et al. *International Journal on Computer Vision, 1:321–331, 1988*

[2]H. H. Thodberg In *Proceedings of IPMI, 2003.*

[3]G. Langs, et al. In *Proceedings of MICCAI'07, 2007*

Results - Morphometry

n=16, 23-32 GW

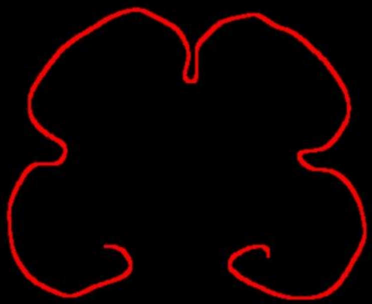

23 GW

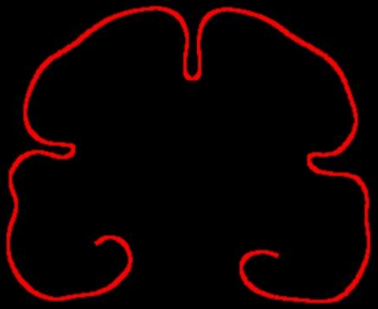

25 GW

29 GW

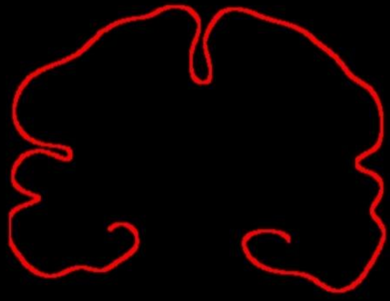

32 GW

G Kaprian, GLangs, PC Brugger, M Arantes, M Weber, D Prayer, Cereb Cortex, October 2010

Results - Morphometry

n=16, 22-32 GW

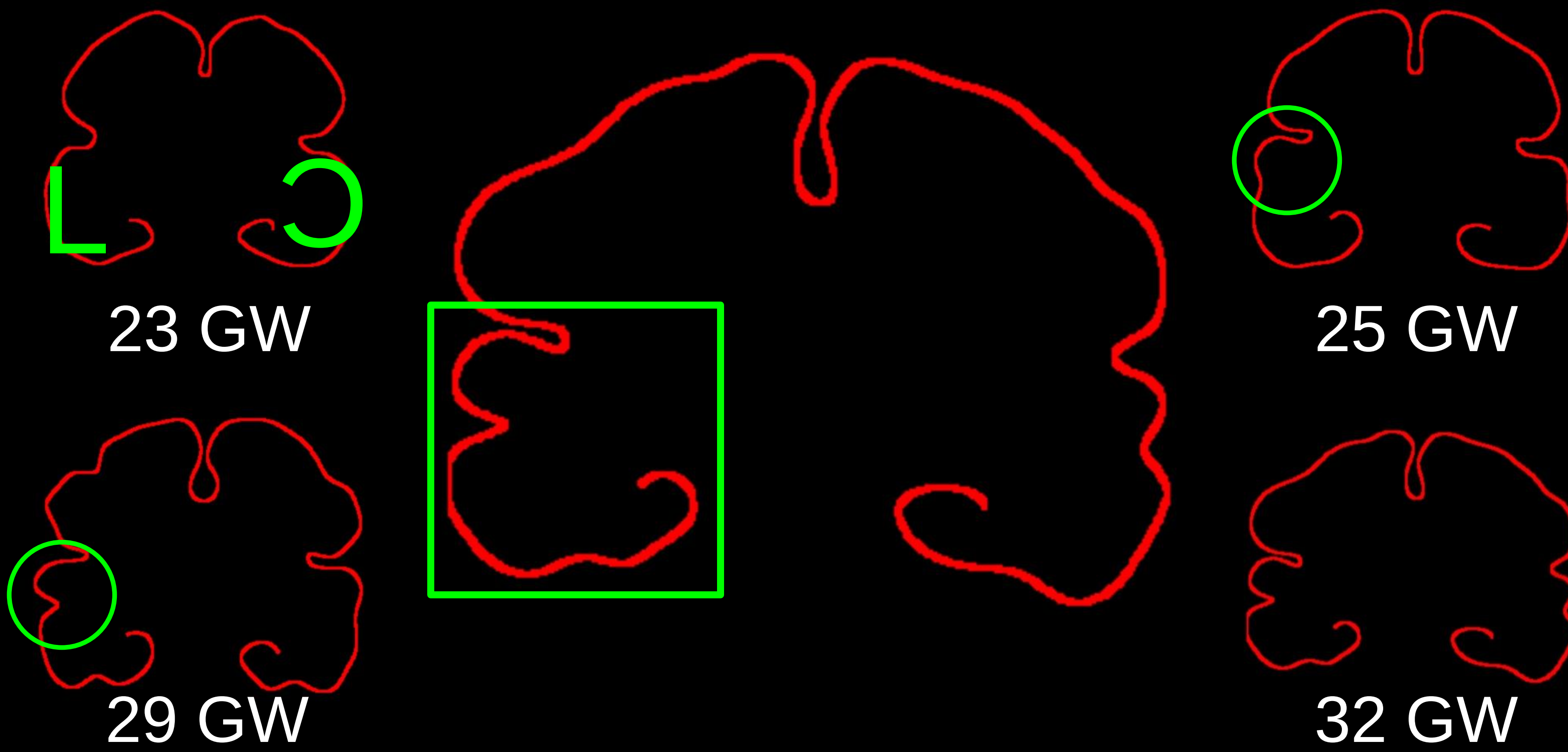

Lamination T2

Histology

Ventricular Zone
+ Ganglionic Eminences
Periventricular Zone
Subventricular Zone
Intermediate Zone
Subplate
Cortical Plate
Marginal Zone

GW 20+4 T2

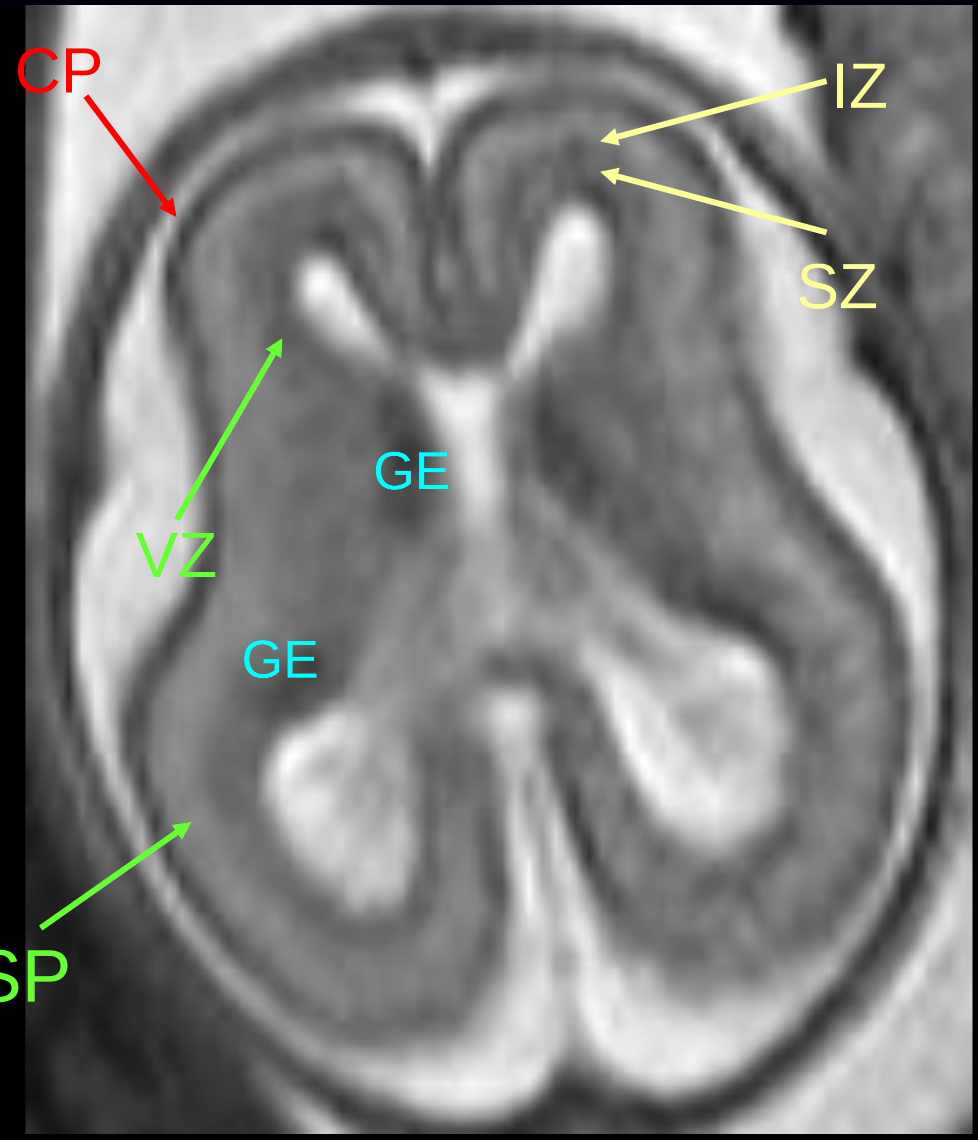

Asymmetry prior to 24GW

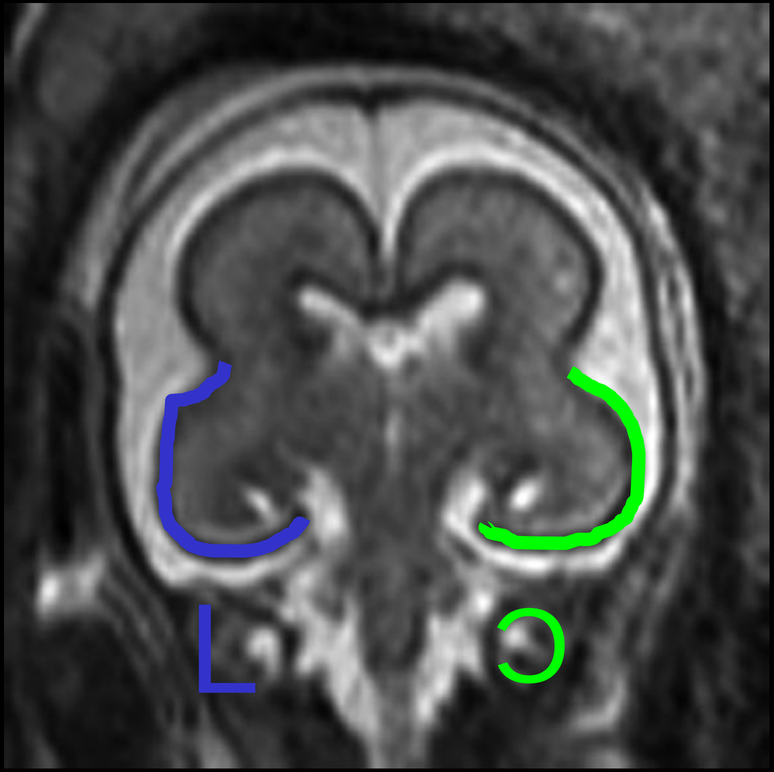

right left

20 GW

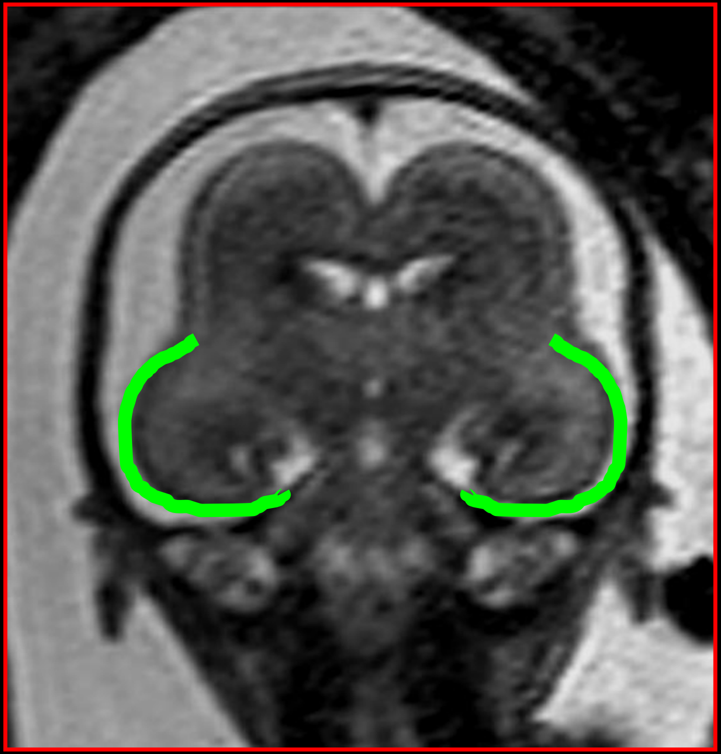

22 GW

Lissencephaly I

Fetal Inflammatory Response Syndrome

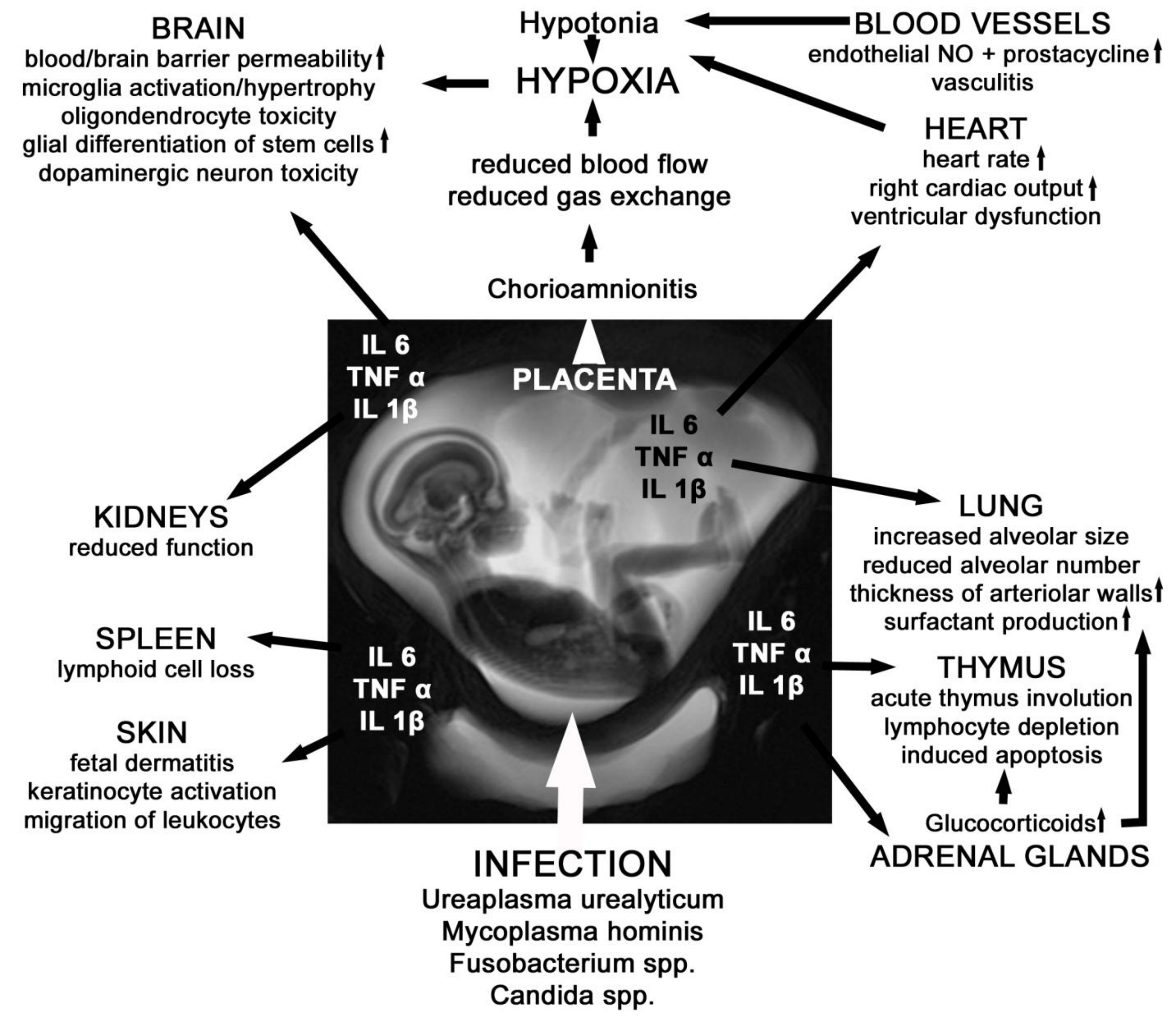

Valentina Ribeiro

Raybaud Castillo Pediatric Neuro radiology

Chapter 91

Fetal Inflammatory Response Syndrome

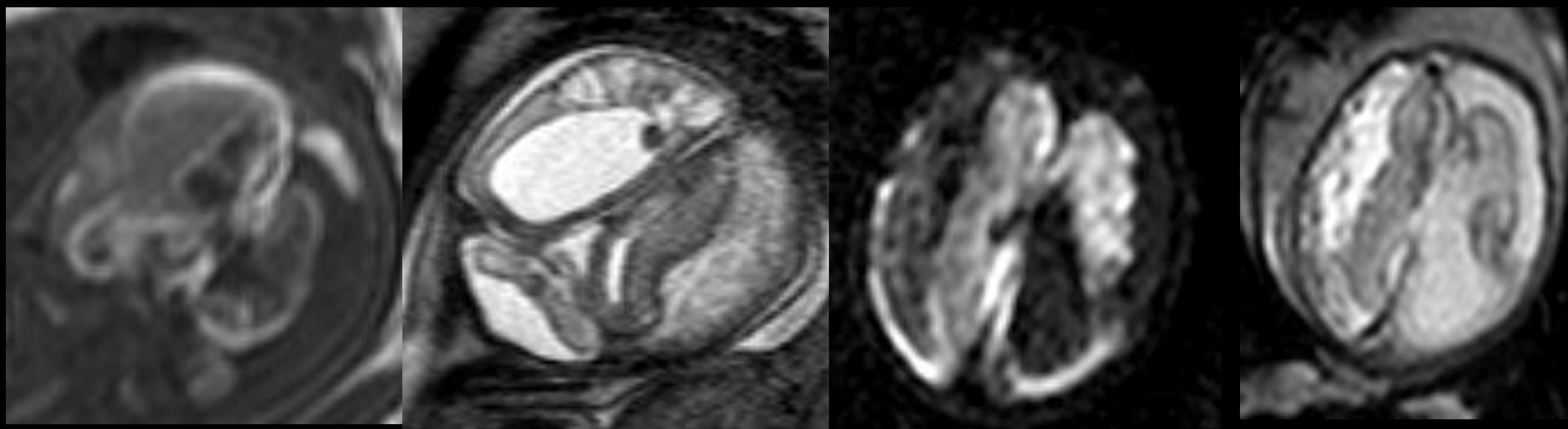

28+2

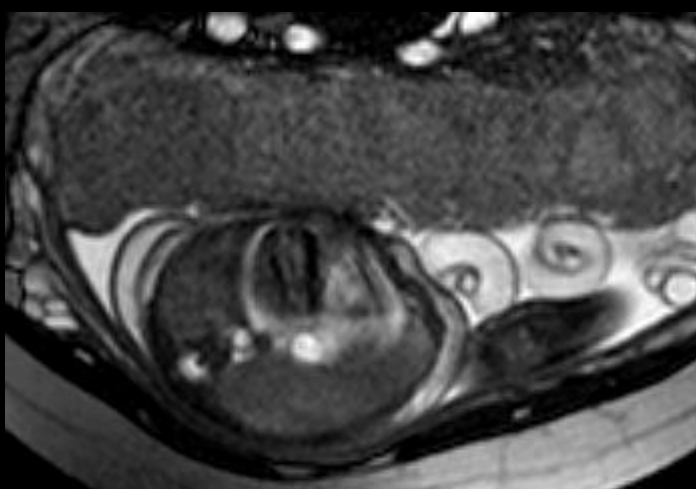

Subcutaneous edema
Cardiac effusion
Placental edema

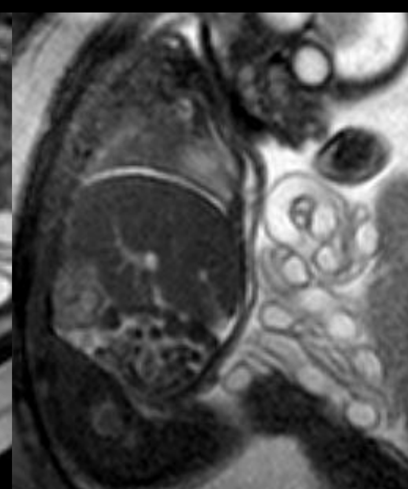

Pleural
effusion

Normal placenta

Linduska N et al, Placenta. 2009 Jun;30(6):555-9

“temporopolar hyperintensities“

„The presence of abnormalities in the anterior part of the temporal lobe increases the likelihood that CMV infection is present.”

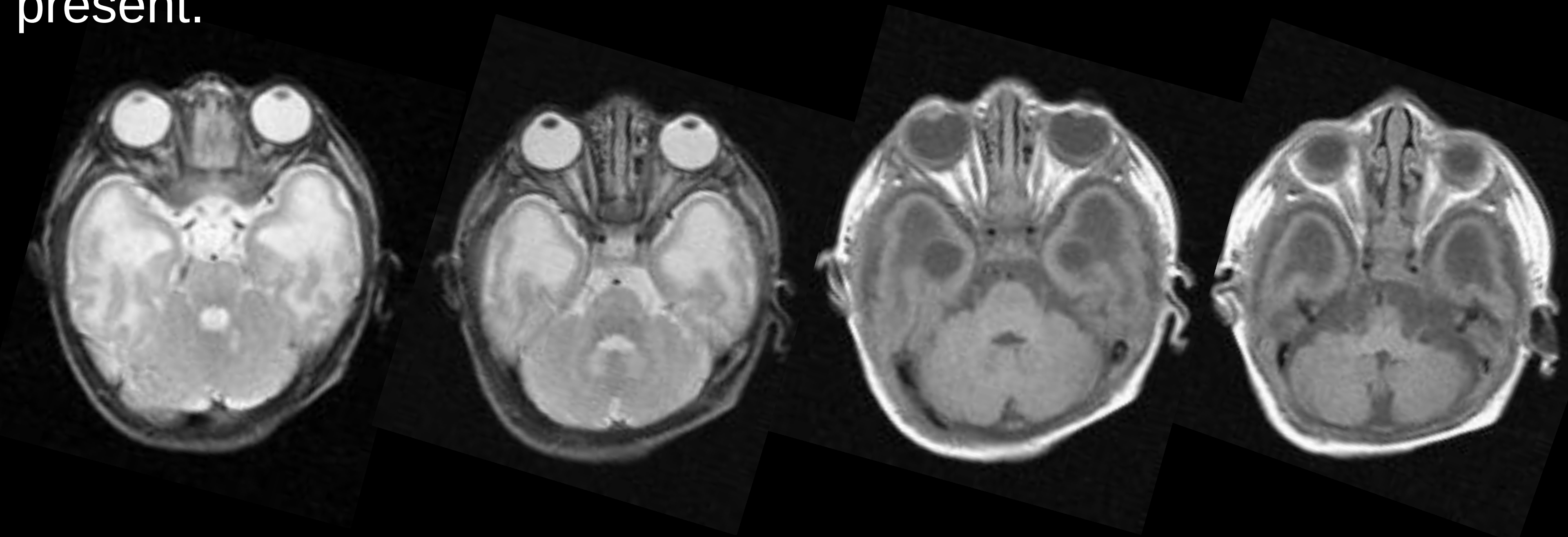

Van der Knaap et al. : Pattern of White Matter Abnormalities at MR Imaging: Use of Polymerase Chain Reaction Testing of Guthrie Cards to Link Pattern with Congenital Cytomegalovirus Infection. Radiology 2004; 230; 529-36

CMV

GW 28

GW 32

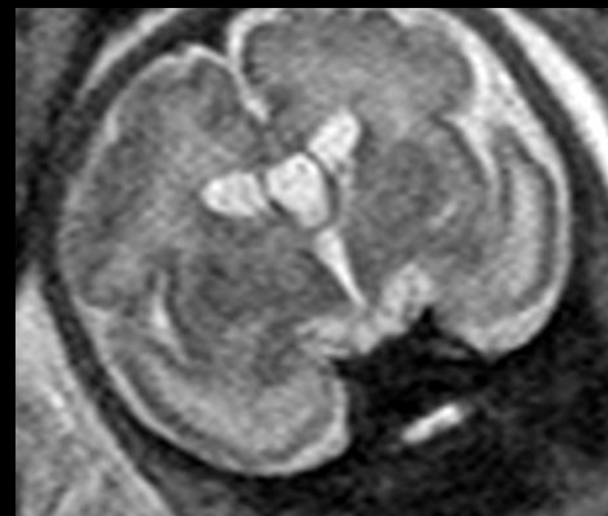

Arthritis

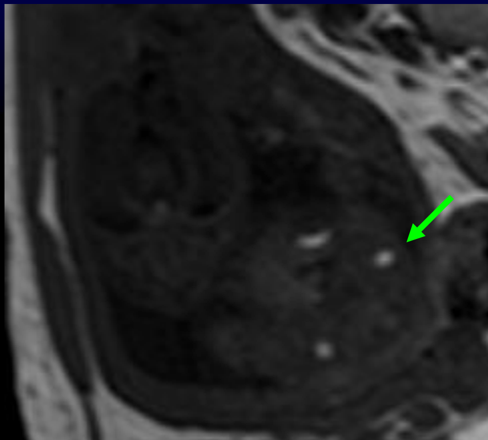
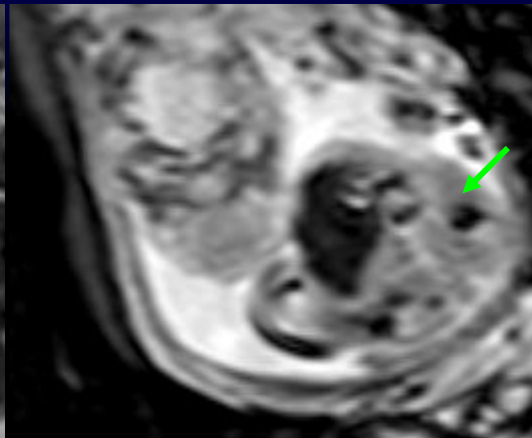

GW 21+5

Hemorrhage in hip joints

“Unlike the adult tissue, prenatal cartilage may be well vascularized“

Reidenbach MM, Schmidt HM. Ann Anat. 1994 176(4):303-10.

“Painful restricted movements of the extremities, Hyperpigmentation over swollen joints….in a 5month old baby with CMV infection“

Kini PG, Baliga M, Ann Trop Paediatr 1993; 13(4):395-7

Arthritis

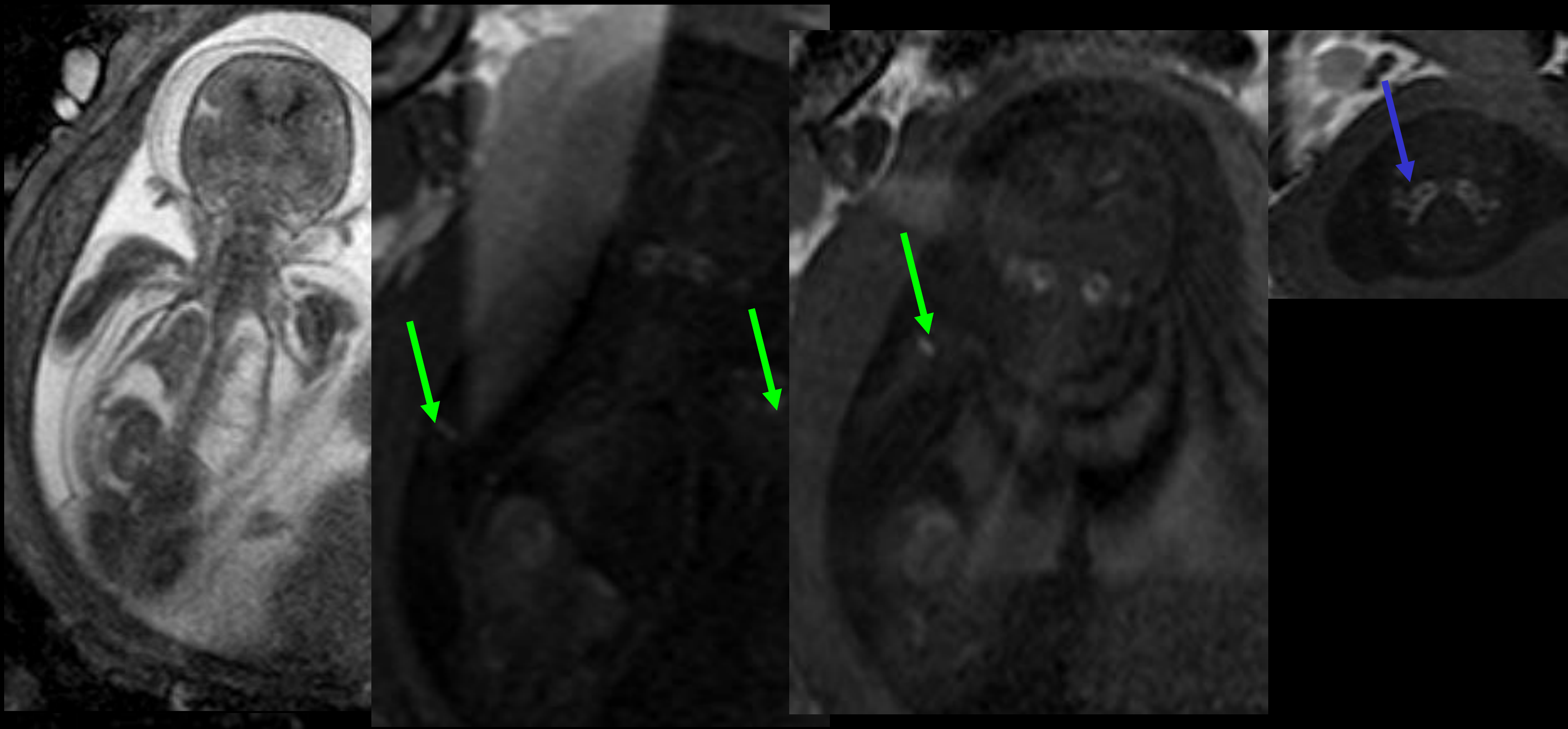

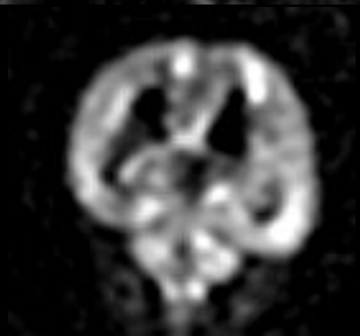

GW 20

Labyrinthitis

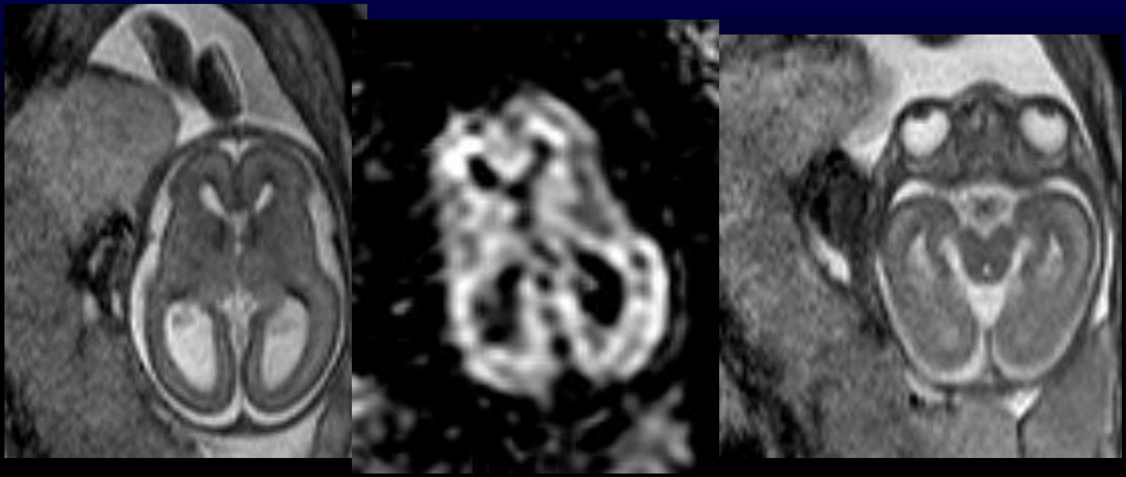

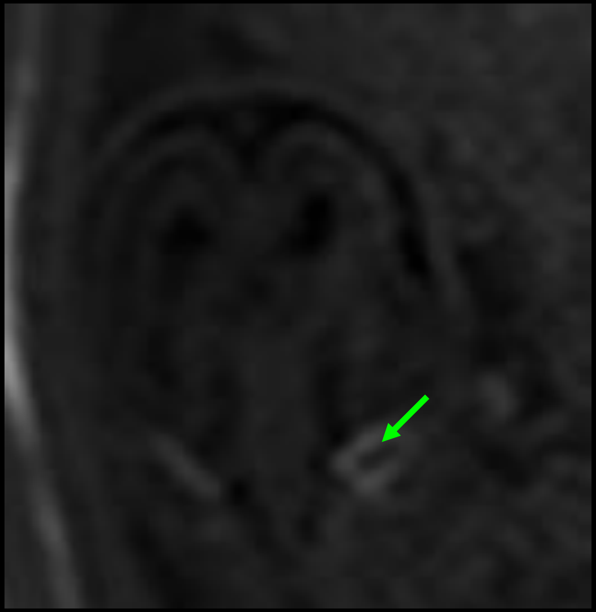

GW 21+5

Woolf et al 1988 antimicrobial agents and chemotherapy

Morphology Image quality

FOV 200 mm, slice thickness 4.0 mm, gap 0.4mm

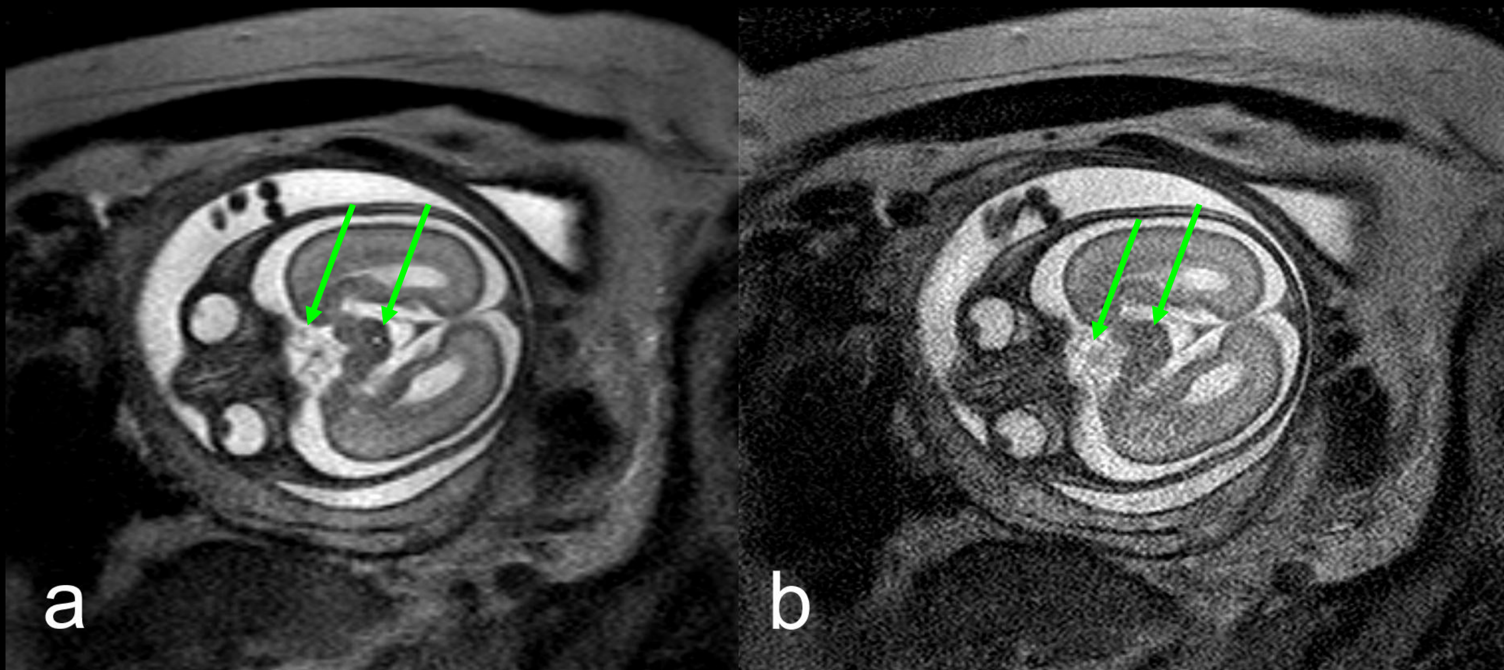

GW
25+0

acquired voxel size
0.78 x 1.18 mm
reconstructed voxel size
0.78 mm
acquis. time/ 18 images:
16 sec

acquired voxel size
0.6 x 0.7 mm
reconstructed voxel size
0.48 mm
acquis. time/ 18 images:
22.4 sec

PC Brugger
In: Fetal MRI
2011, Springer
Ed. D Prayer

Small structures

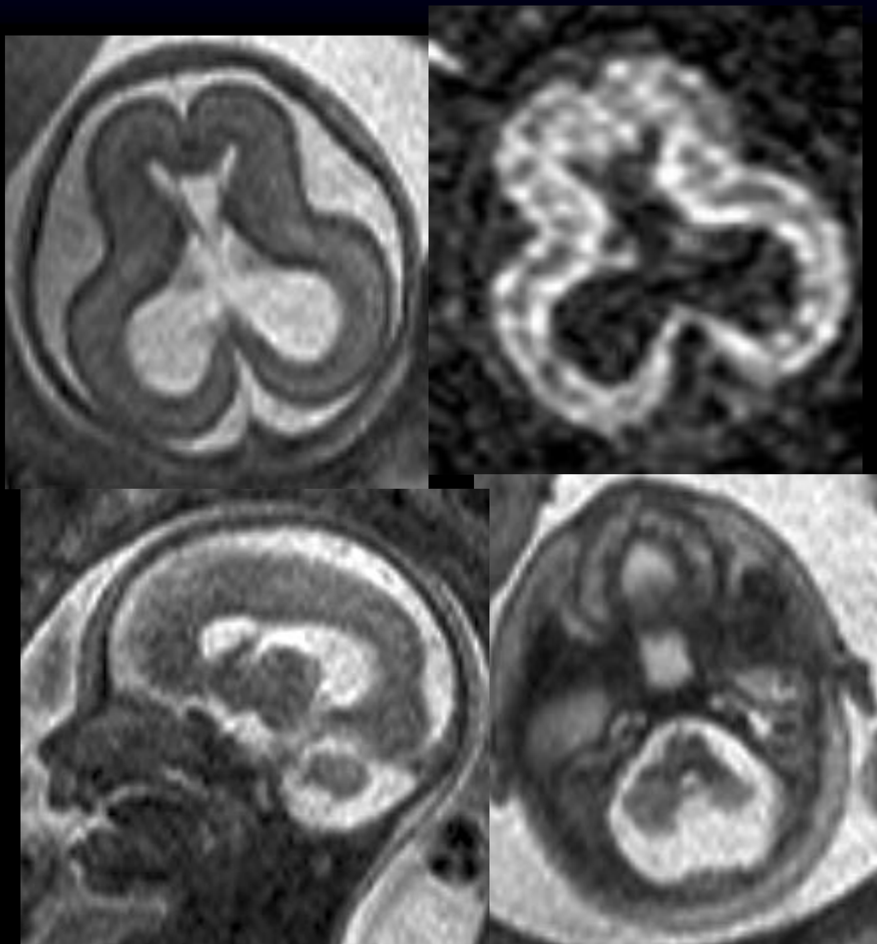

GW 20+6

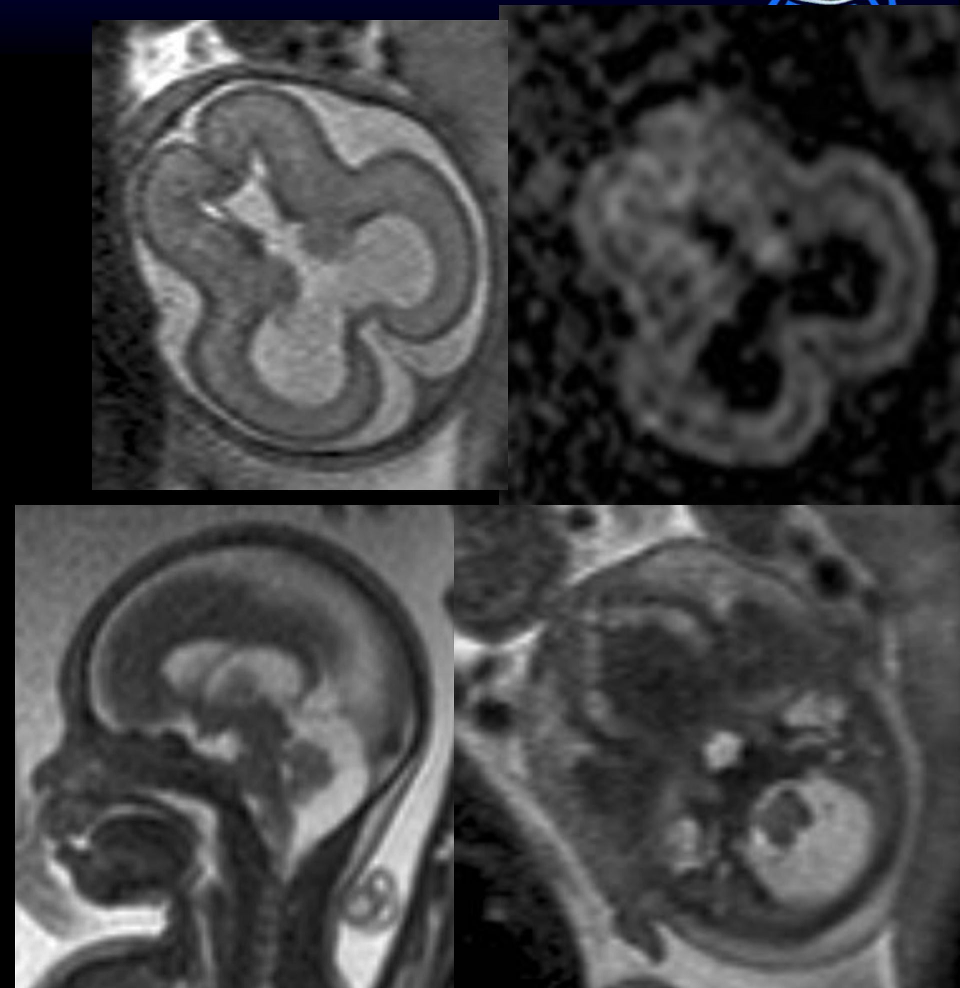

GW 23+2

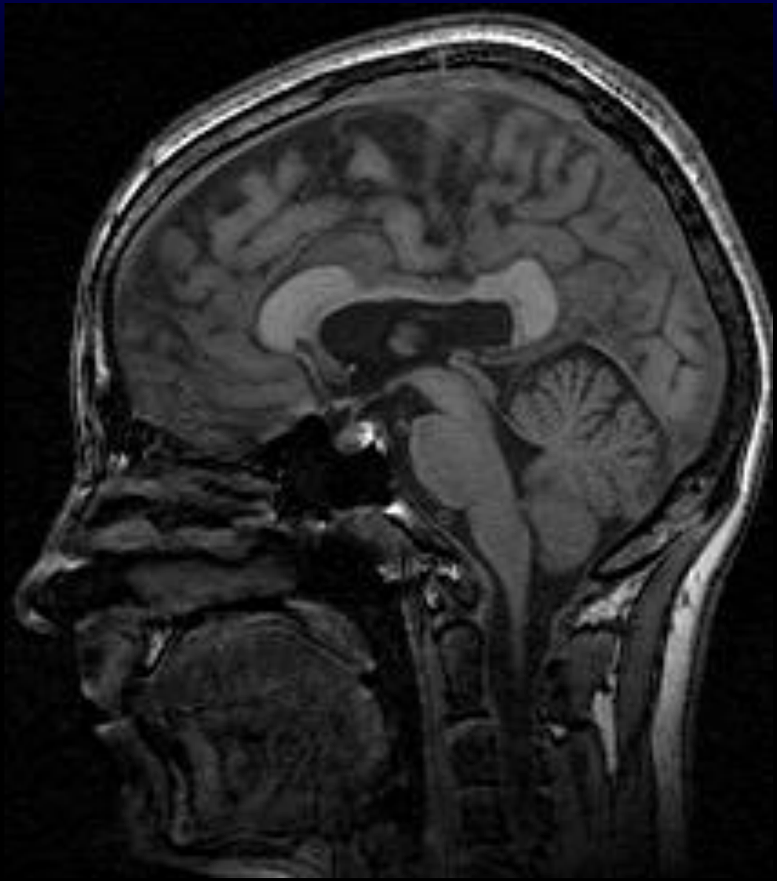

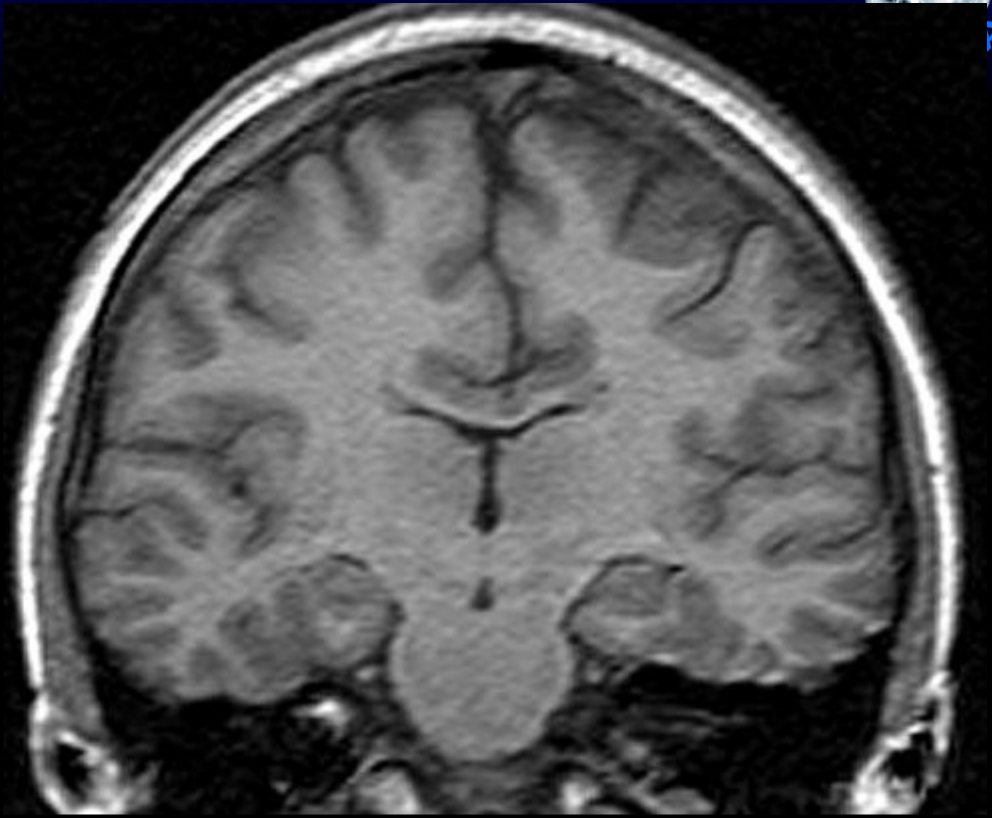

HPE with midline interhemispheric fusion

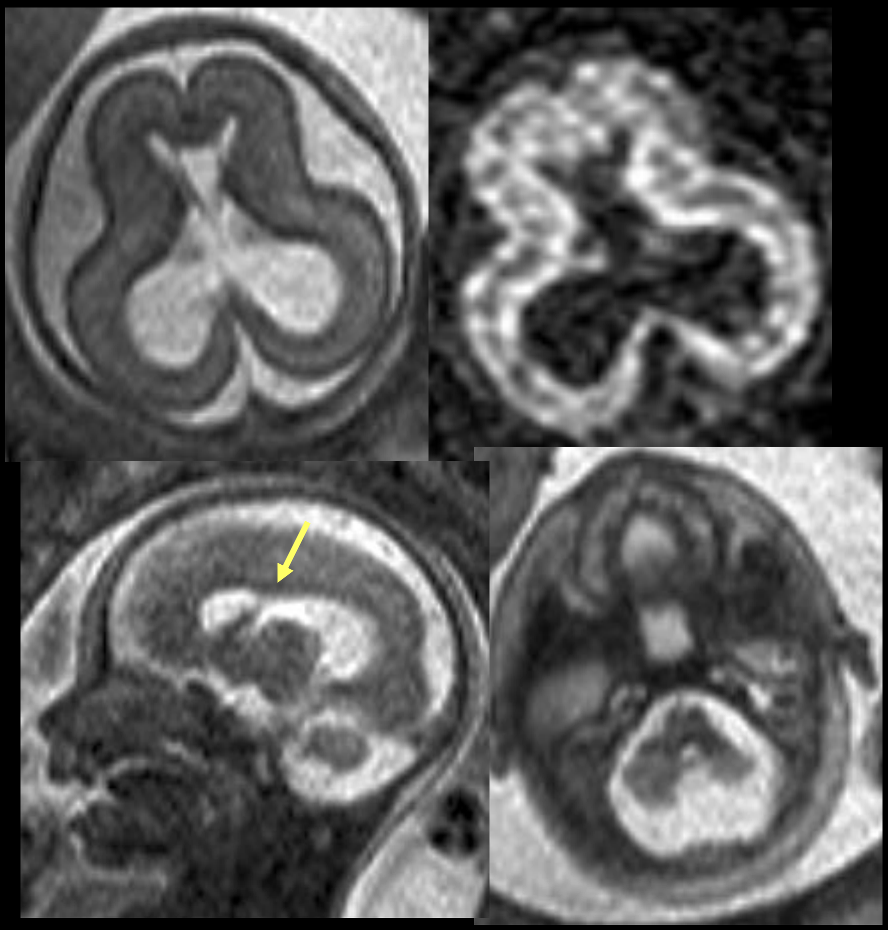

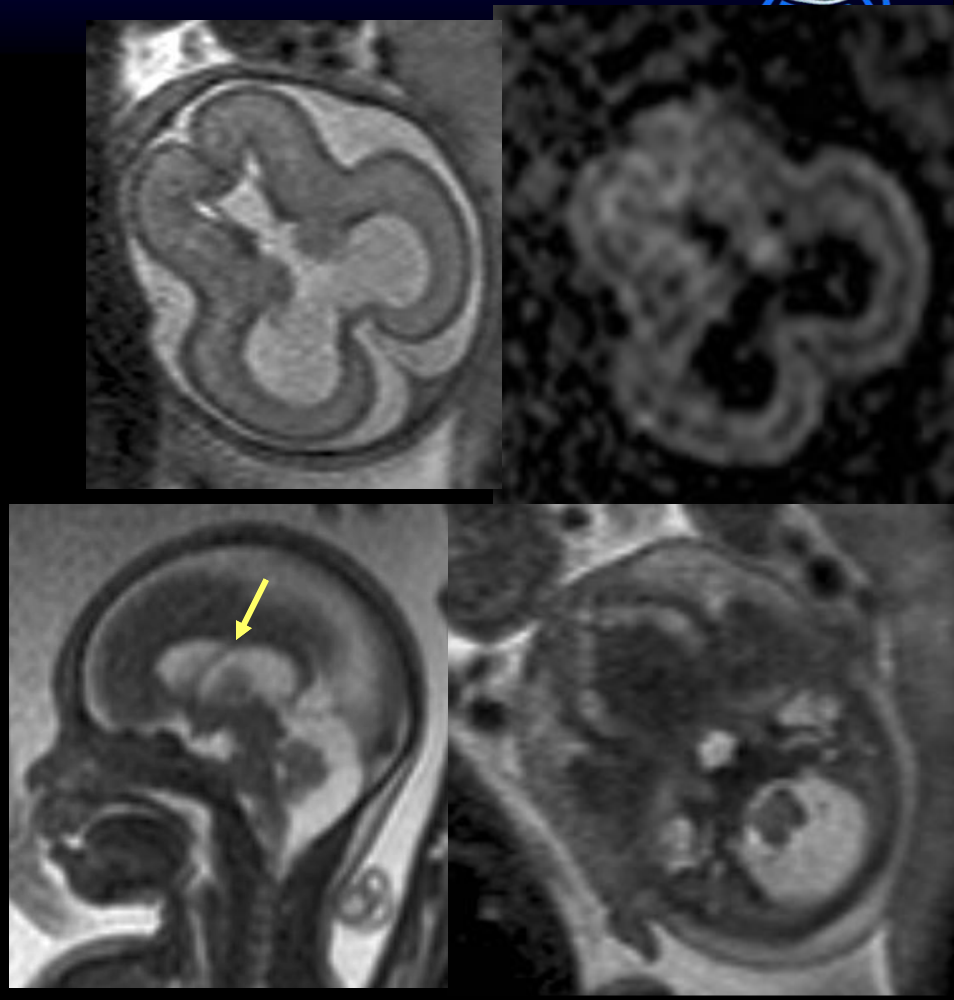

GW 20+6

GW 23+2

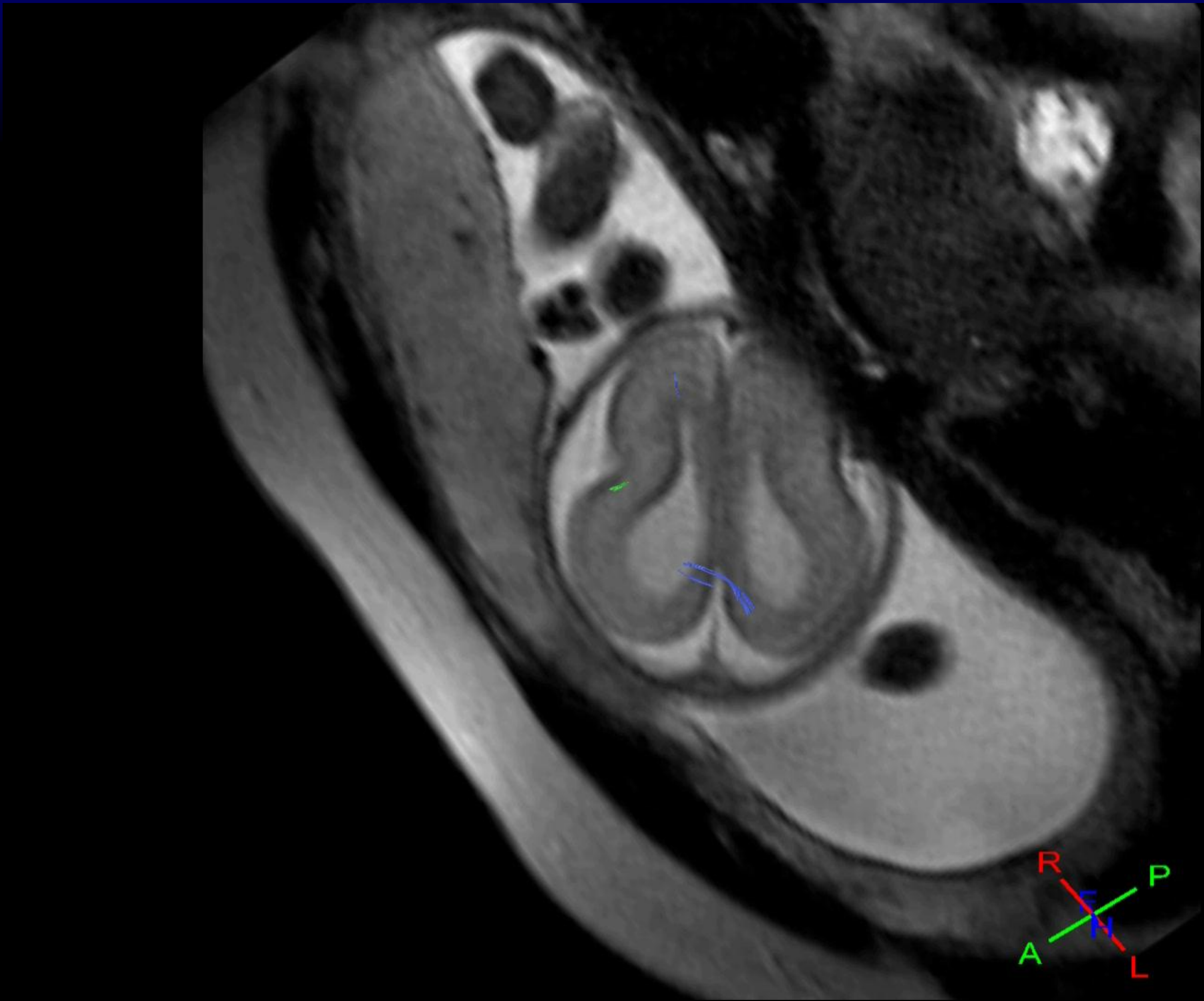
R
P
A
L

Genetical
Diabetes mellitus

Di Base At, Couborne MT
Beware the solitary median central incisor
J Orthod. 35 (1) 16-19. 2008

Small structures

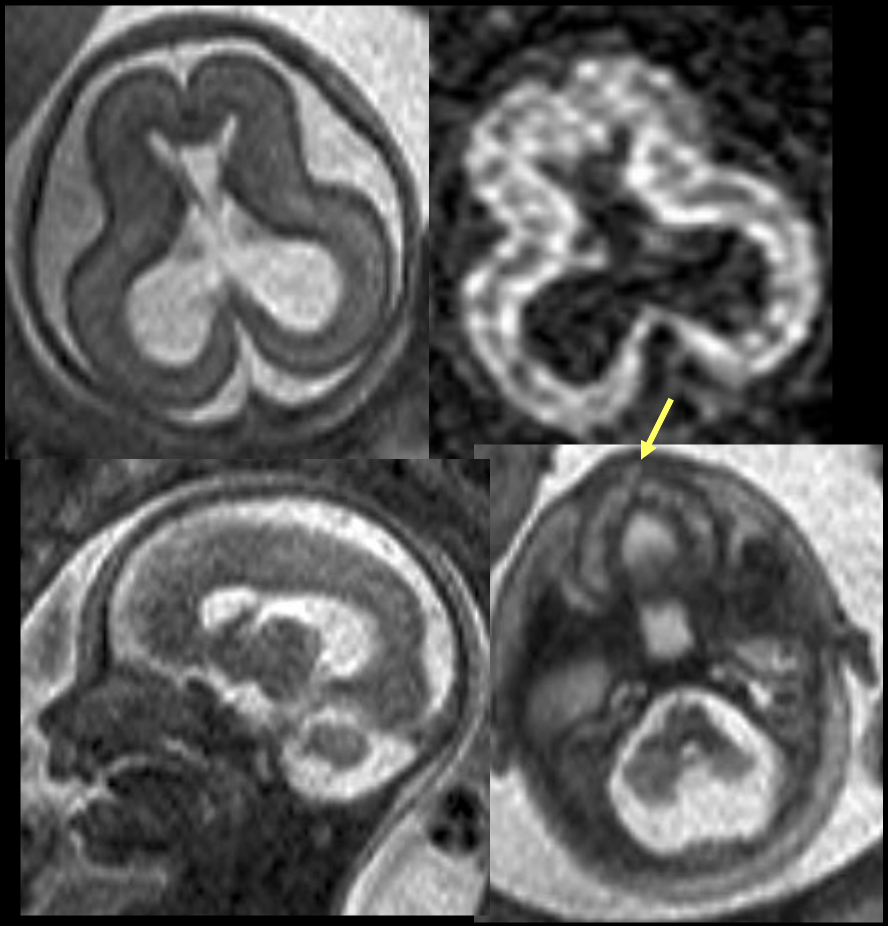

GW 20+6

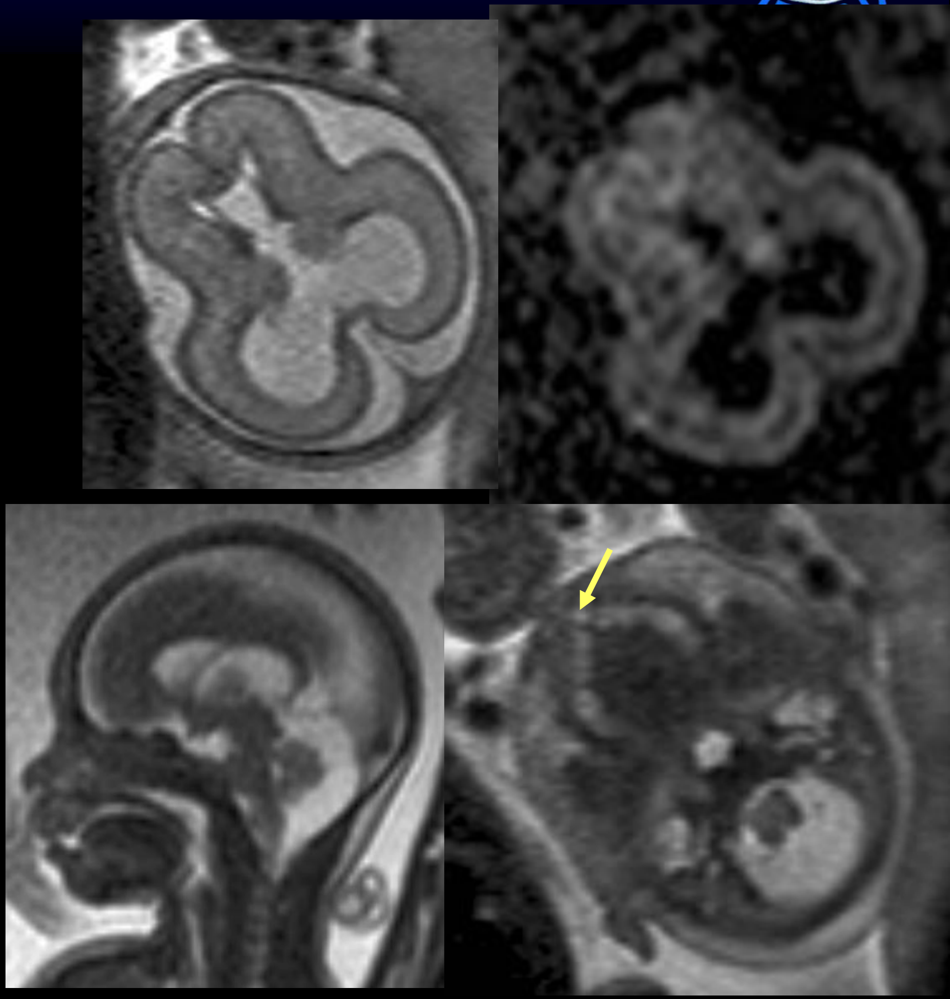

GW 23+2

DWI prenatally

Ischemia

Disordered lamination

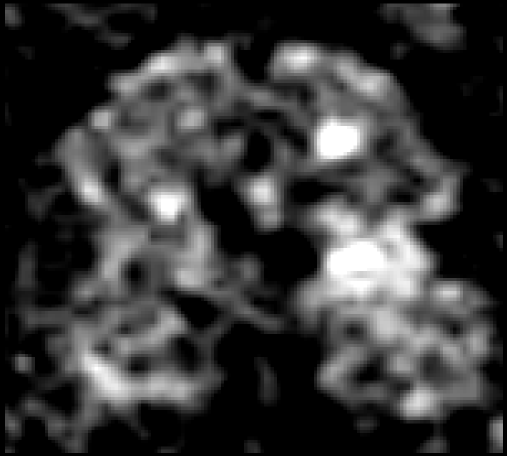

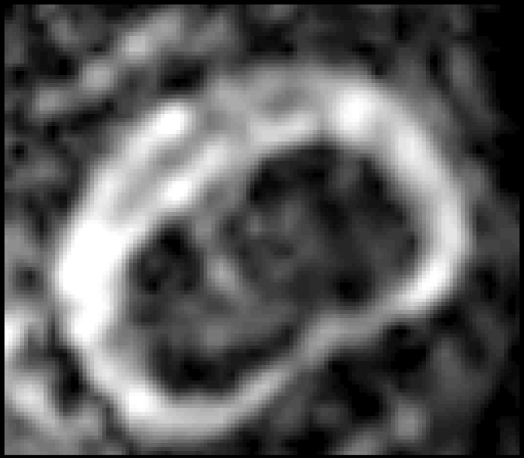

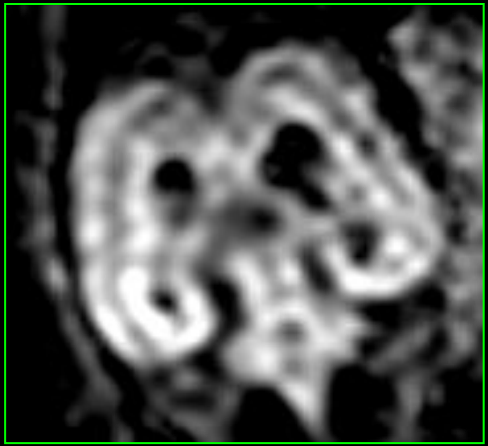

GW 26+2

GW 20+0

GW 20+4

Acute ischemic lesions

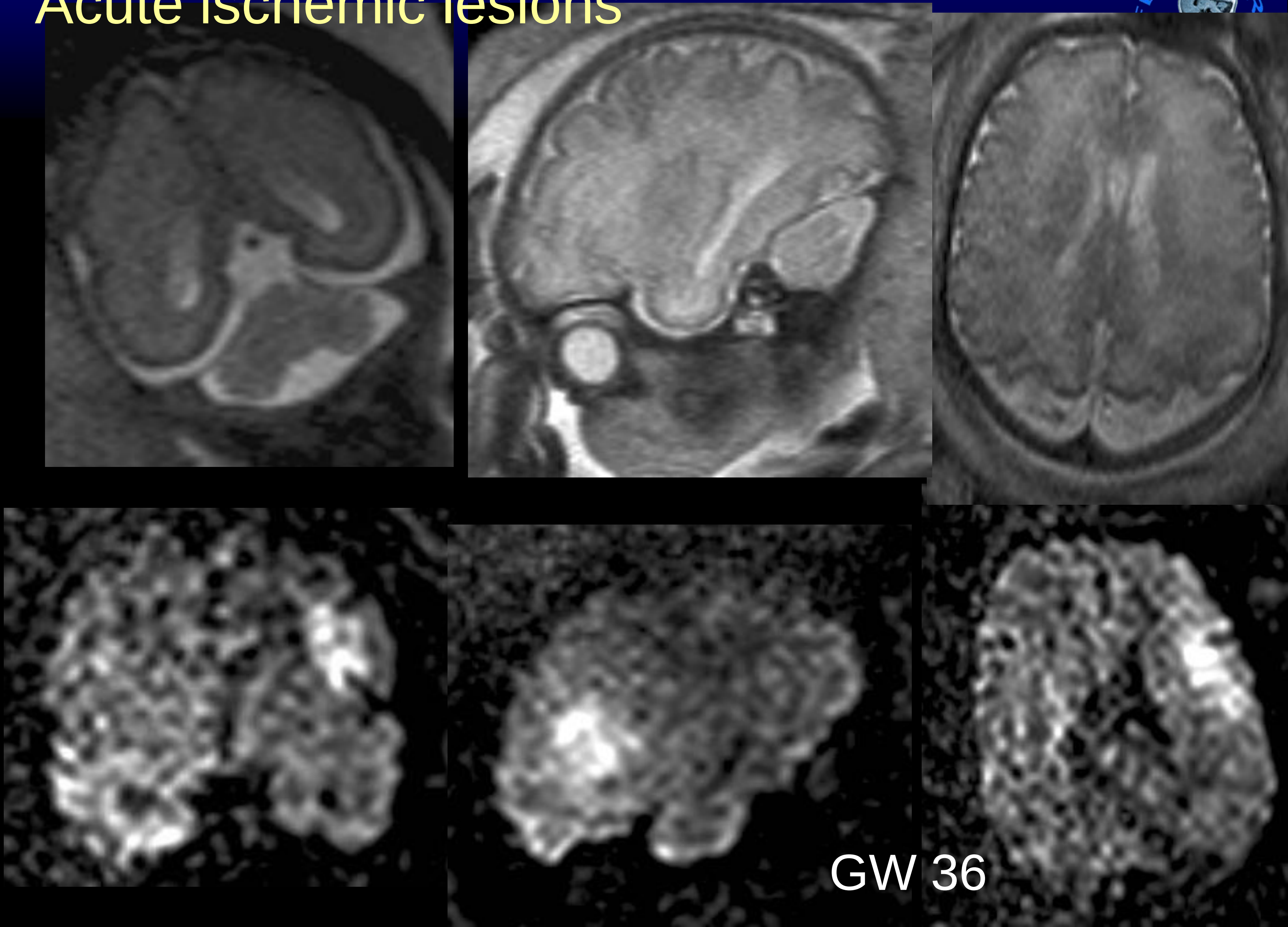

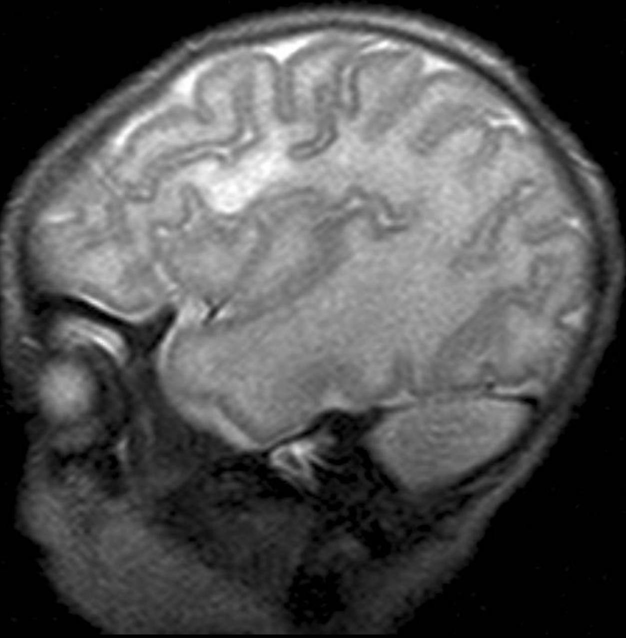

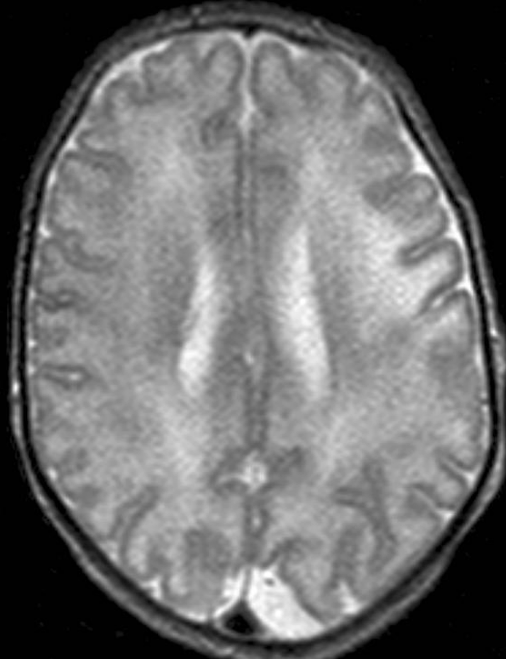

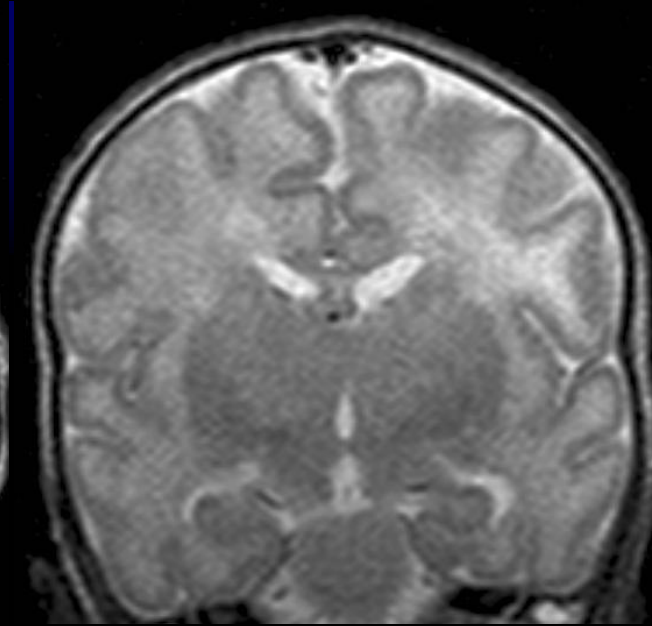

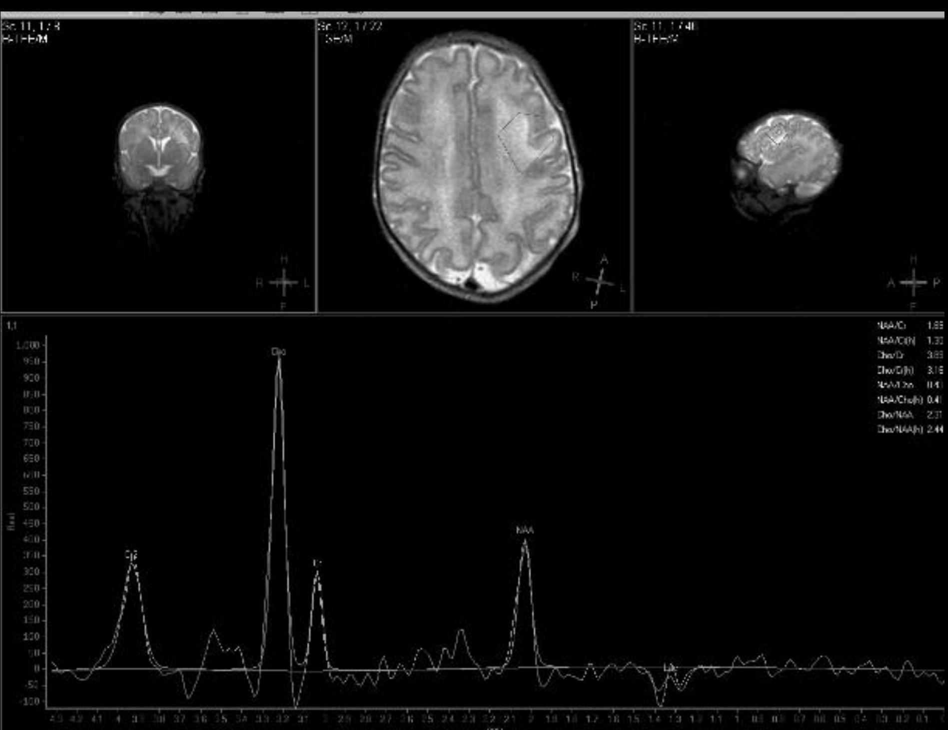

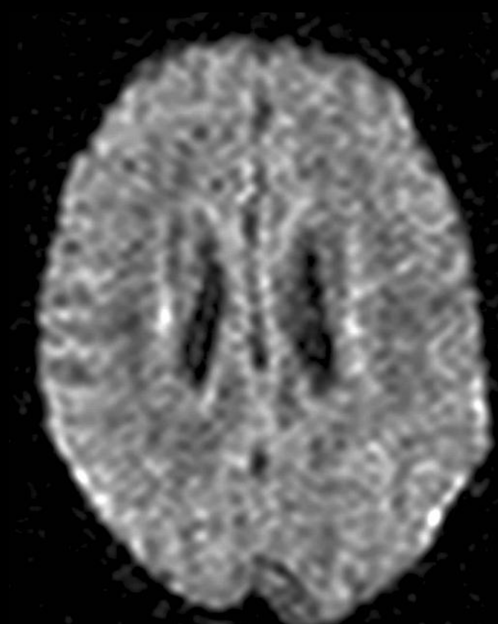

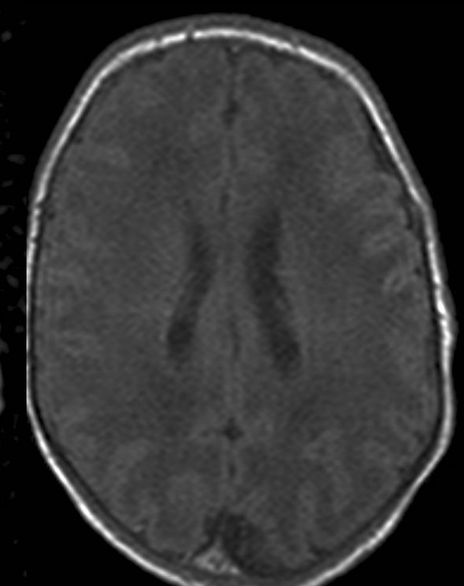

GW 40

Anisotropic Diffusion-weighted Imaging

Corpus callosum

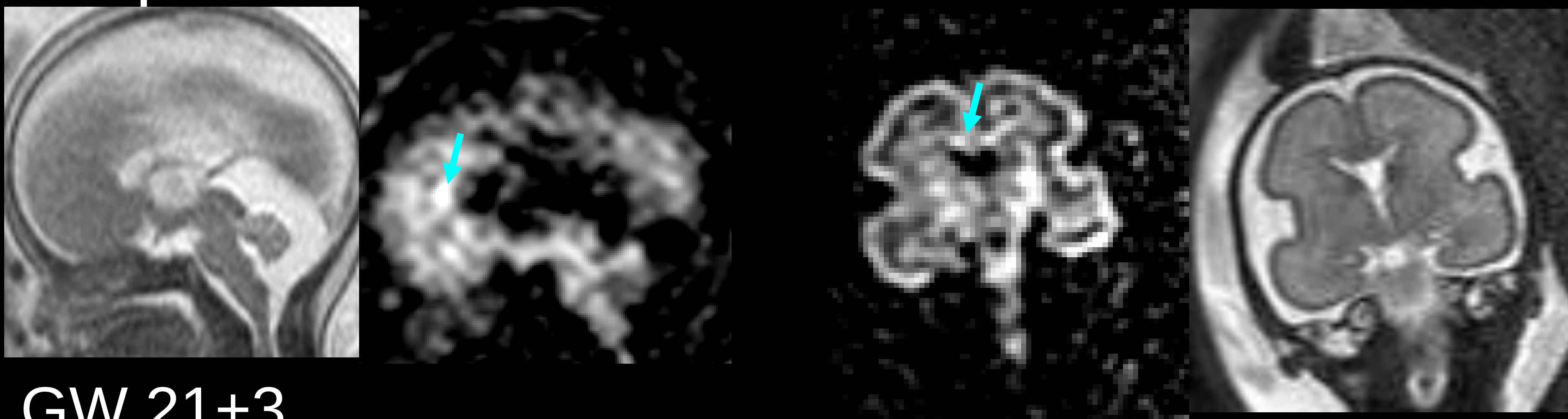

GW 21+3

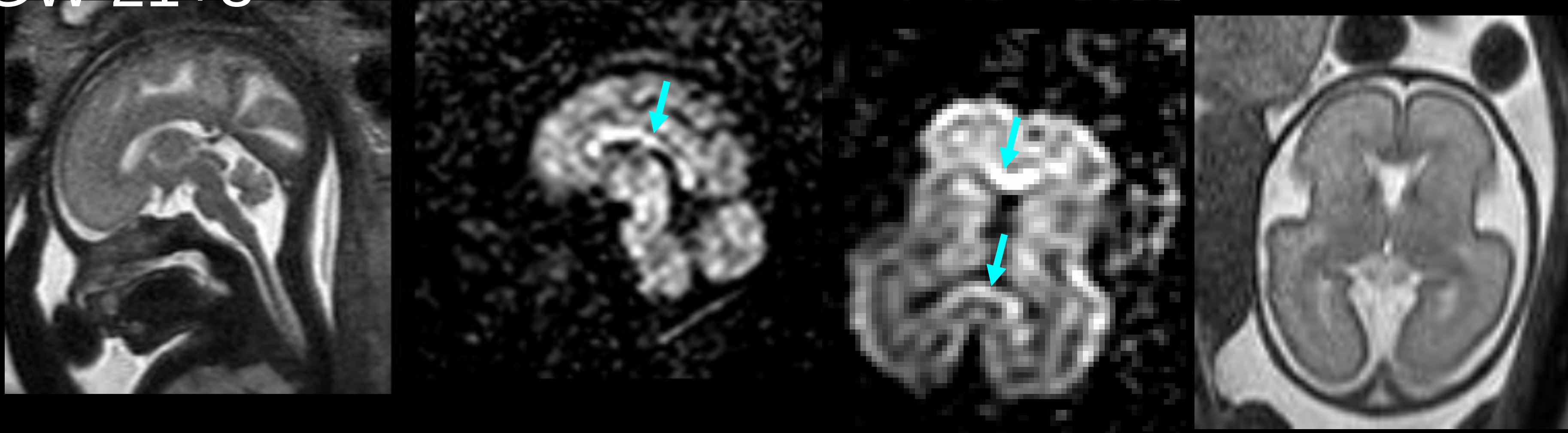

GW 25+6

Tractography:
Technical Background

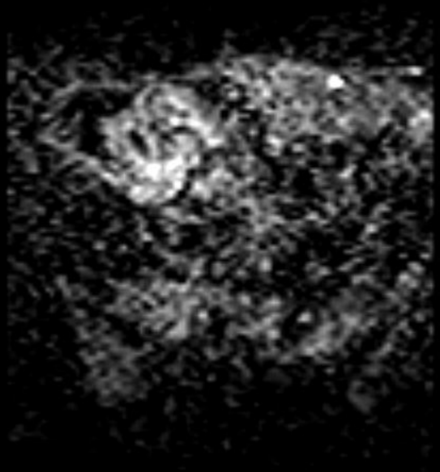

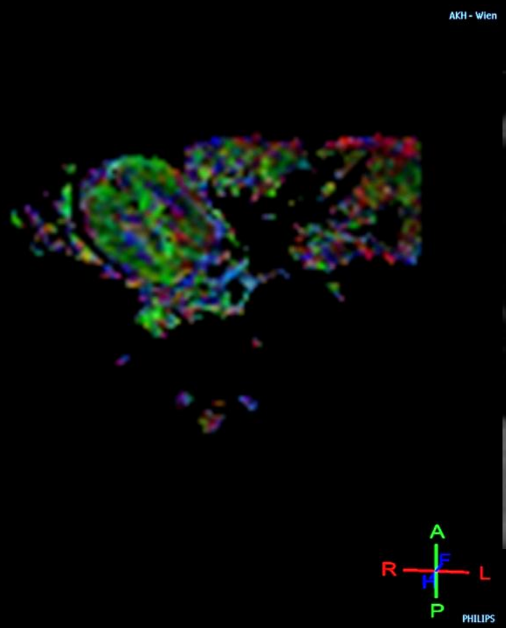

Diffusion weighted sequence
DTI 16-32 directions
Voxel size 1.8x1.8x4mm
b-value 0s/mm^2 and 700s/mm^2

FA color coded map

T2-w sequence

Technical Background

ROI definition

Corticospinal/
Thalamocortical

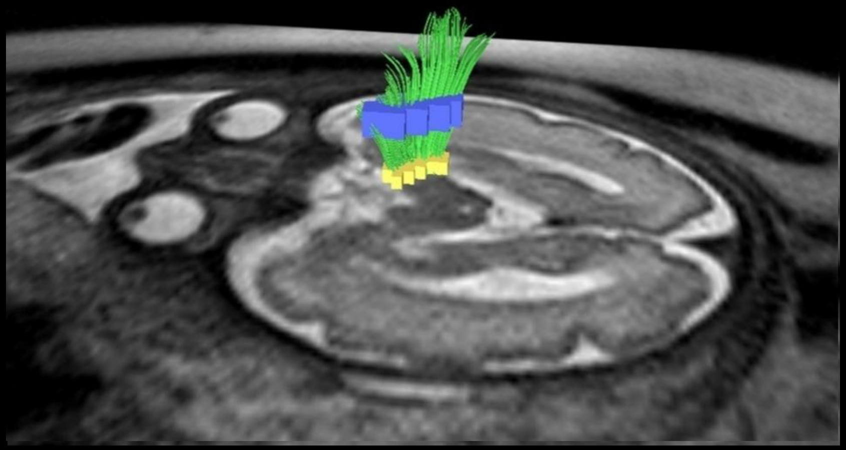

Corpus Callosum

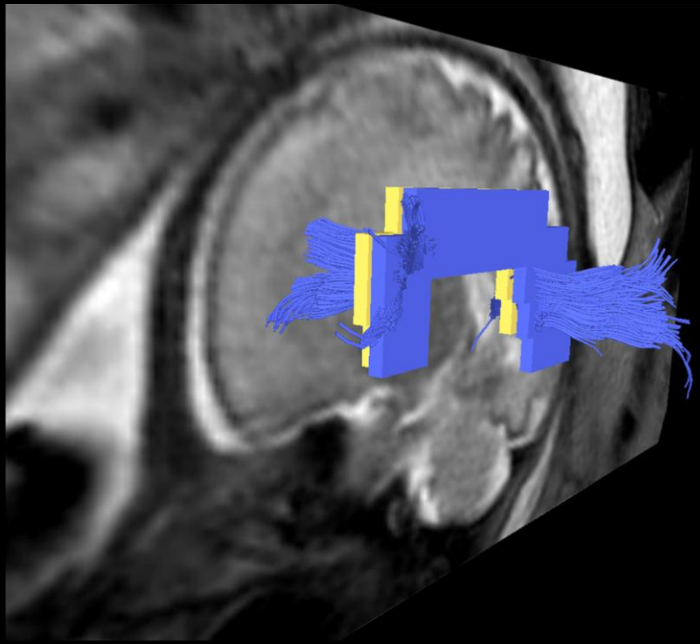

Minimum FA: 0.15
Max. angle change: 27
Min. fiber length: 10mm

Technical Background

limiting factors

number of diffusion directions

fetal head position

acquisition time

fetal movements

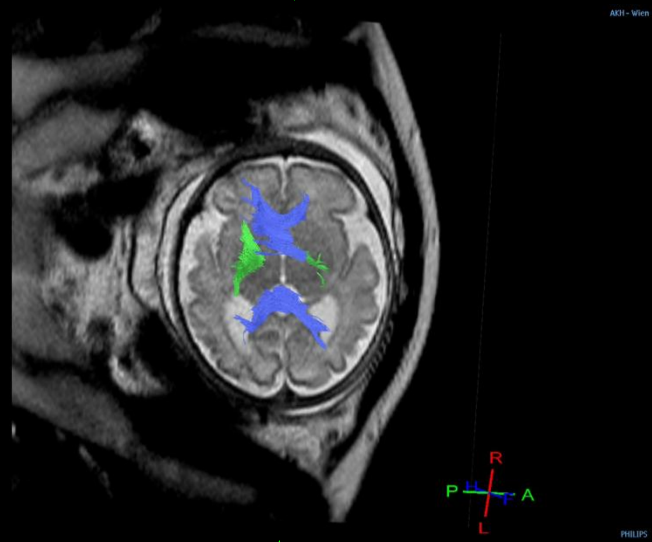

slice thickness

gestational age

coil position

amount of amniotic fluid

maternal (breathing) movements

Normal connectivity
Motor and Sensory tracts

18 GW

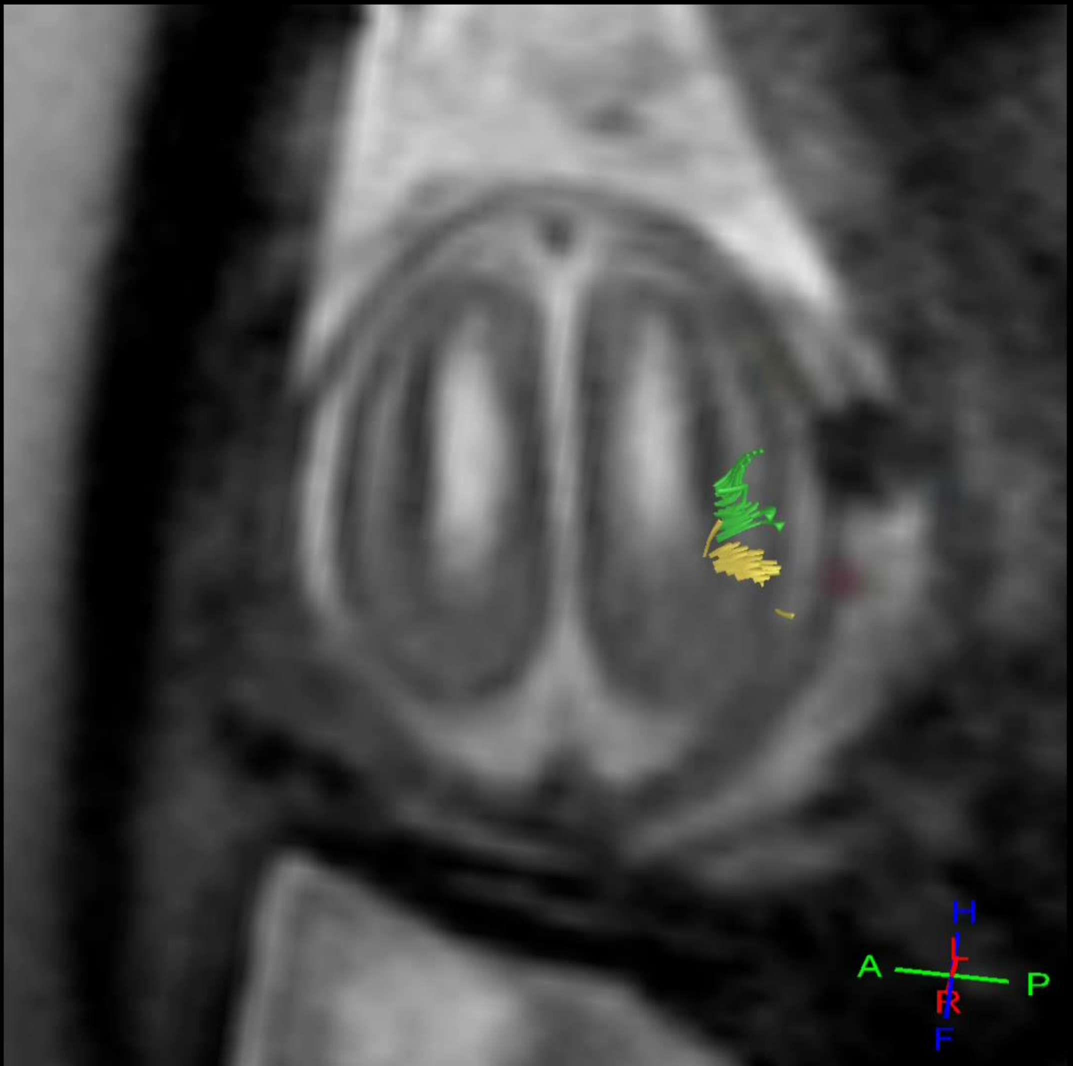

Normal connectivity
Motor and Sensory tracts

Kostovic et al. Cereb. Cortex 2002

18 GW

Cortical plate

Subplate

Intermediate zone

Ventricular zone

Motor

Sensory

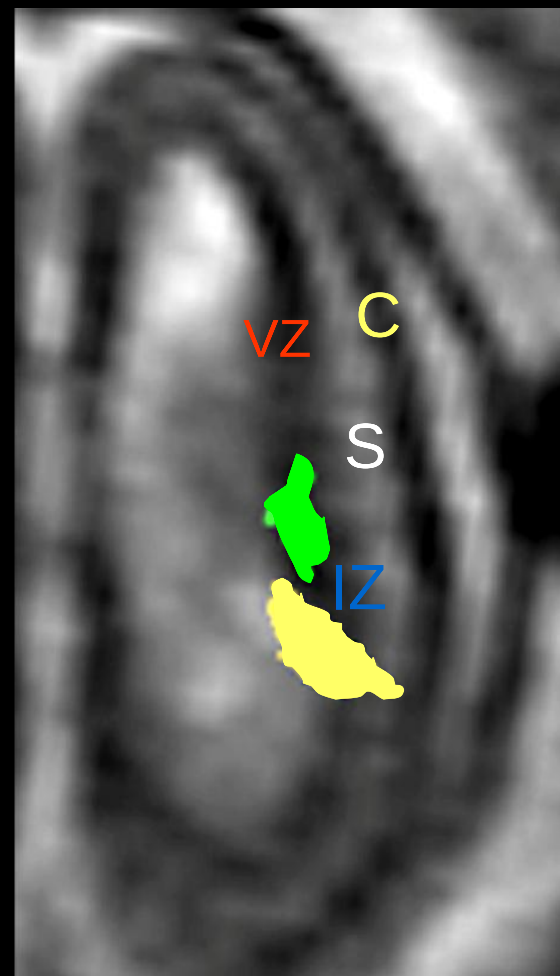

In vivo 2D-projection

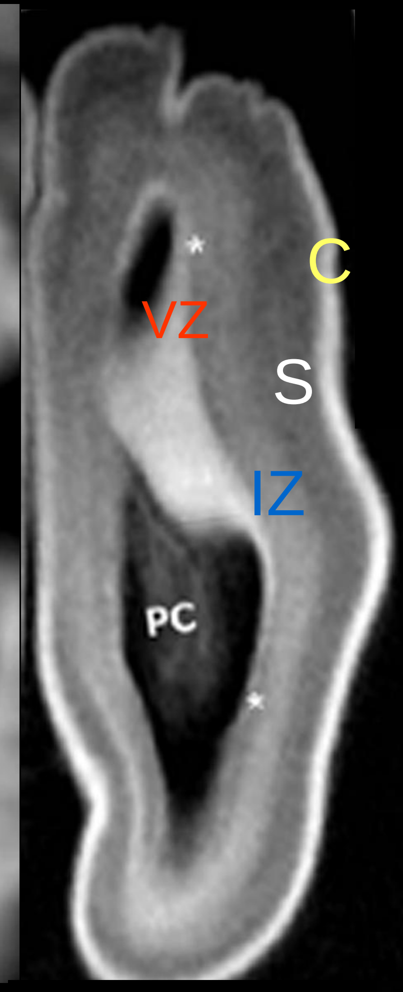

In vitro T1w

Normal connectivity
Connectivity at 23GW

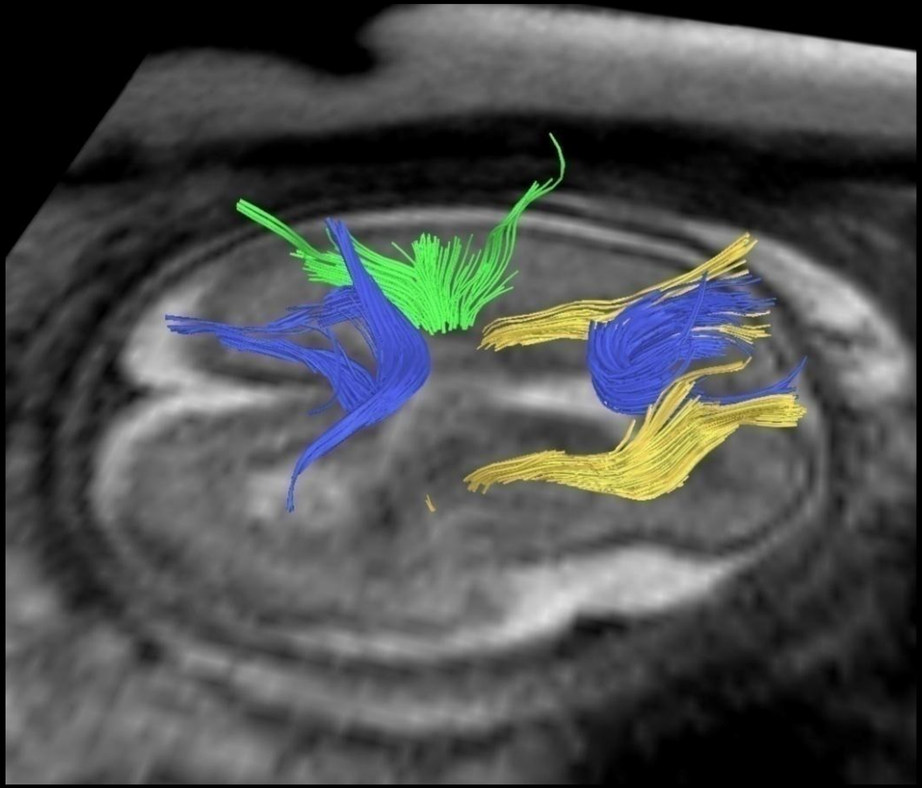

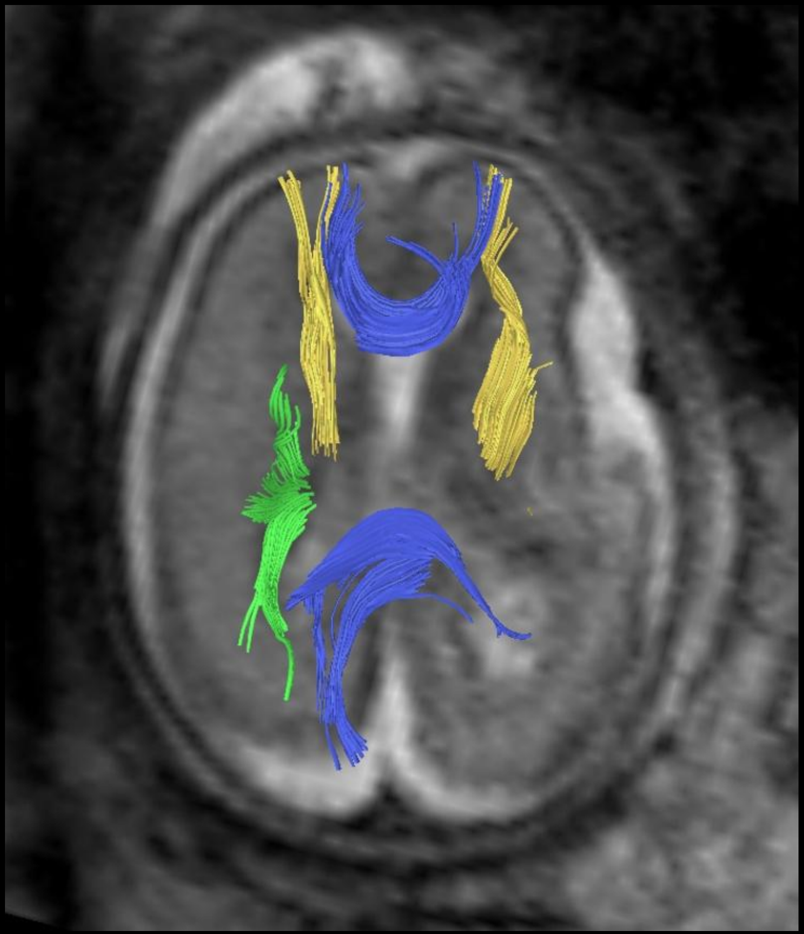

Normal Connectivity
Association fibers GW34

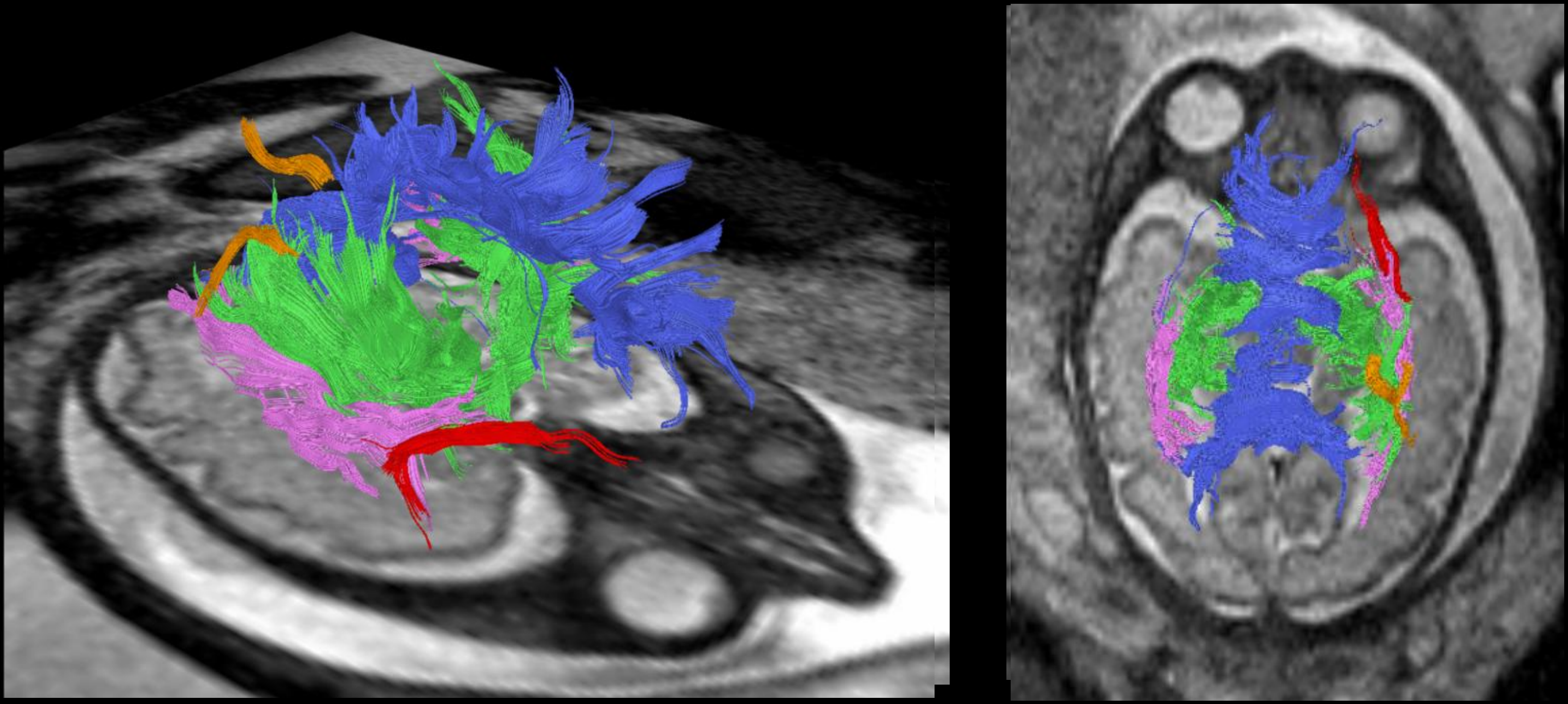

Inferior longitudinal fascicle/optic radiation

Uncinate fascicle

Superior longitudinal fascicle

C. Mitter, UOG Feb 2011

Normal connectivity?

GW 36

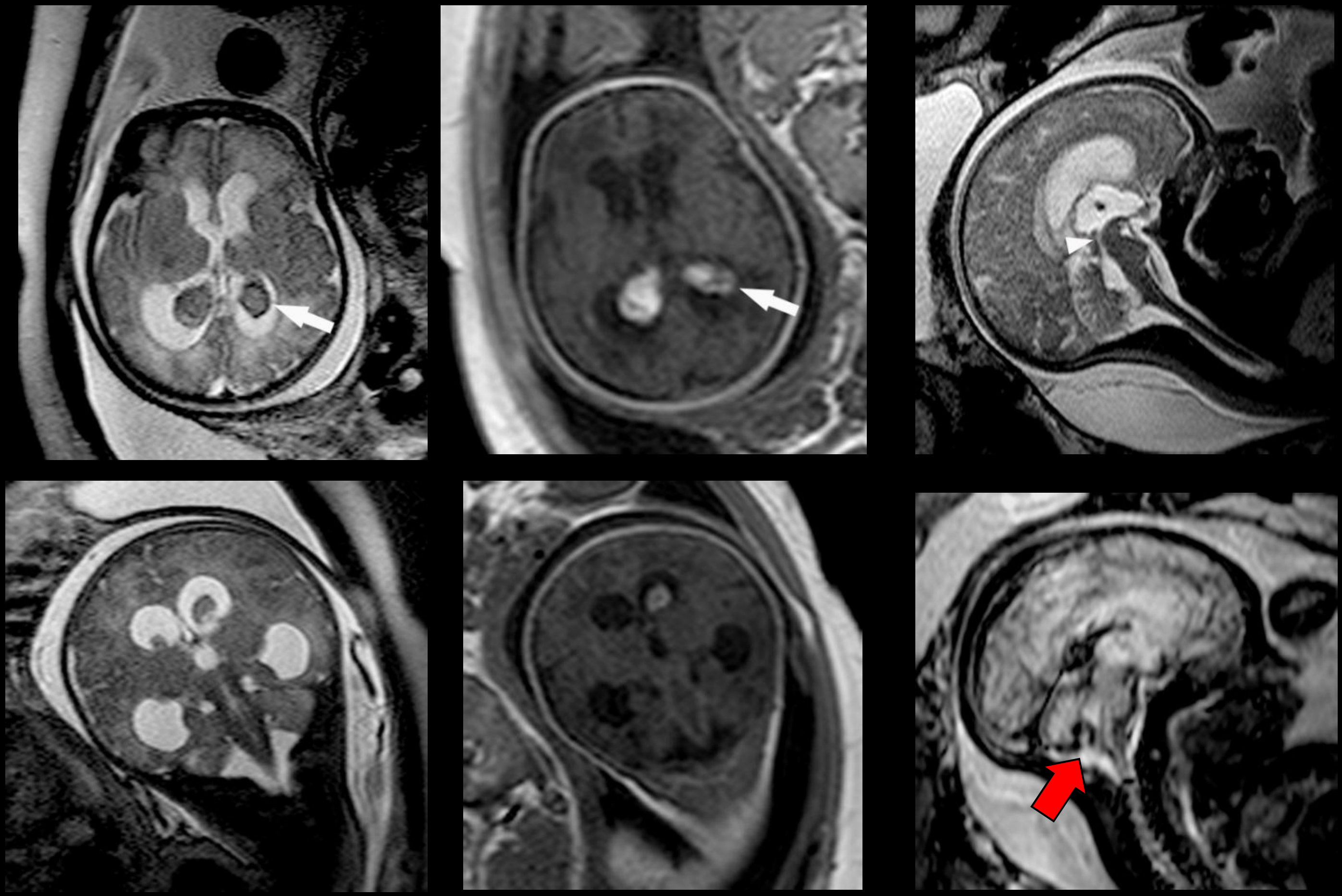

Normal connectivity?

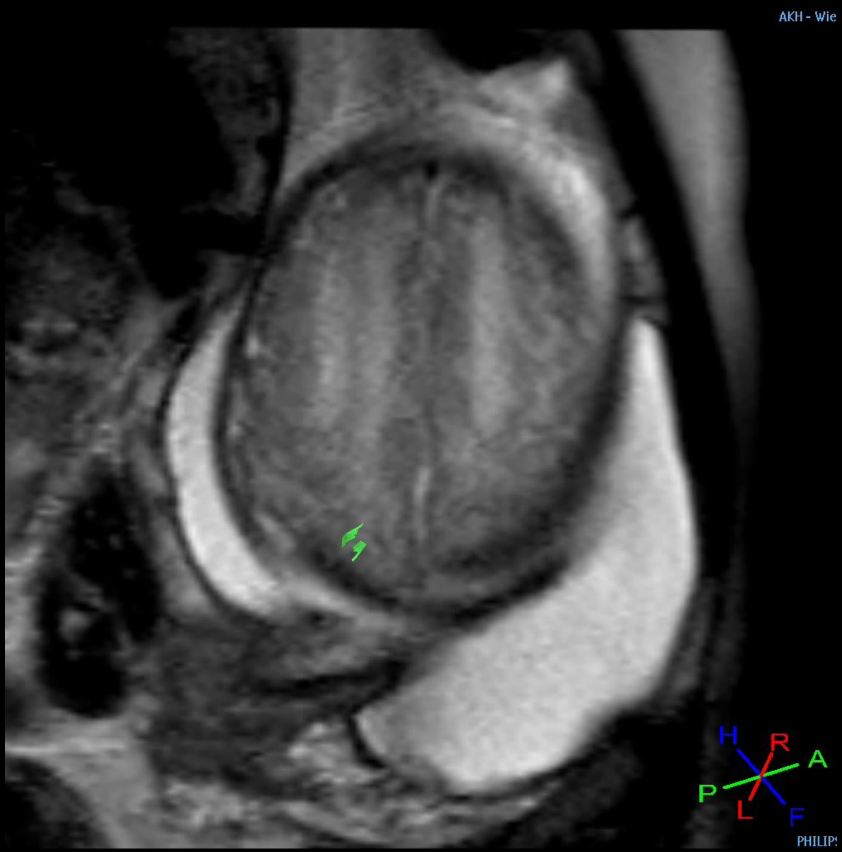

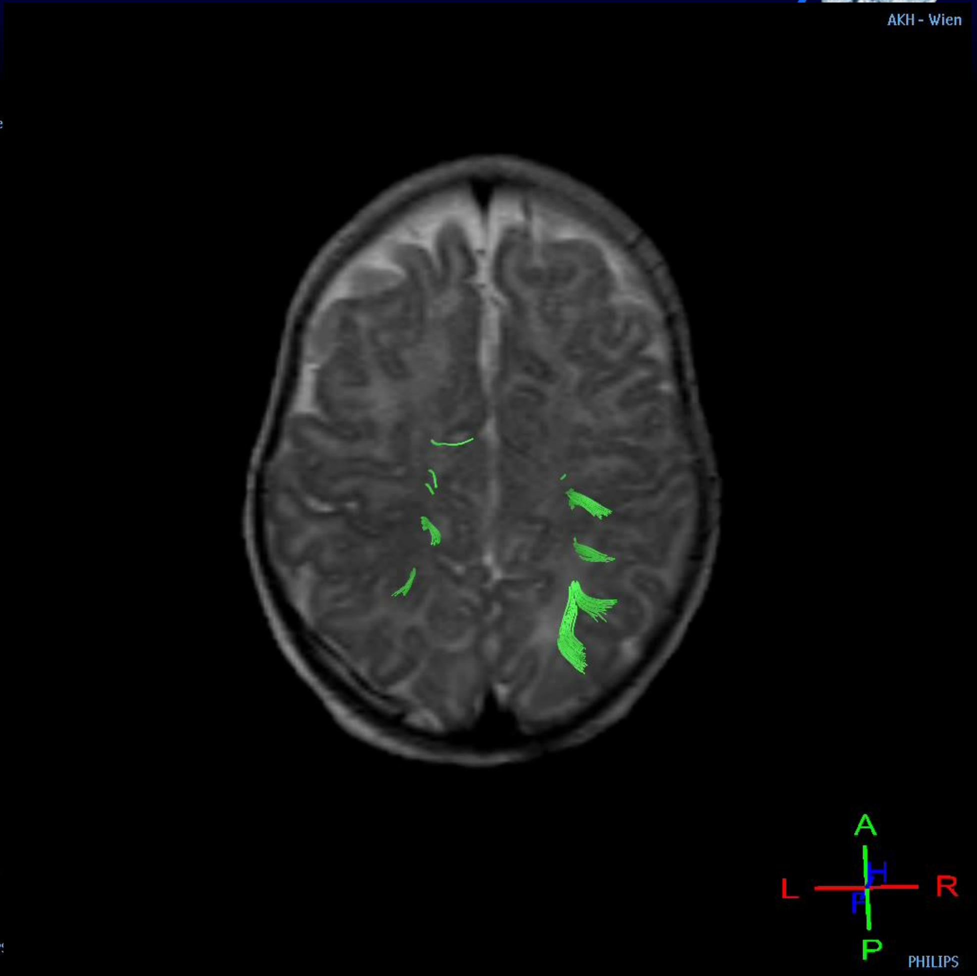

GW 40

3 Month

Pathological connectivity
Probst bundles

Trisomy 13, CCA

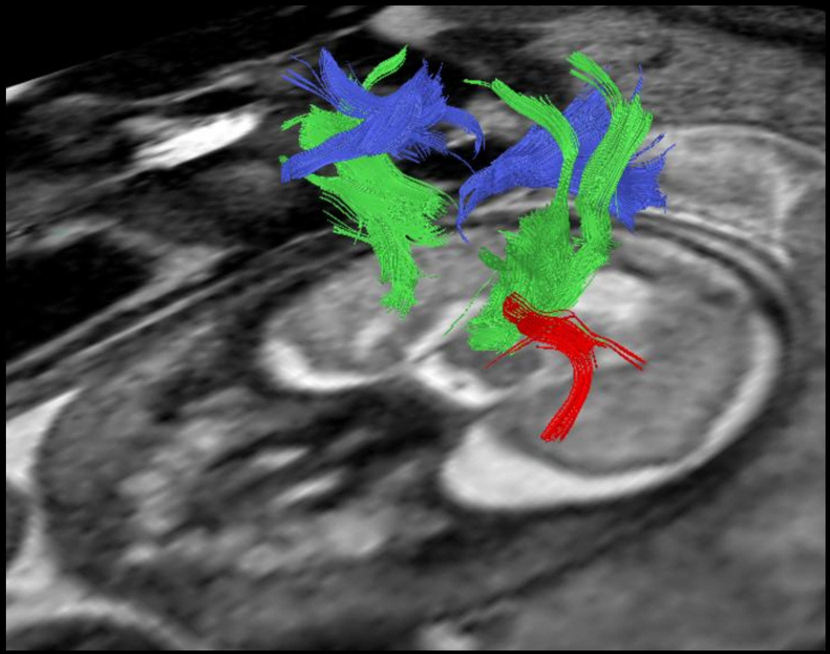

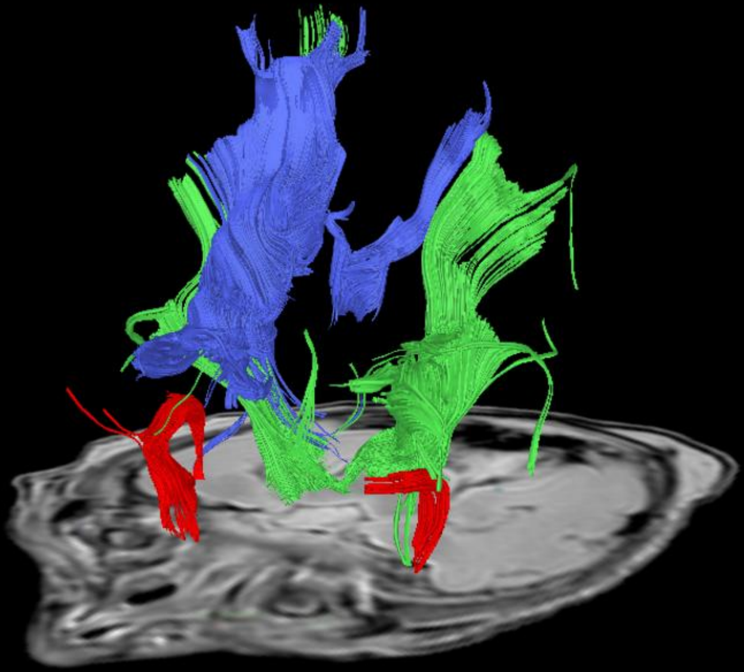

Prenatal, in vivo 28GW

Postmortem, 31GW

Pathological connectivity

Sensorimotor tracts, Discontinouity

34 GW

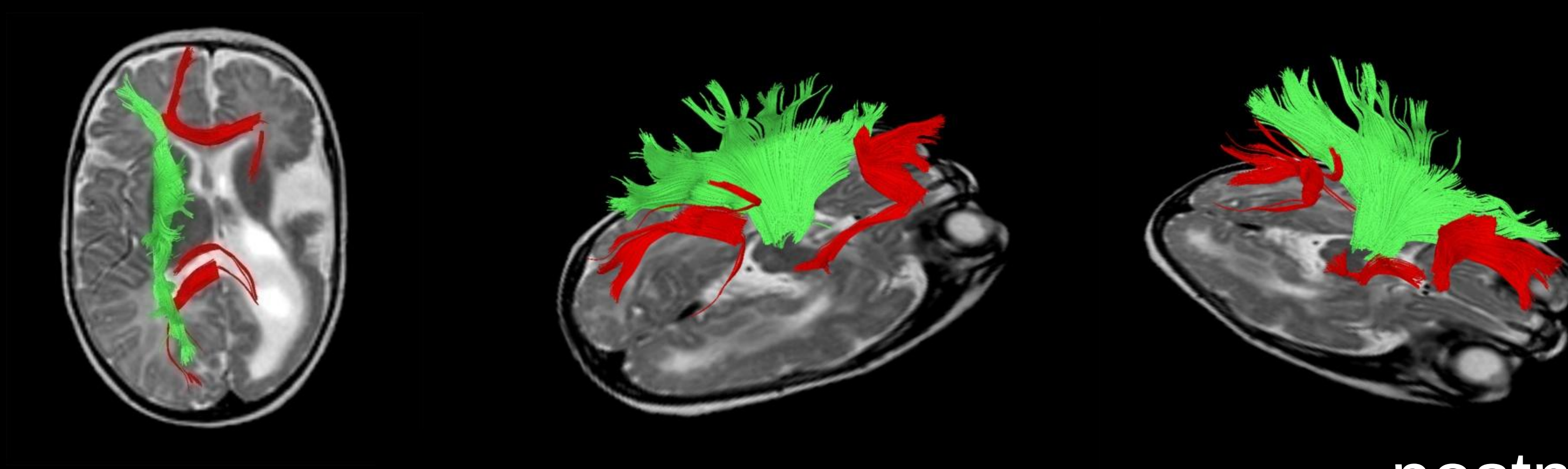

postnatal

?

GW 34+4

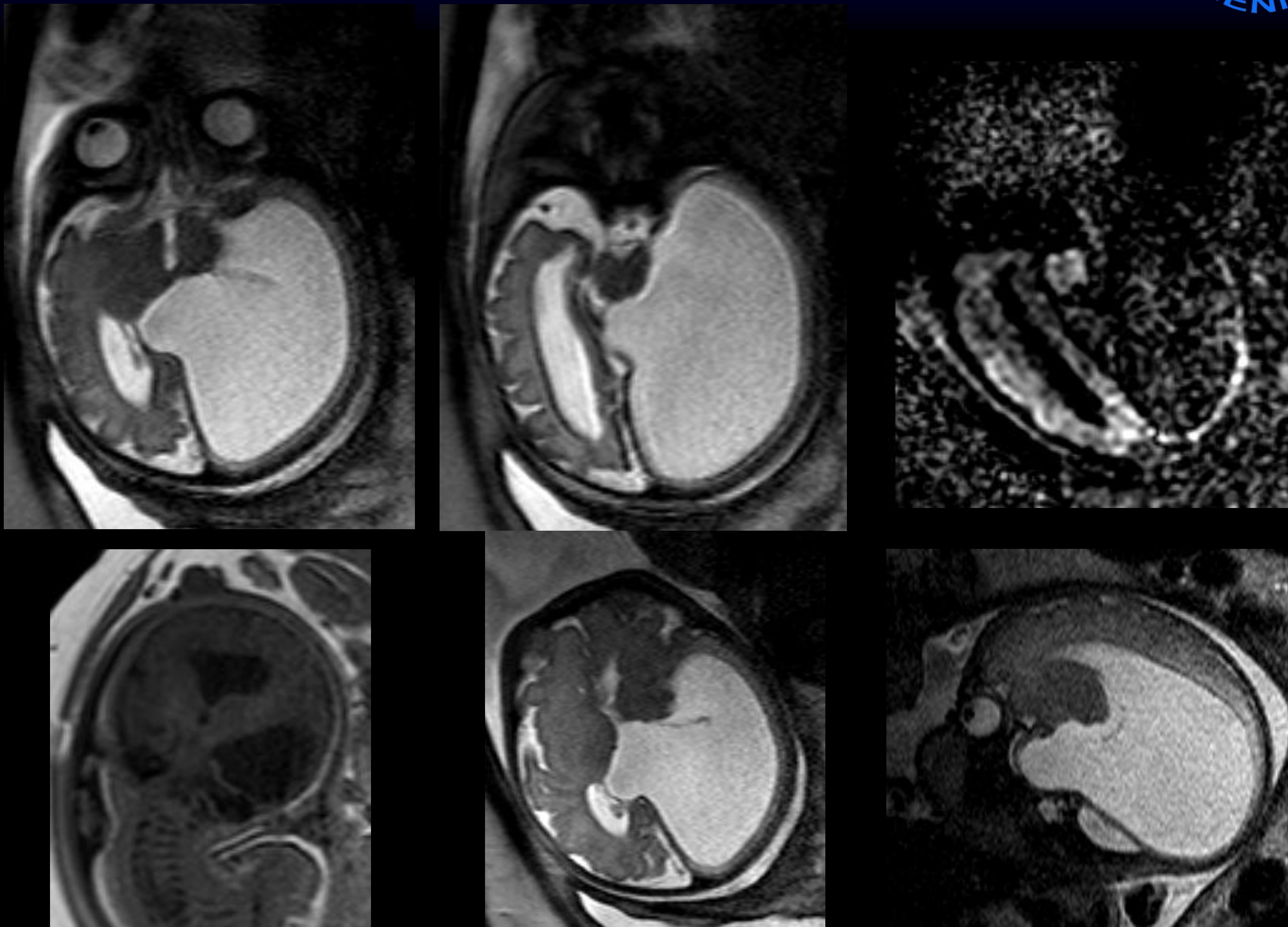

Pathological connectivity
Sensorimotor tracts, Displacement

GW 34+4

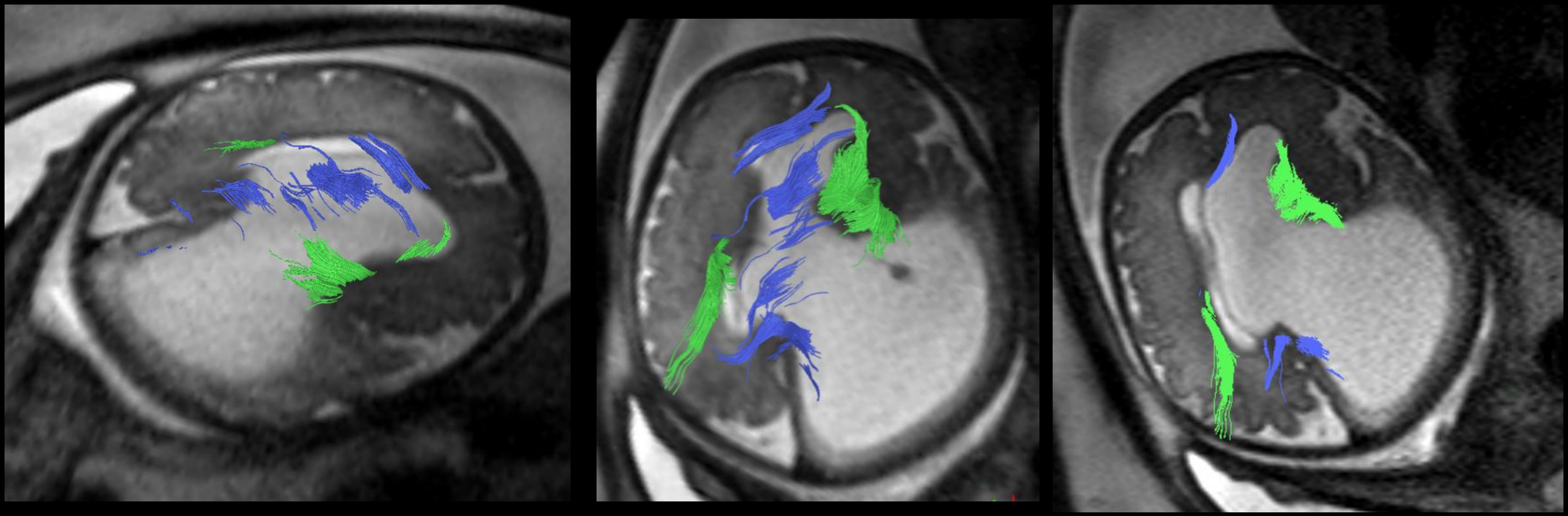

Pathological connectivity

Corpus callosum

„The striking and particularly interesting structure of brains, with complete absence of the corpus callosum is the Balkenlängsbündel,..“

„..absence of the corpus callosum is rather a heterotopia then an agenesis…”

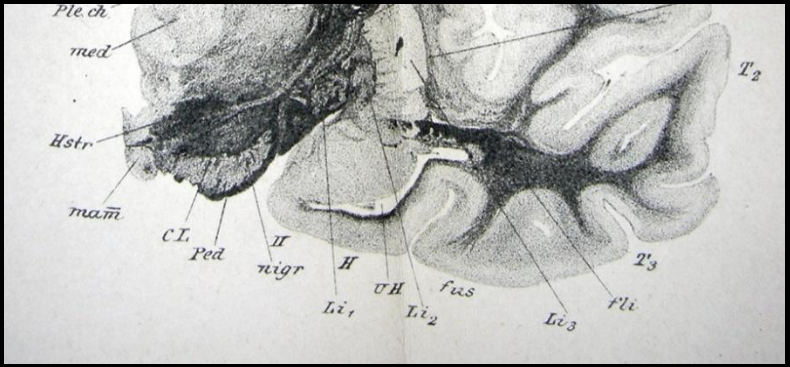

Probst, M., 1901. Über den Bau des vollständigen balkenlosen Großhirns sowie über Microgyrie und Heterotopie der Grauen Substanz. Arch Psychiat Nervenkr 34, 709-786.

Pathological connectivity
Callosal agenesis - background

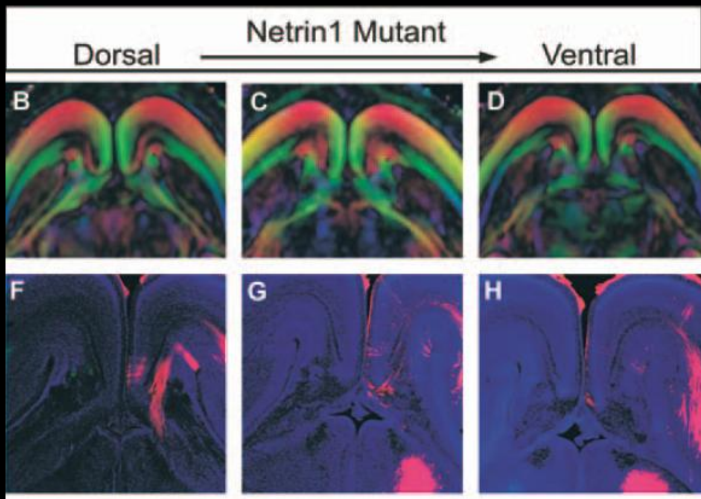

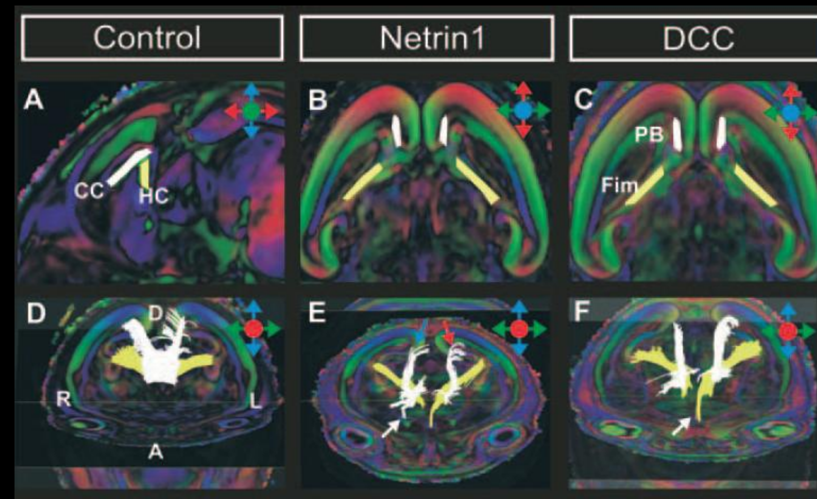

Ren, T., Zhang, J., et al. 2007. J Neurosci 27, 10345-10349.

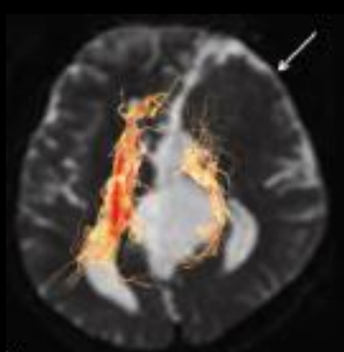

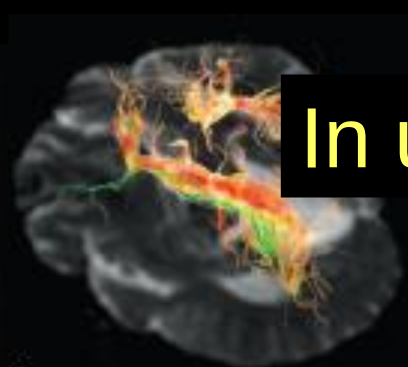

In utero?

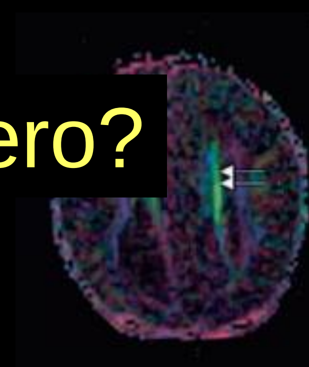

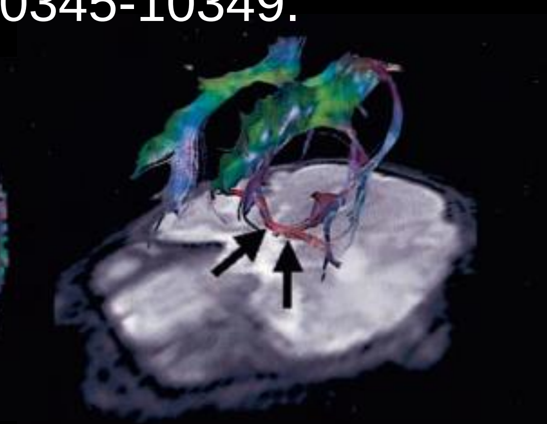

Utsunomiya H, Yamashita S, et al. 2006. Acta Radiol 47, 1063-1066
Lee, S.K., Mori, S., et al. 2004. AJNR Am J Neuroradiol 25, 25-28.

Pathological connectivity
Callosal agenesis

29GW Premyelination of Probst Bundles

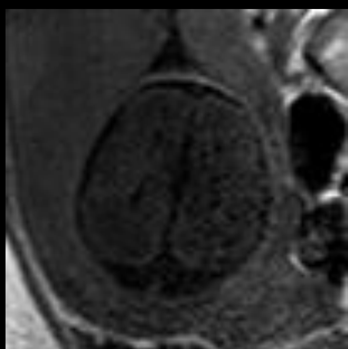

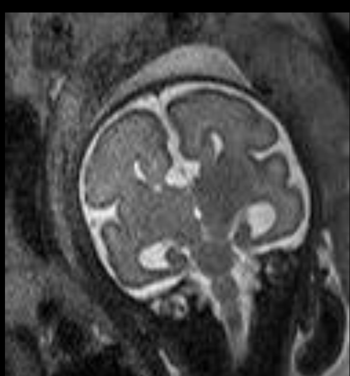
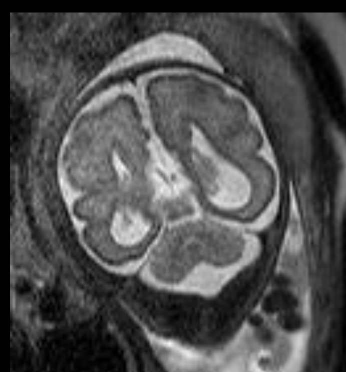
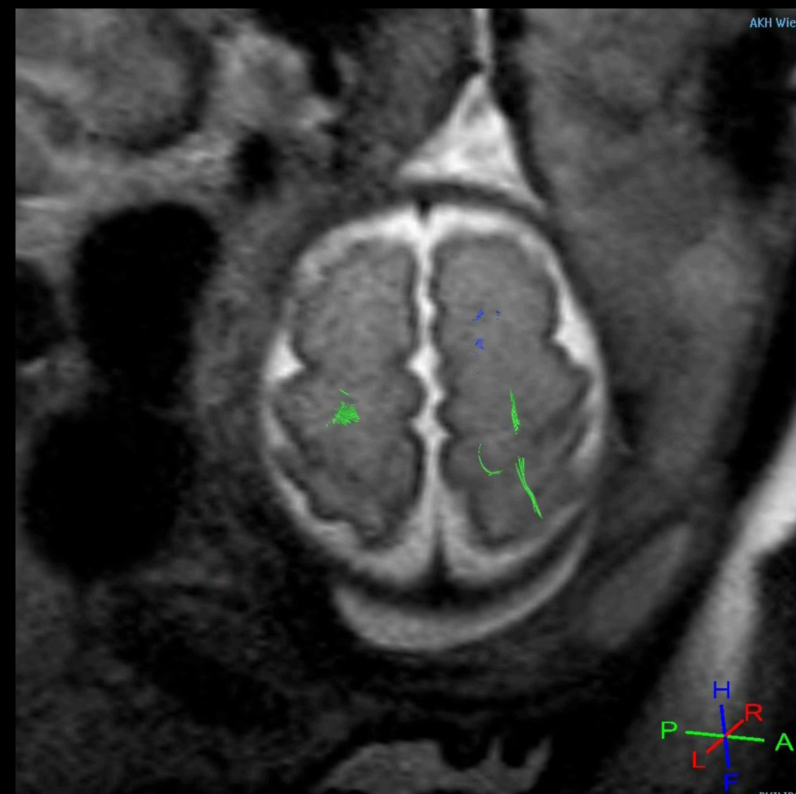

No Myelin!

Pathological connectivity
Callosal agenesis

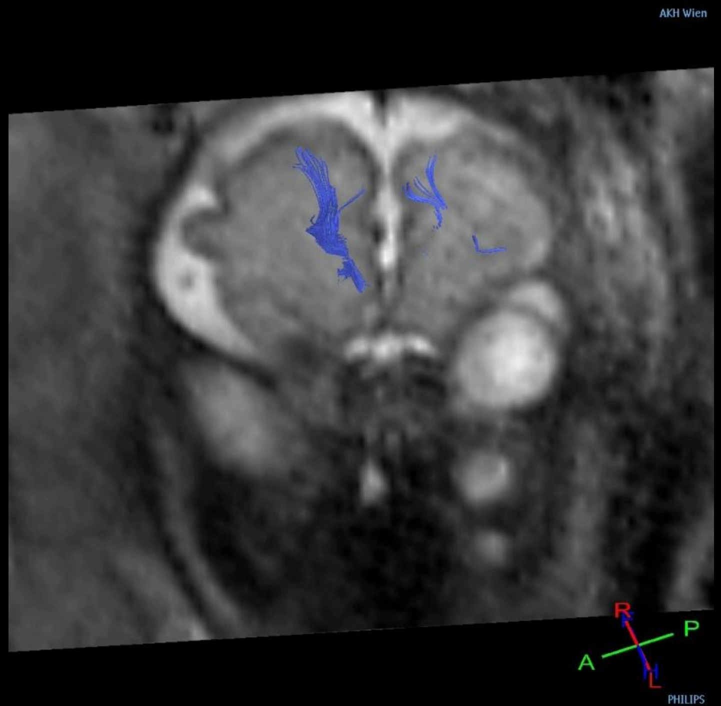

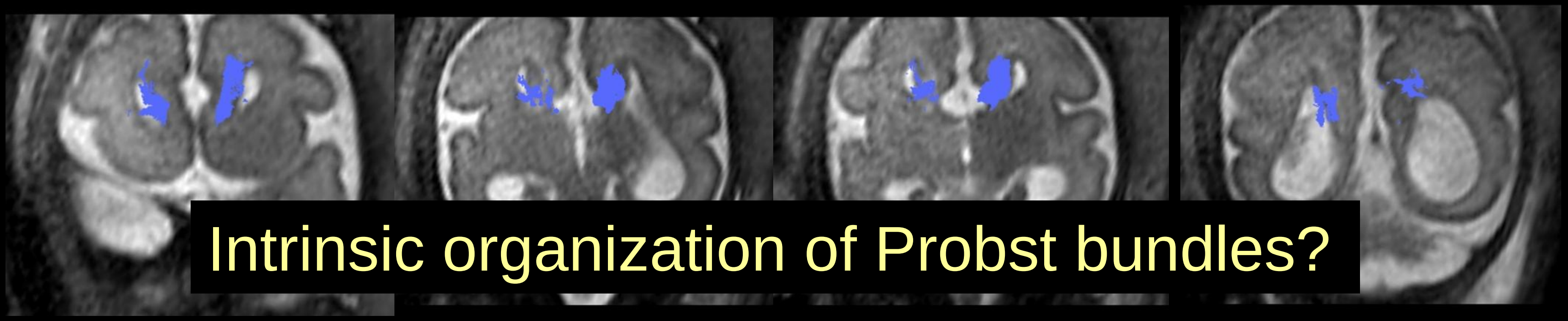

Intrinsic organization of Probst bundles?

Pathological connectivity
Callosal agenesis

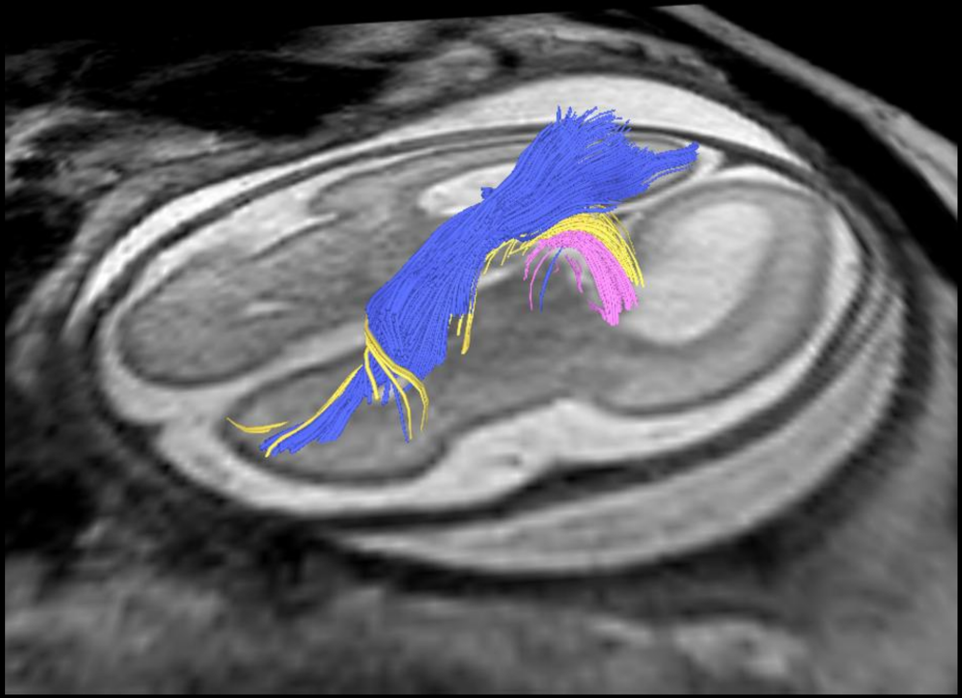

Cingulum
Fornix
Intrinsic organization of Probst bundles?

Pathological connectivity

Callosal agenesis

= disorder of axon guidance

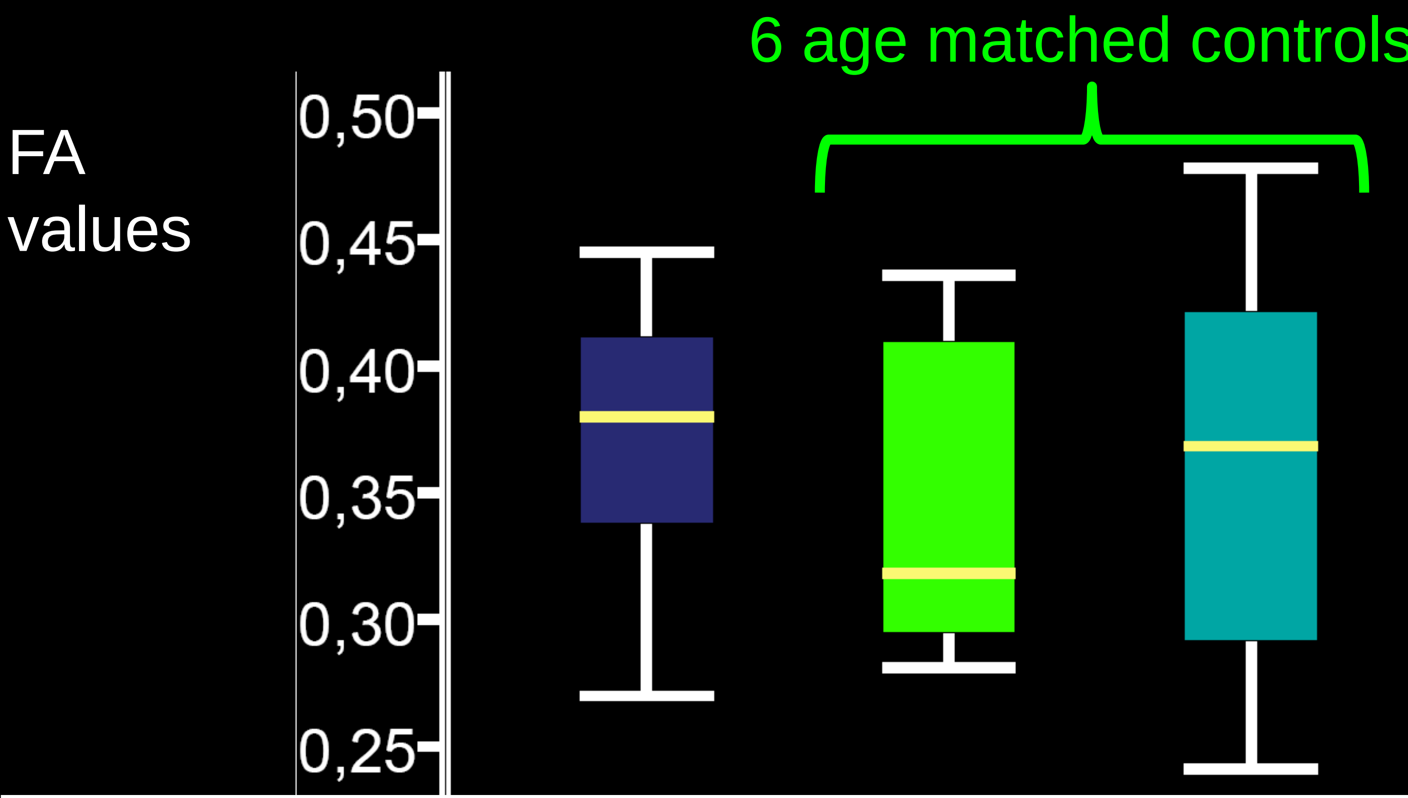

structural integrity and maturity:
Probst Bundle similar to the corpus callosum

Partial callosal agenesis

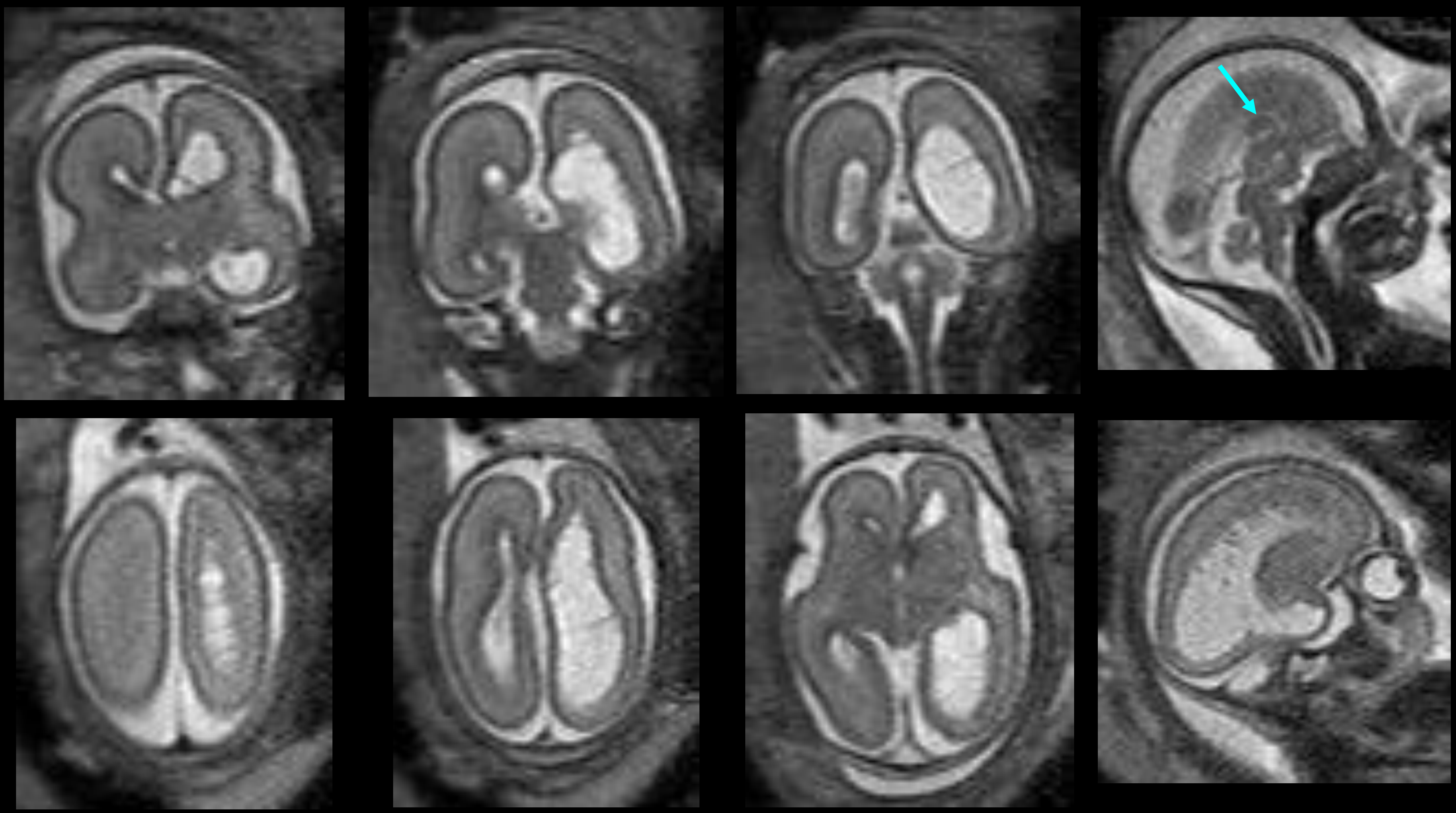

Partial callosal agenesis

Sigmoid Bundle?

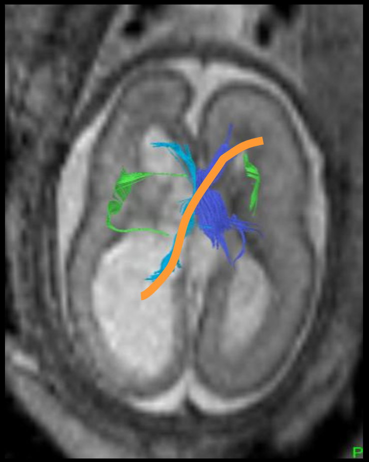

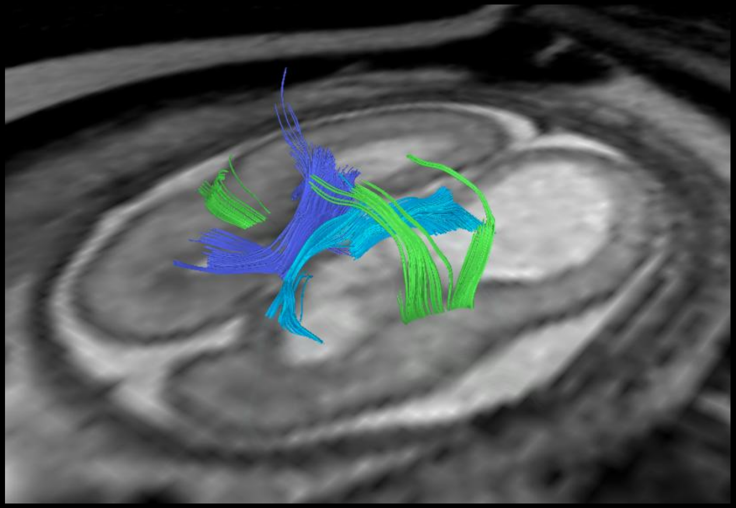

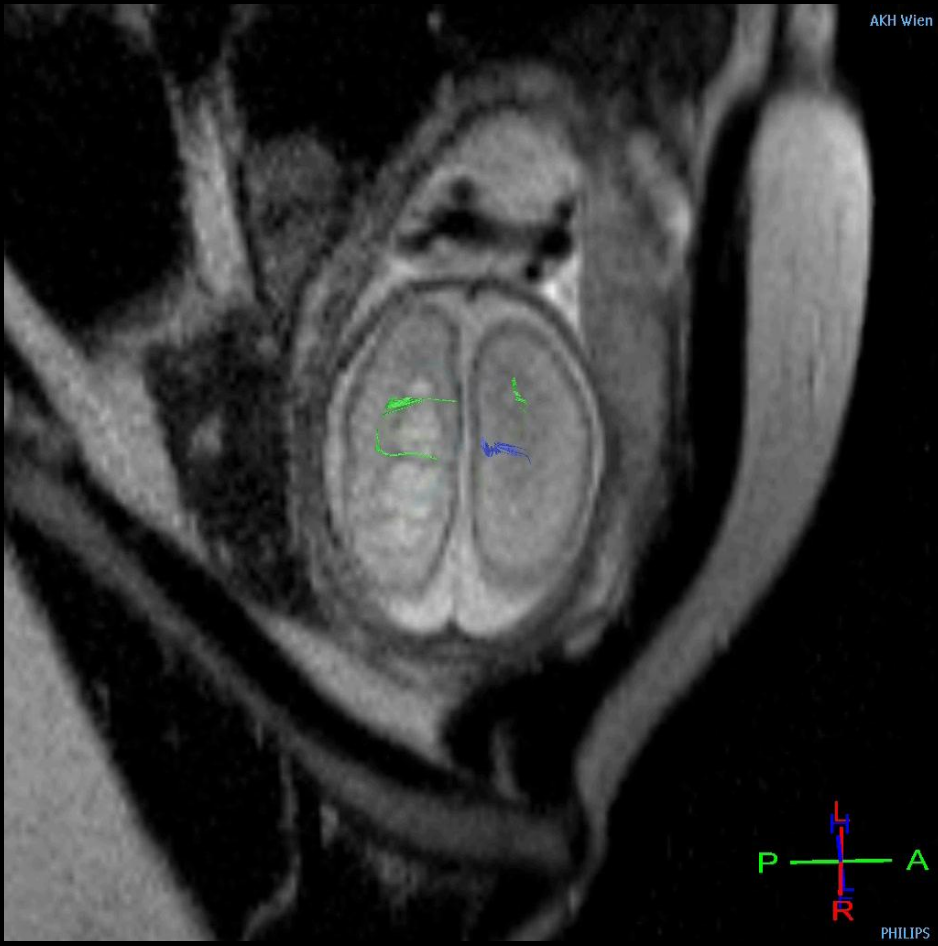

Partial callosal agenesis

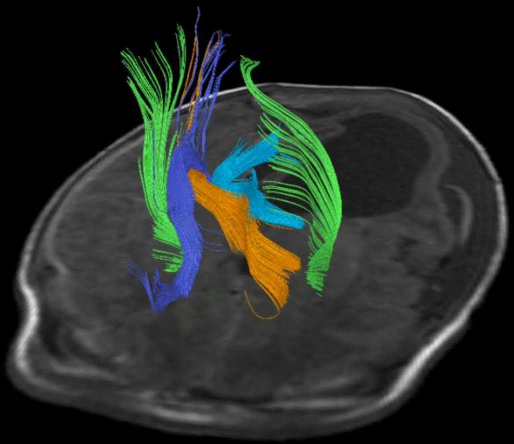

Sigmoid Bundle

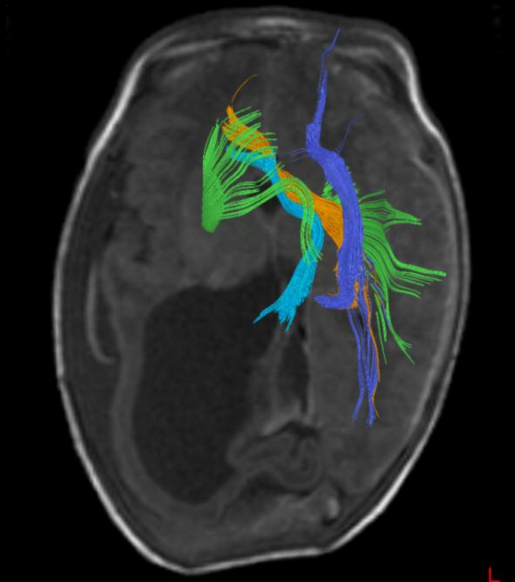

postnatally

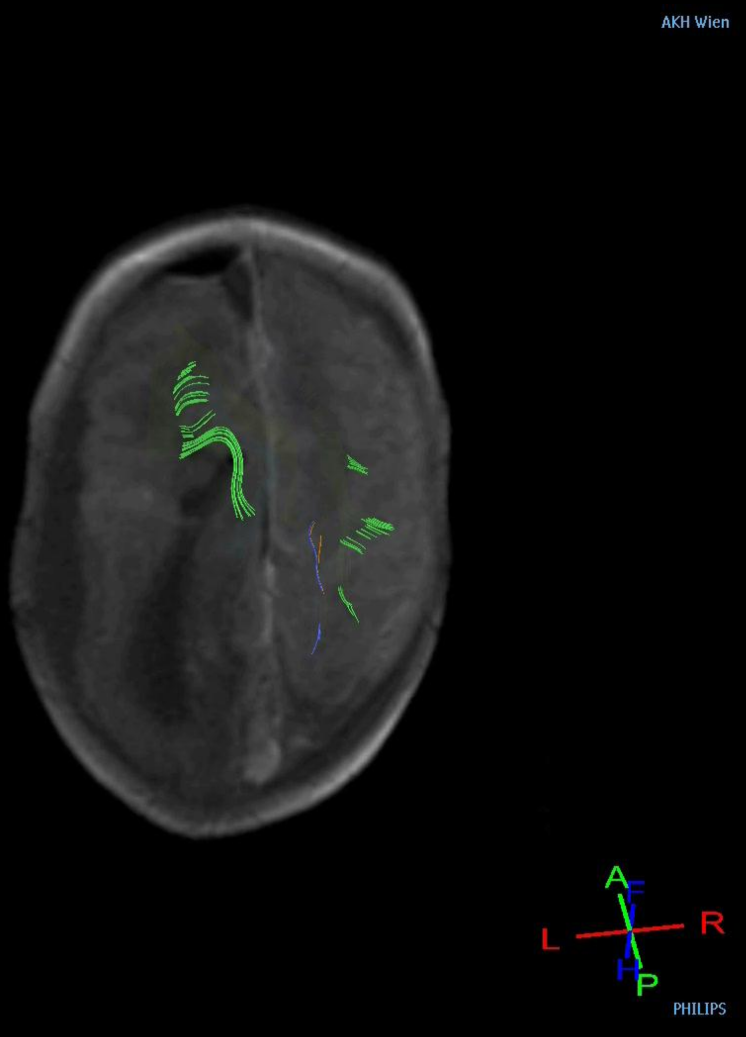

Disorders of axon guidance

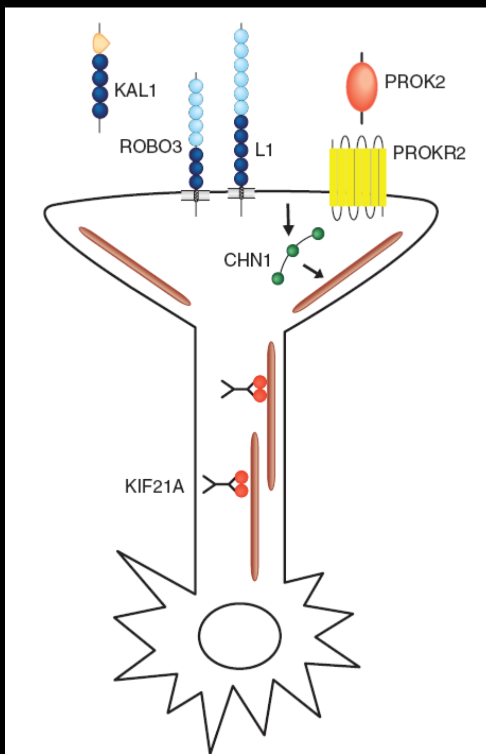

With identified genes[‡]
Andermann syndrome (*KCC3*)
XLAG (*ARX*)
Mowat Wilson syndrome (*ZFHX1B*)
AgCC with fatal lactic acidosis (*MRPS16*)
HSAS/MASA syndromes (*L1CAM*)
AgCC seen consistently, no gene yet identified
Acrocallosal syndrome
Aicardi syndrome
Chudley–McCullough syndrome
Donnai–Barrow syndrome
FG syndrome
Genitopatellar syndrome
Temtamy syndrome
Toriello–Carey syndrome
Vici syndrome

AgCC seen occasionally (partial list)[§]
AgCC with spastic paraparesis (*SPG11*)
Craniofrontonasal syndrome
Fryns syndrome
Marden–Walker syndrome
Meckel–Gruber syndrome
Microphthalmia with linear skin defects
Opitz G syndrome
Orofaciodigital syndrome
Pyruvate decarboxylase deficiency
Rubinstein–Taybi syndrome
Septo-optic dysplasia (DeMorsier syndrome)
Sotos syndrome
Warburg micro syndrome
Wolf–Hirschhorn syndrome

Engle EC (2010) Human genetic disorders of axon guidance. Cold Spring Harb Perspect Biol

Paul LK et al. (2007) Agenesis of the corpus callosum: genetic, developmental and functional aspects of connectivity. Nat Rev Neurosci 8: 287-299

Pathological connectivity of the fetal brain

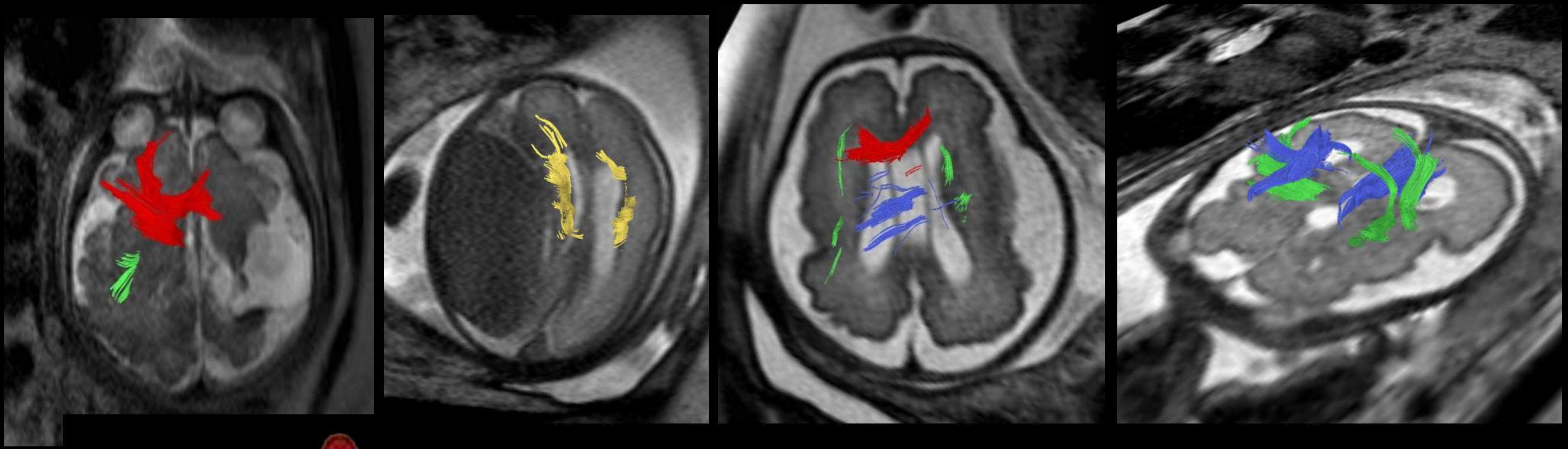

!Postnatal Correlation!

Brainstem development :

Measurement of FA in the midbrain

r= .496 p=. 005**

significant **positive correlation**: **GA and FA measured in the midbrain**

no significant correlation: GA and ADC

r=-.205 p=.268)

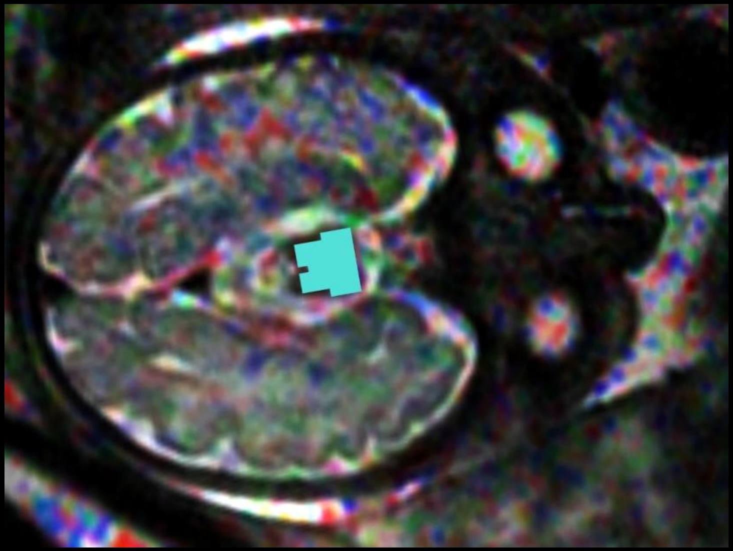

45 Fetuses
17-38 GW
normal CNS development

Intrinsic movements as output of brainstem functions:

Type I a single, transient, linear deviation, usually from a mid-position to a lower, outer orbital margin, followed by a return to the initial position;

Type II a prolonged, but single deviation to a medial or lateral position;

Type III a complex sequence of deviations including rotary components, without apparent spatial or temporal periodicity, observed to be typically brisk and jerky; and

Type IV a repetitive or nystagmoid deviation of the eye.

Birnholz, J. C. (1981). The development of human fetal eye movement patterns. *Science*, **213**, 679–81

GW 29+3

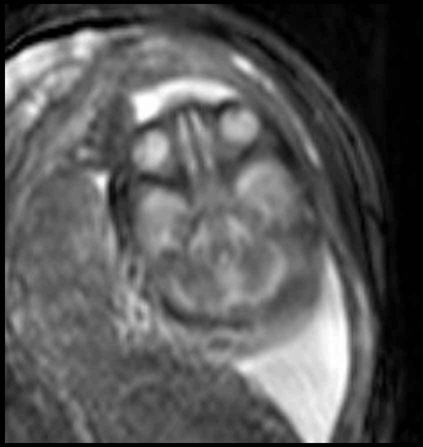

GW 32+3

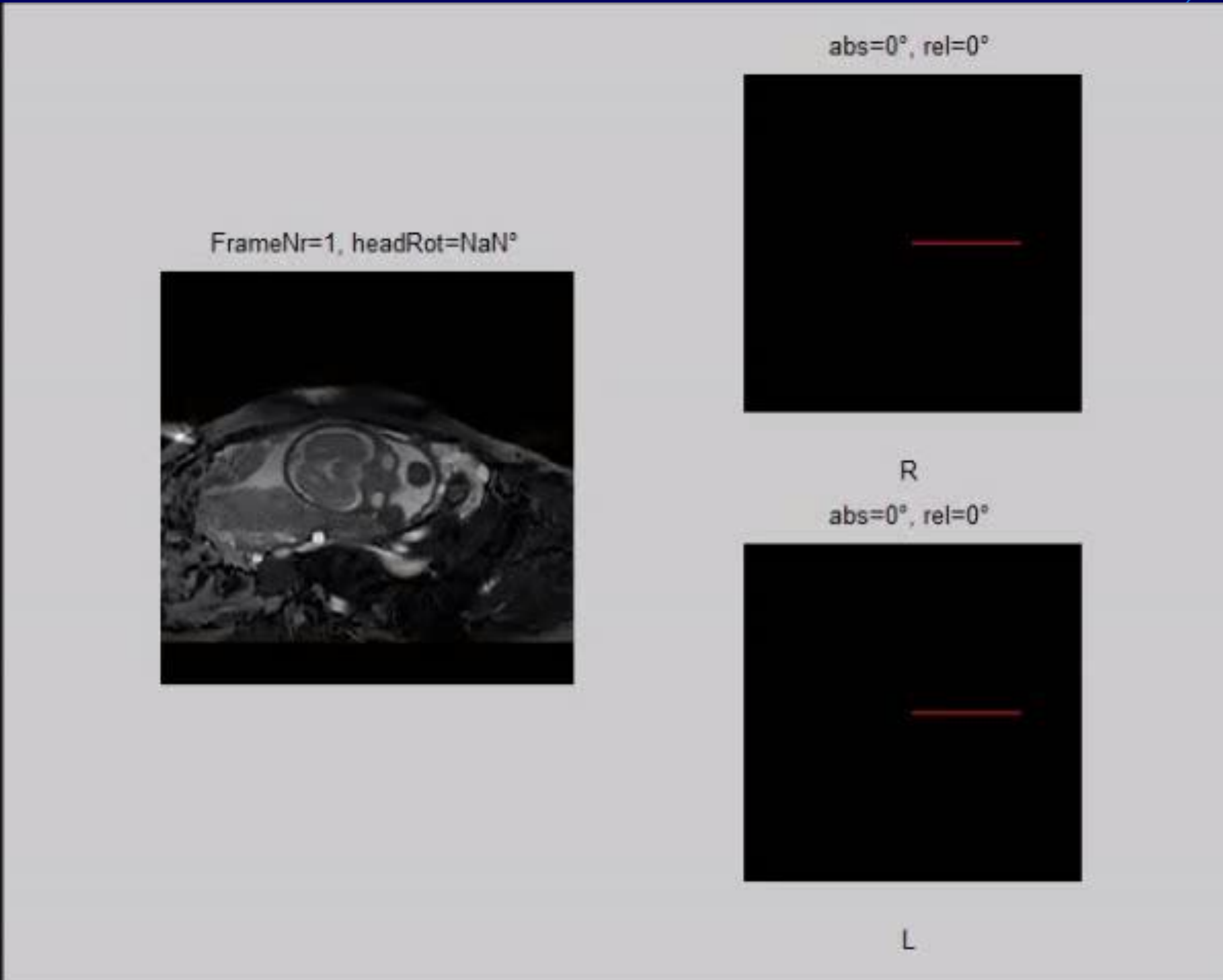
FrameNr=1, headRot=NaN°
abs=0°, rel=0°
R
abs=0°, rel=0°
L

Vestibulo ocular Reflex

Allows to see sharply when head moves

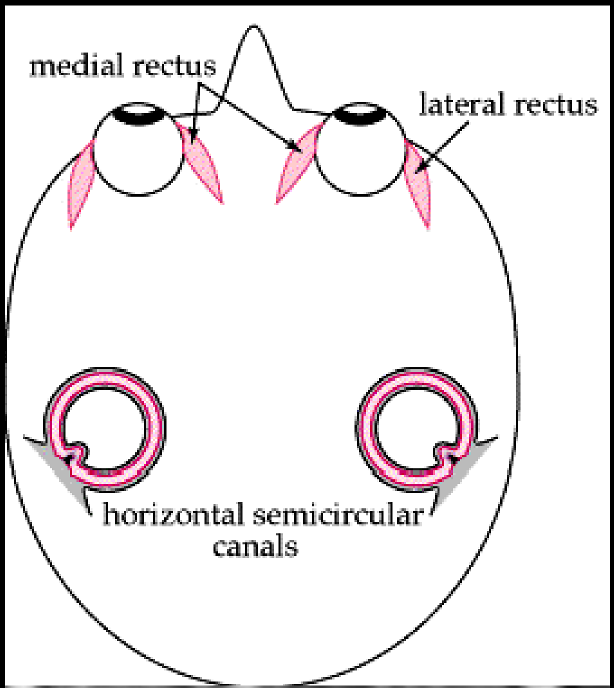

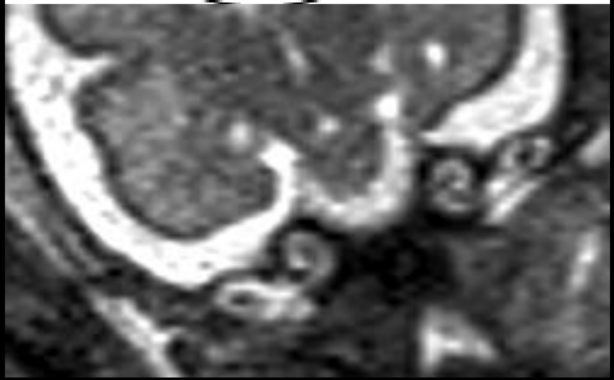

Semicircular canals detect head rotation
Otholiths detect head translation

Vestibular nerve-vestibular nuclei (brainstem)
fibers cross to the contralateral abducens nucleus

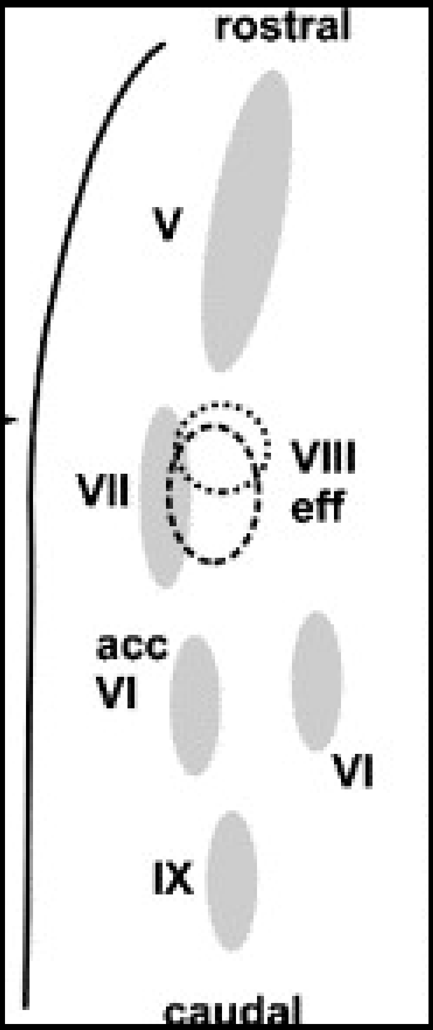

-Directly to rectus lateralis and via medial - longitudinal fasciculus to the oculomotor nuclei- medial rectus

Neural integrators prevent eye from rolling back to center when head stops moving: nucleus prepositus hypoglossi (medulla) nucleus of cajal (midbrain)

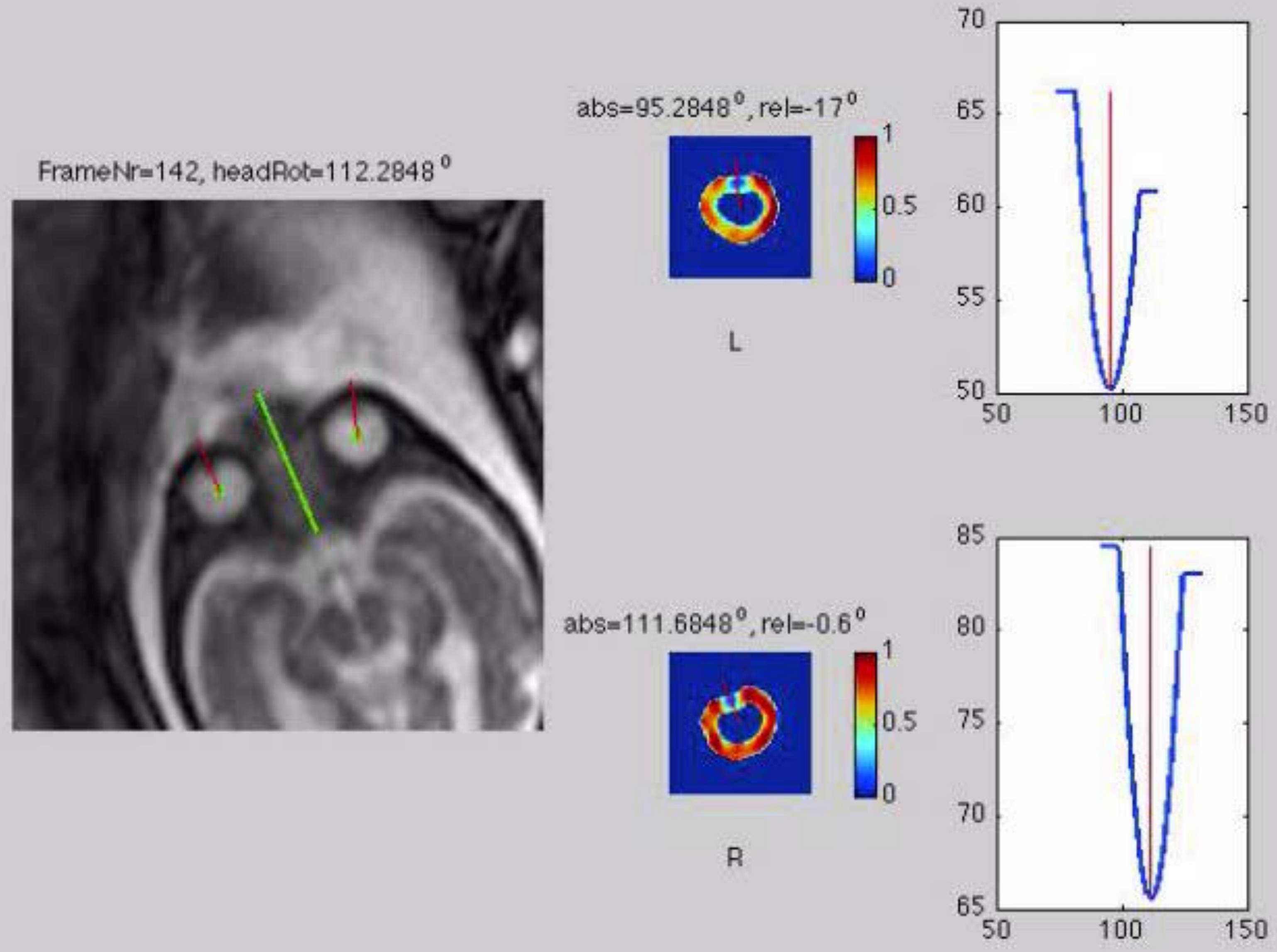

FrameNr=142, headRot=112.2848 °
abs=95.2848 °, rel=-17 °
L
abs=111.6848 °, rel=-0.6 °
R
1
0.5
0
70
65
60
55
50
50
100
150
85
80
75
70
65

Proton spectroscopy

Choline: cell turnover

Creatine: energy level

Myo-inosiol: glial function

Lactate/Lipids/Macromolec.

N-acetyl aspartate: neuronal function

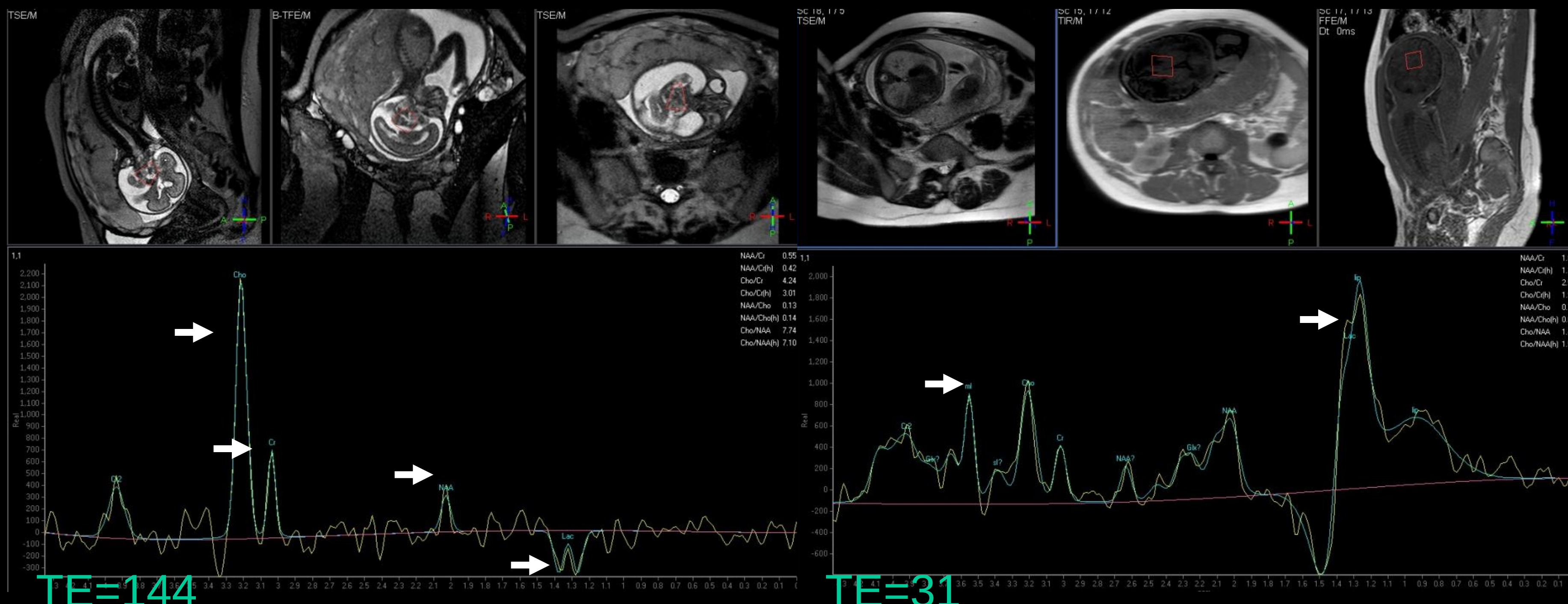

GW 35 ventriculomegaly

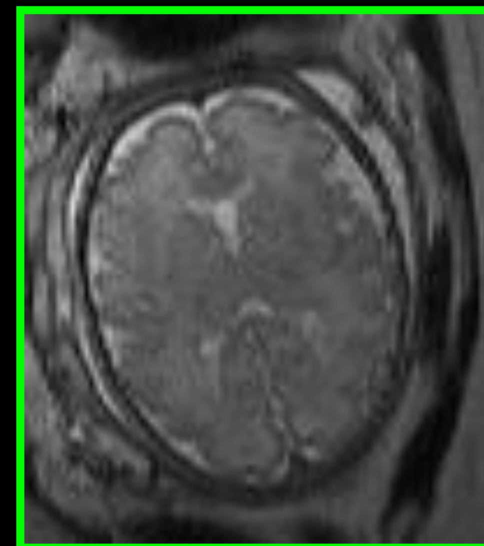

Germinolytic cysts

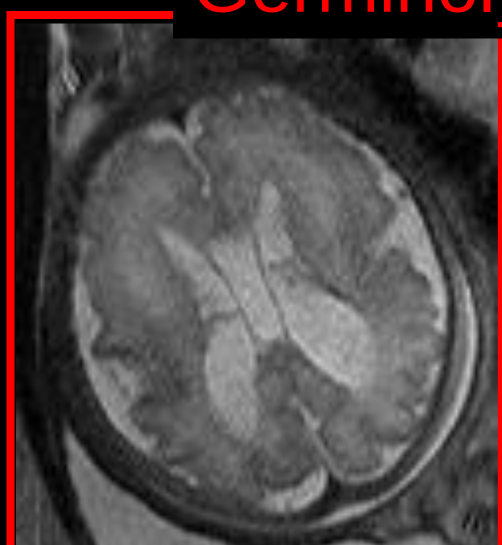

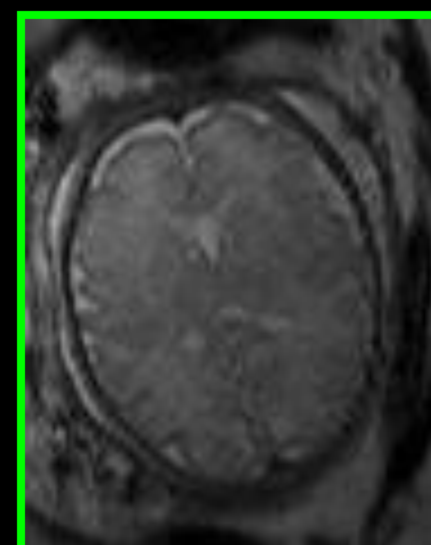

35+0

GW 35 ventriculomegaly

Renal cysts

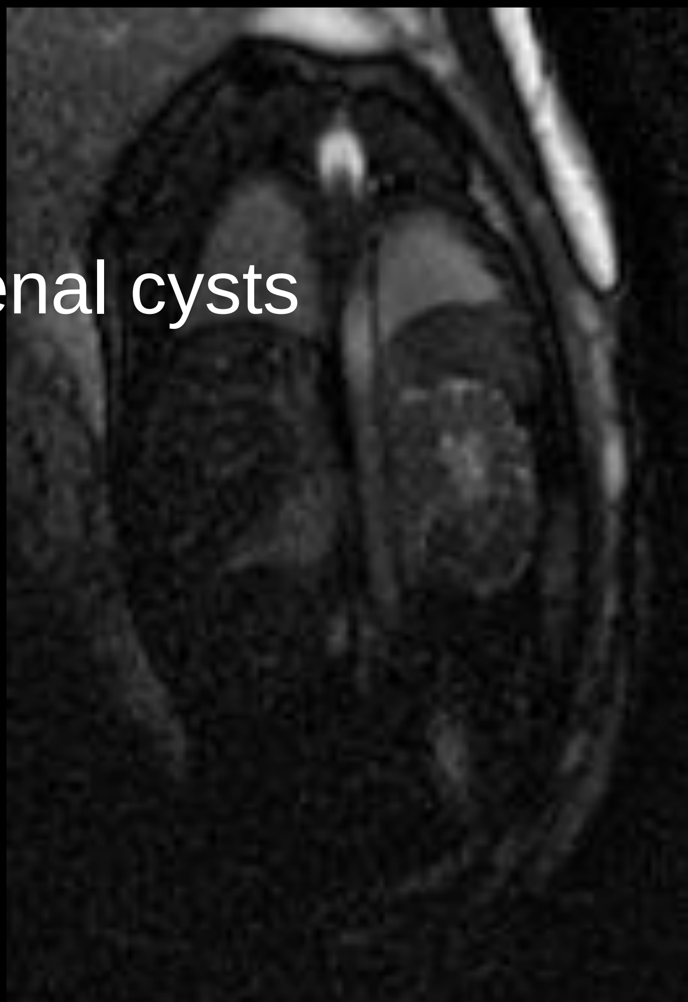

35+0

GW 35 ventriculomegaly

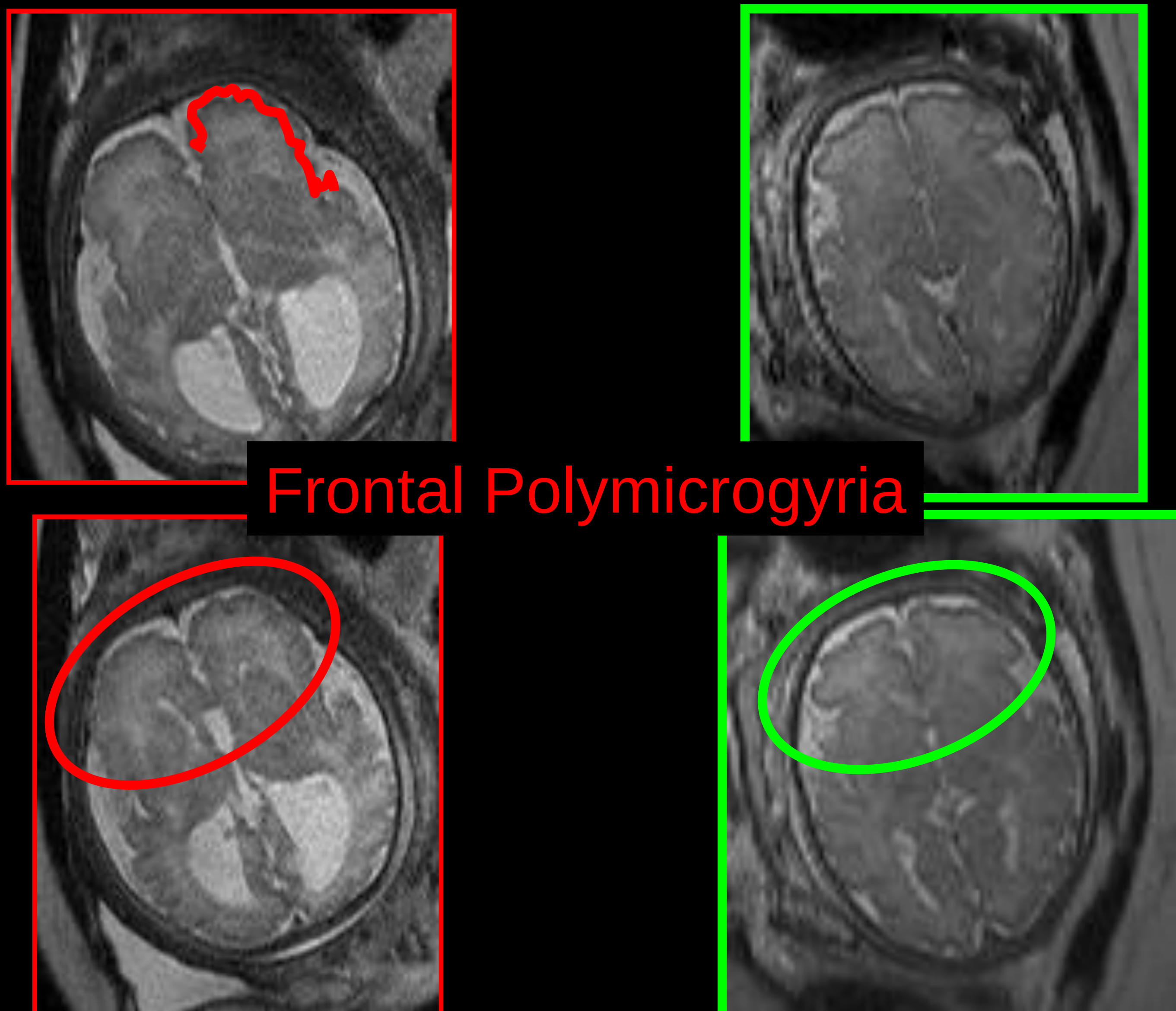

35+0

GW 35 ventriculomegaly

In+opposed phase

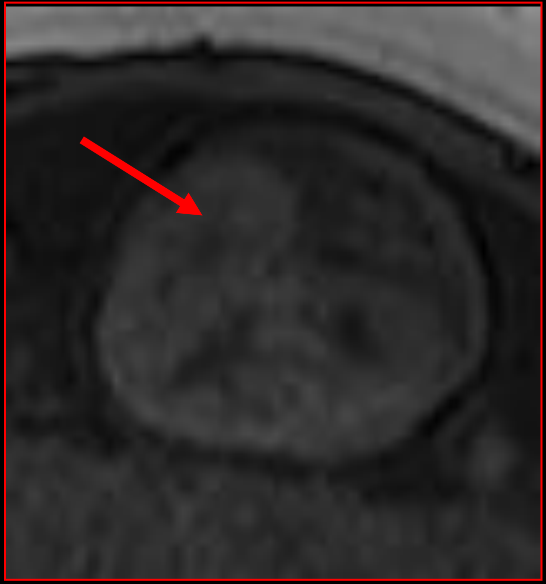

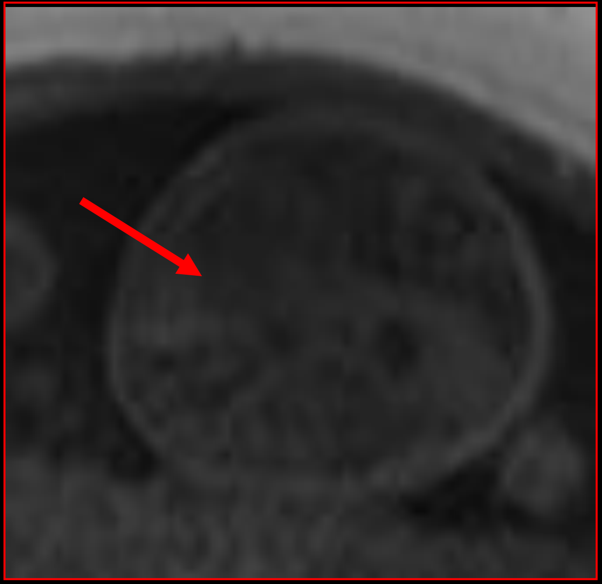

Pathological
Signals
In the
liver

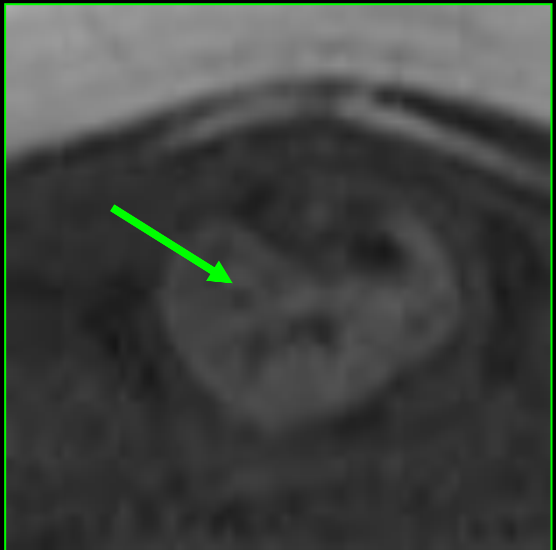

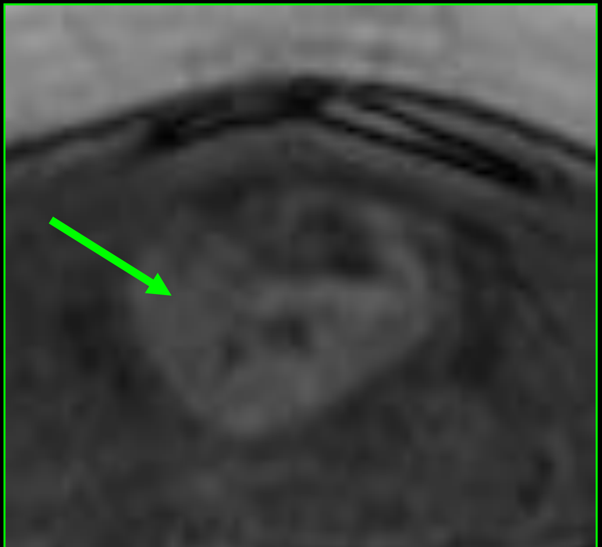

GW 35 ventriculomegaly

White matter ?

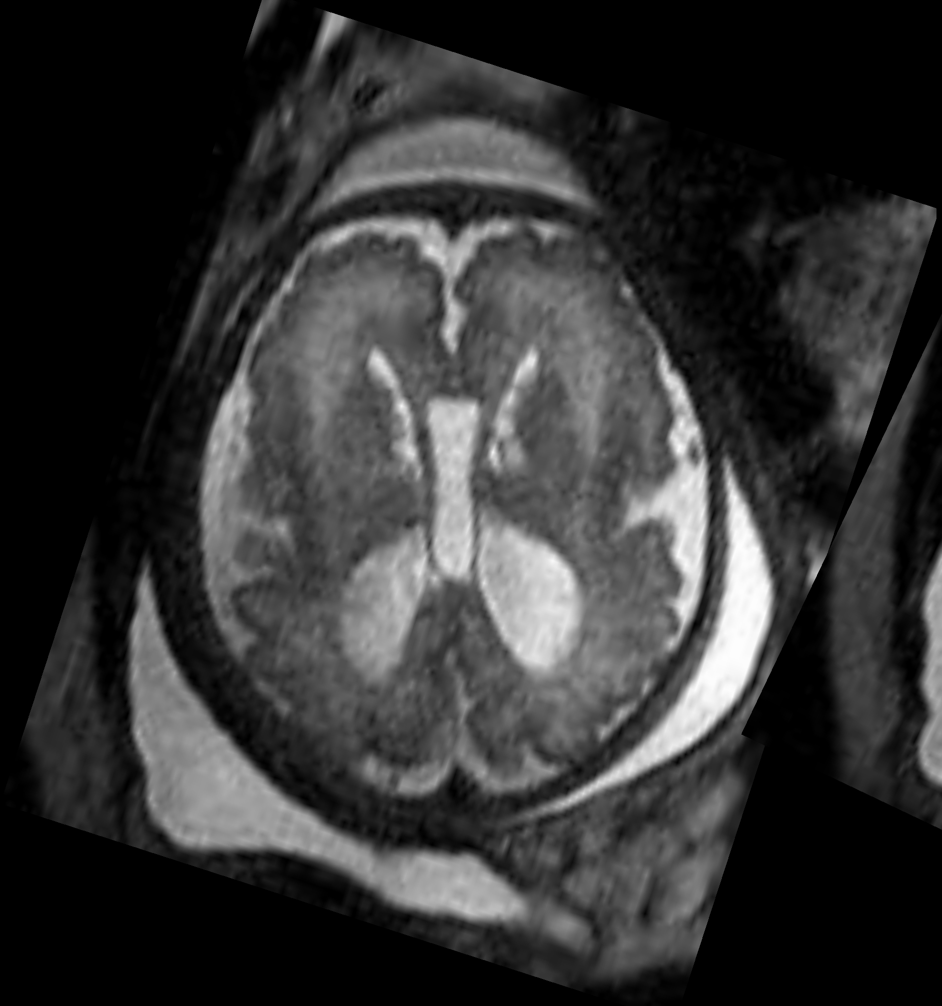

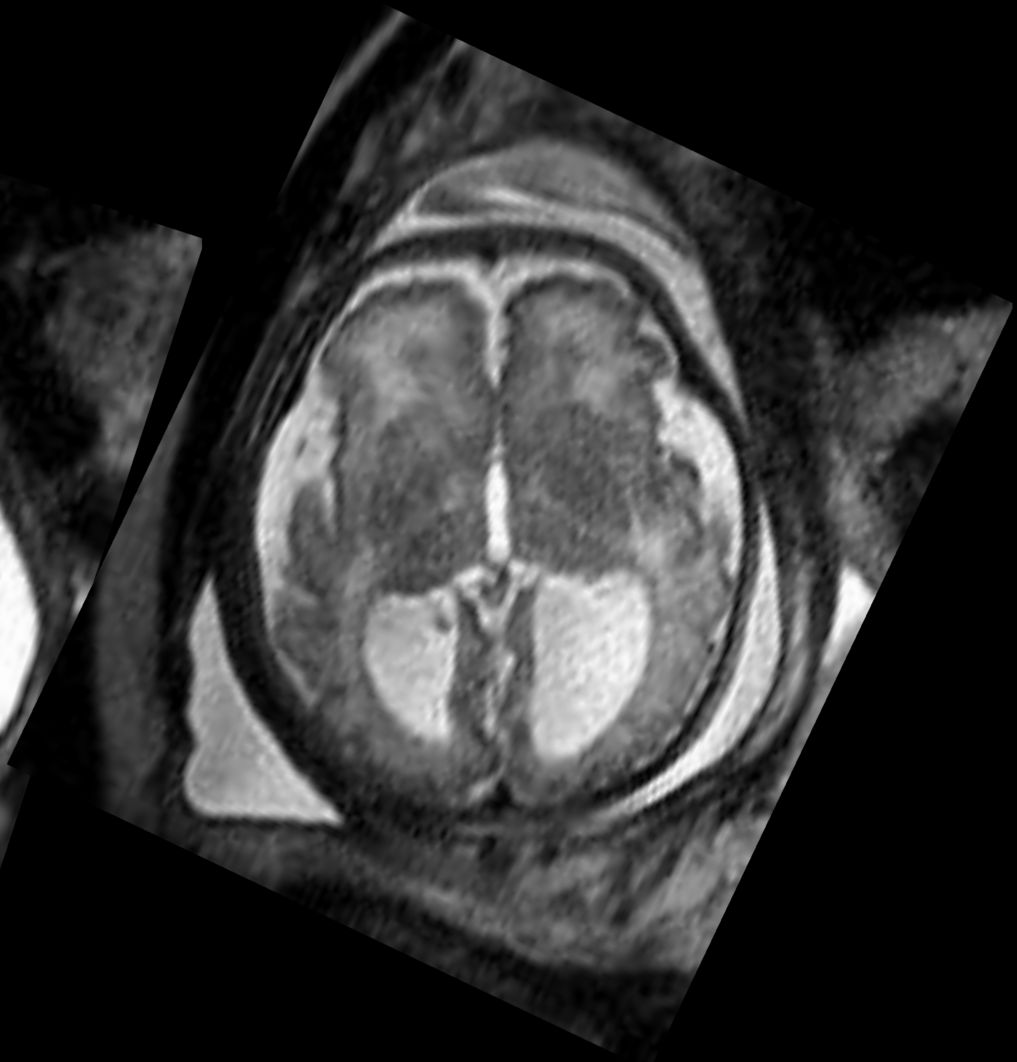

GW 35 ventriculomegaly

tractography!

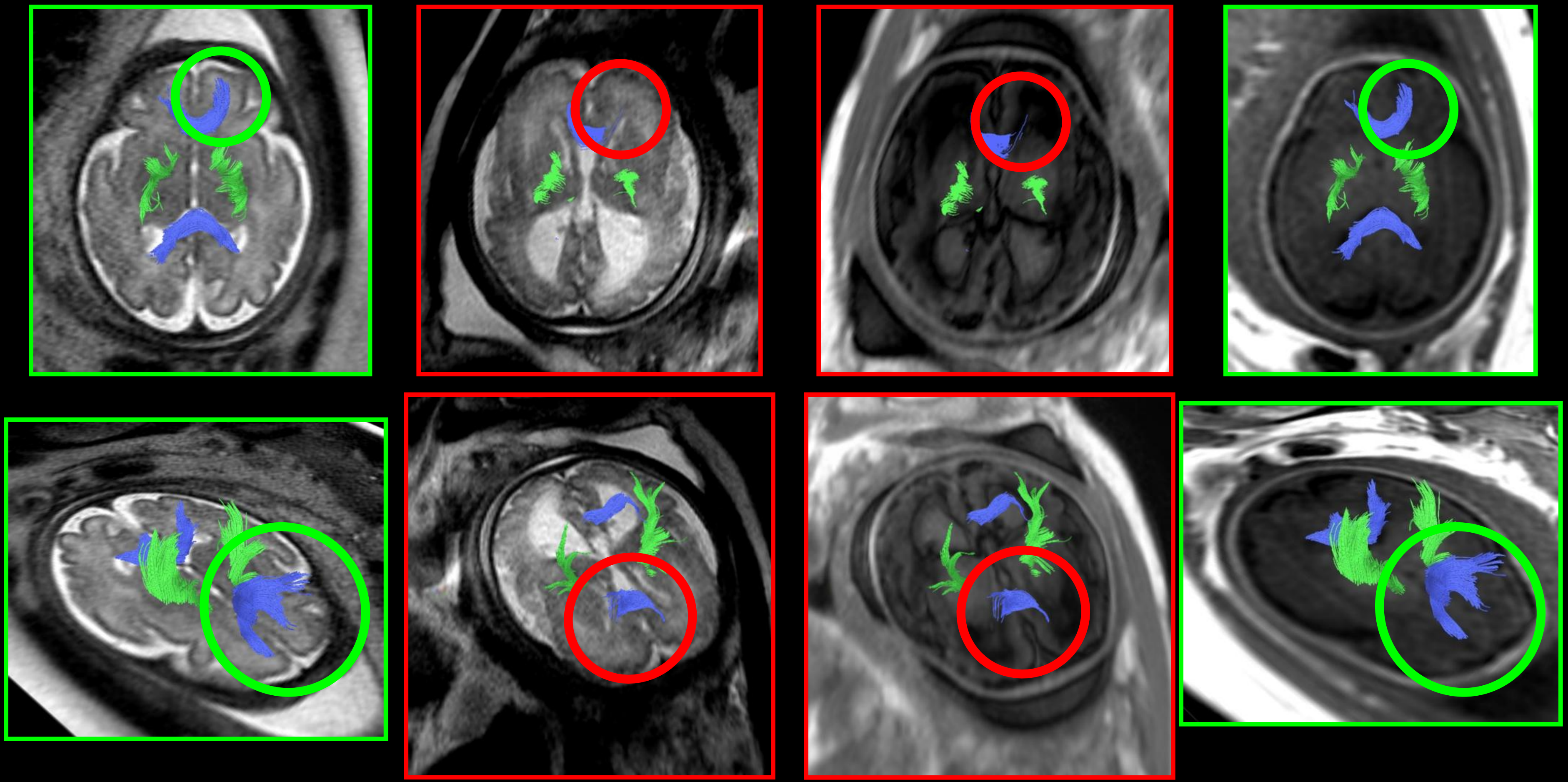

GW 35 ventriculomegaly

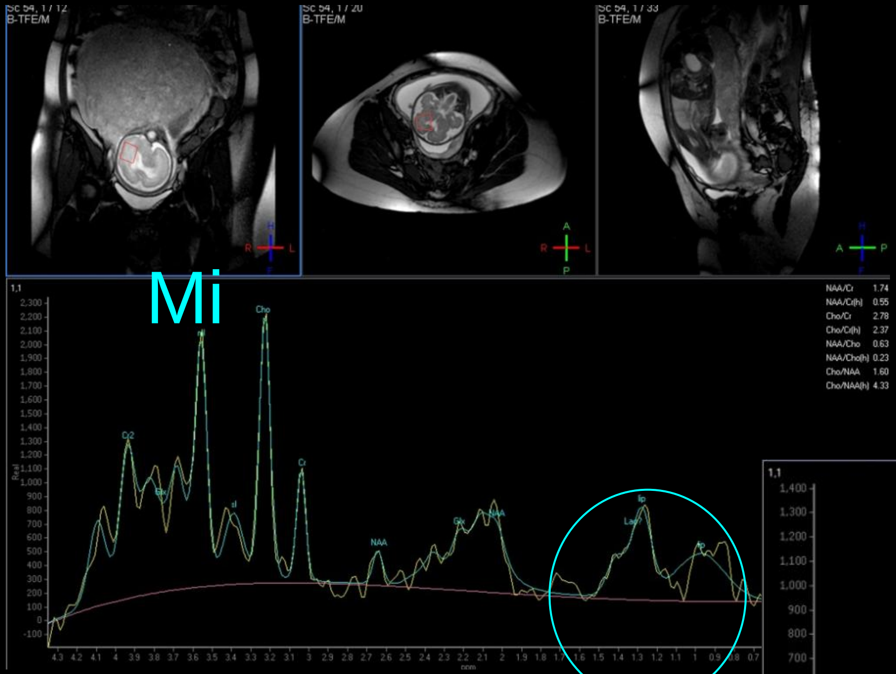

Proton
spectroscopy

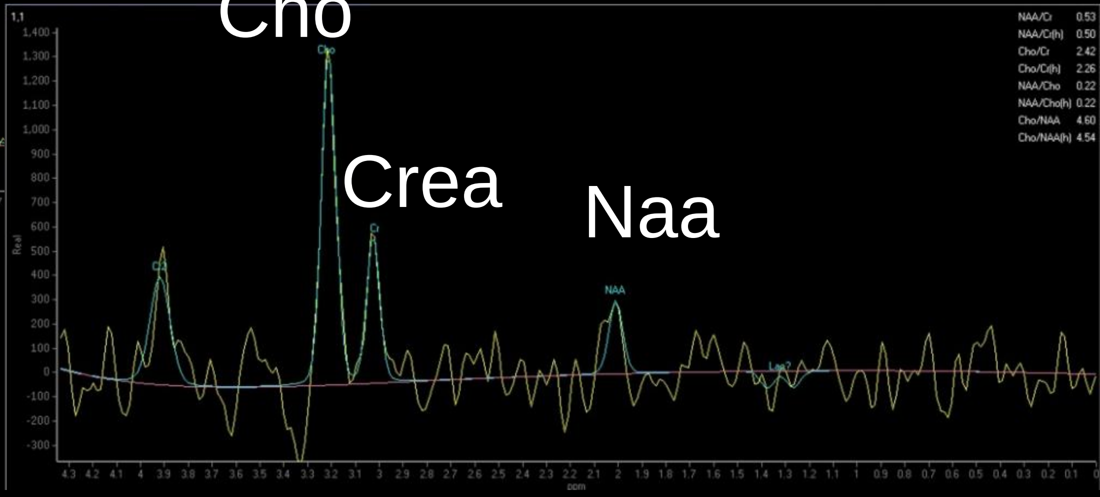

Peaks in Lipid/
Lactate/
Macromolecule
Region

GW 35 ventriculomegaly

Bilateral frontal polymicrogyria

Abnormal white matter

Germinolytic cysts

Lipid/ Lactate/ Macromolecules

Renal cysts

Pathologic liver

Zellweger Syndrome

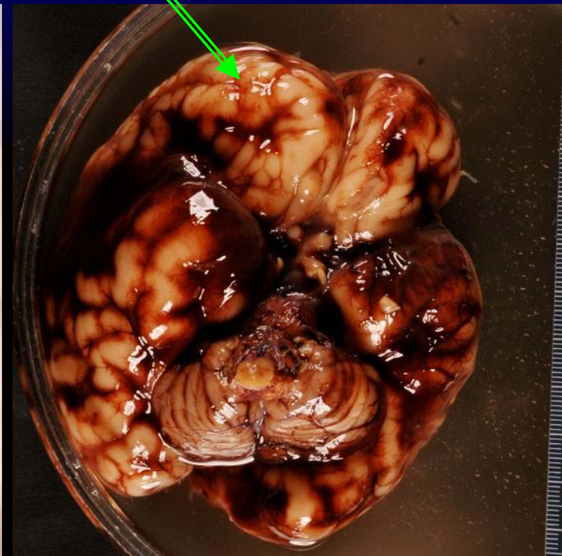

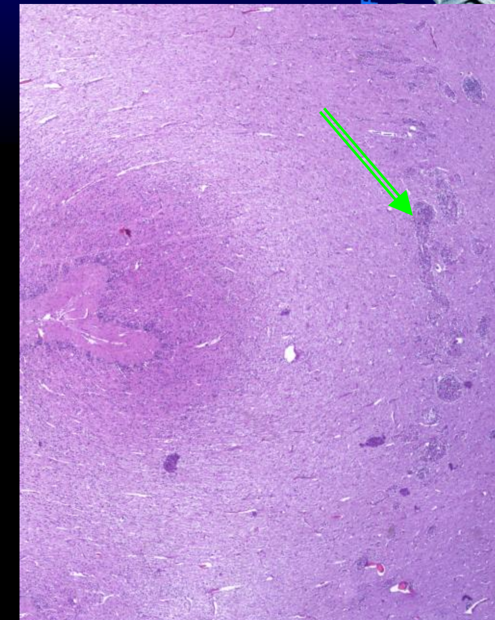

Functional MRI (fMRI)

Blood Oxygen Label Dependent imaging

More oxygene demand in active than nonactive regions- oxyhemoglobin gives different signals than deoxyhb

Statistical analysis of temporal oxygene consumption- activity

Finger movement

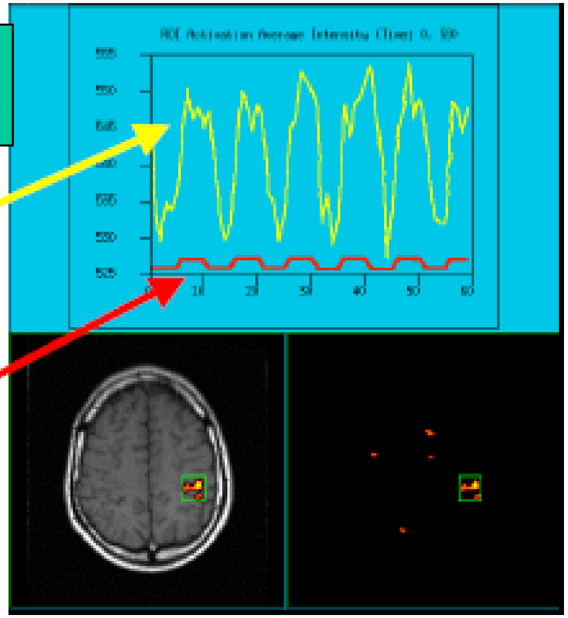

Signal from active Region

Stimulus

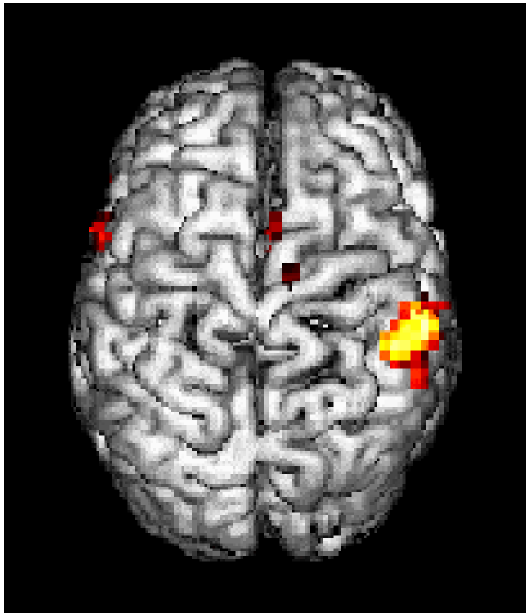

Functional MRI

Resting state

= basic cerebral activity
„ relax, stay awake, lie still, eyes closed think of nothing"

Low frequency (<0,1Hz) fluctuations are measured

These fluctuations are organized in networks under resting-state conditions

Resting-State in adults

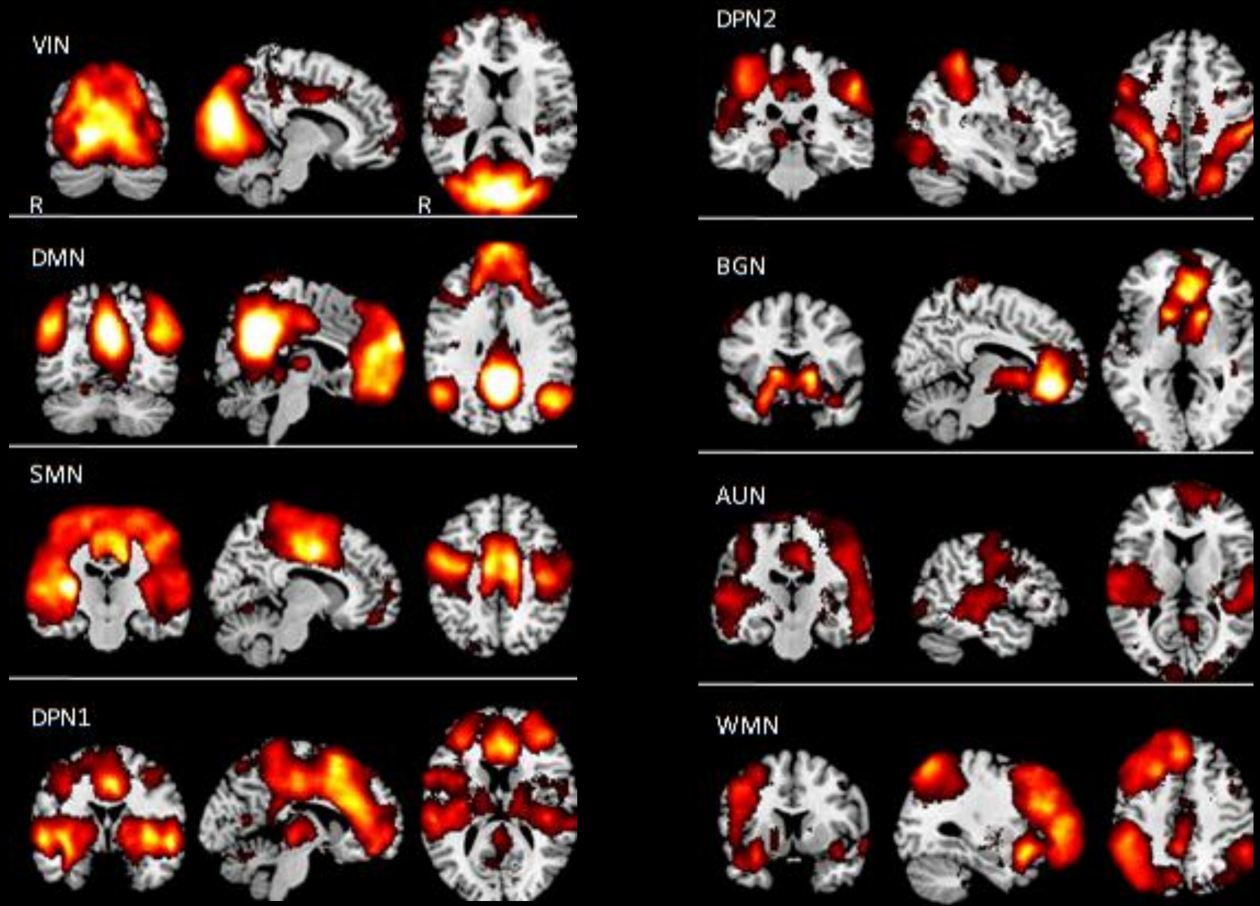

Schöpf et al, Neuroimage (2010)

Frontal Network

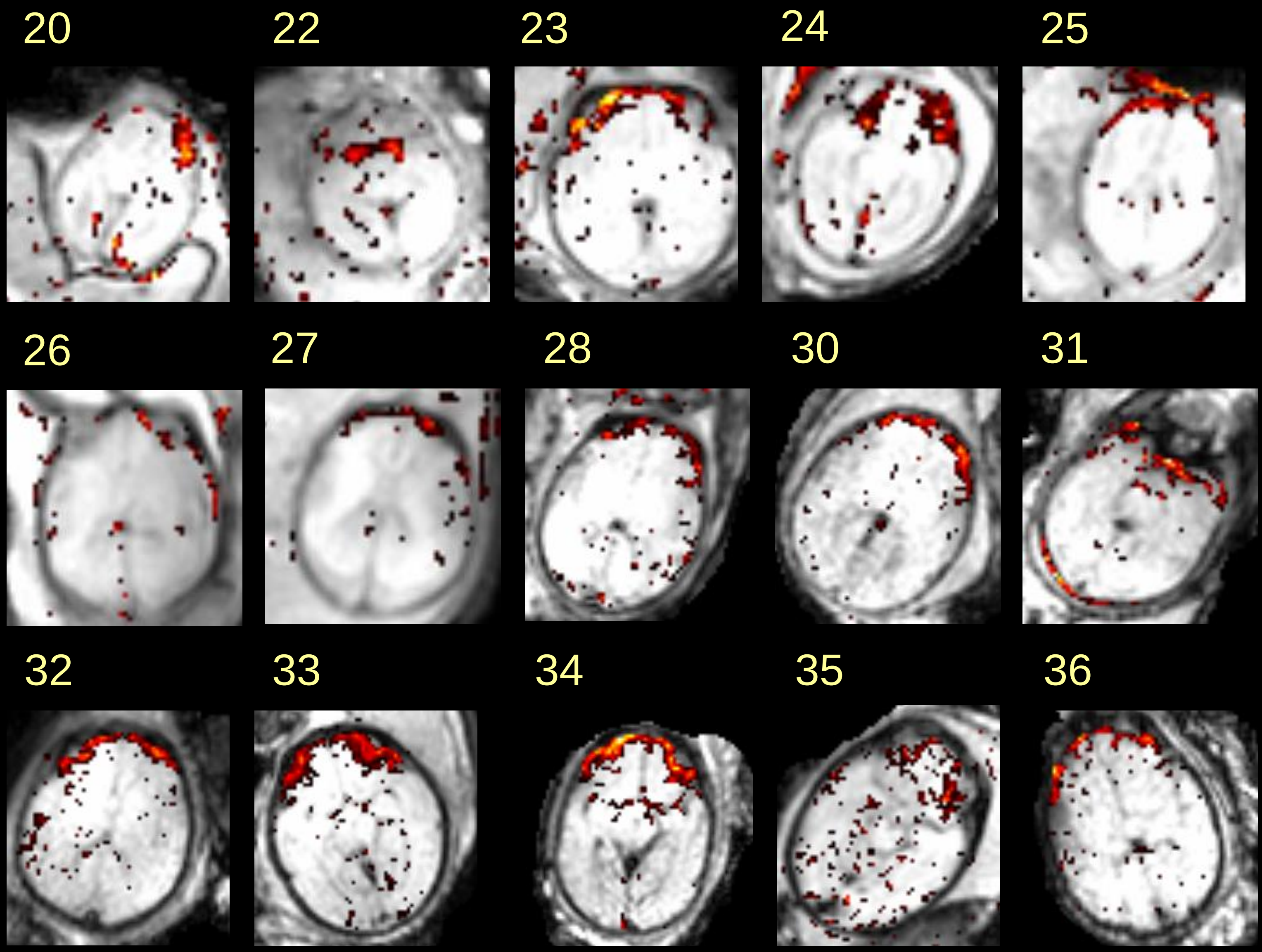

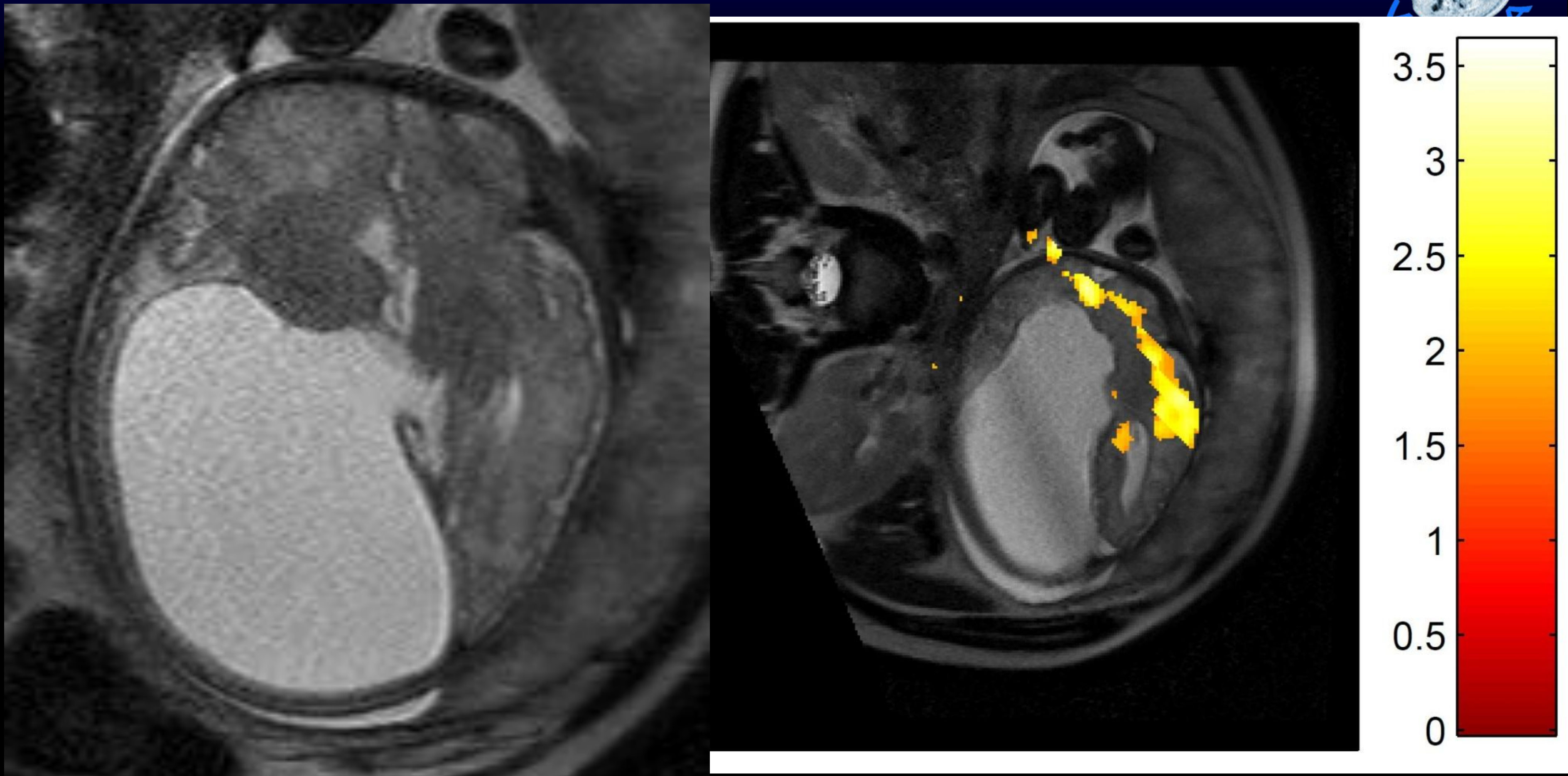

resting state fMRI

Visuelle Stimulation

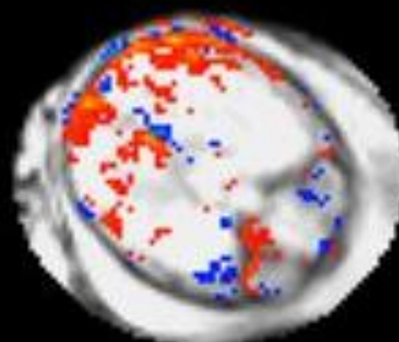

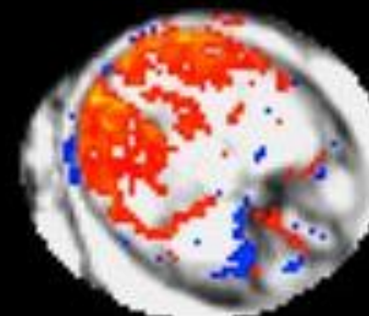

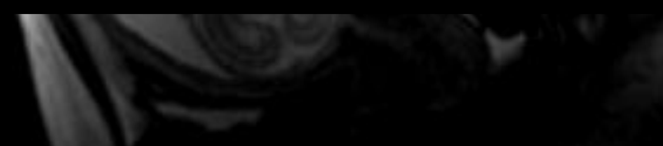

Future aspects

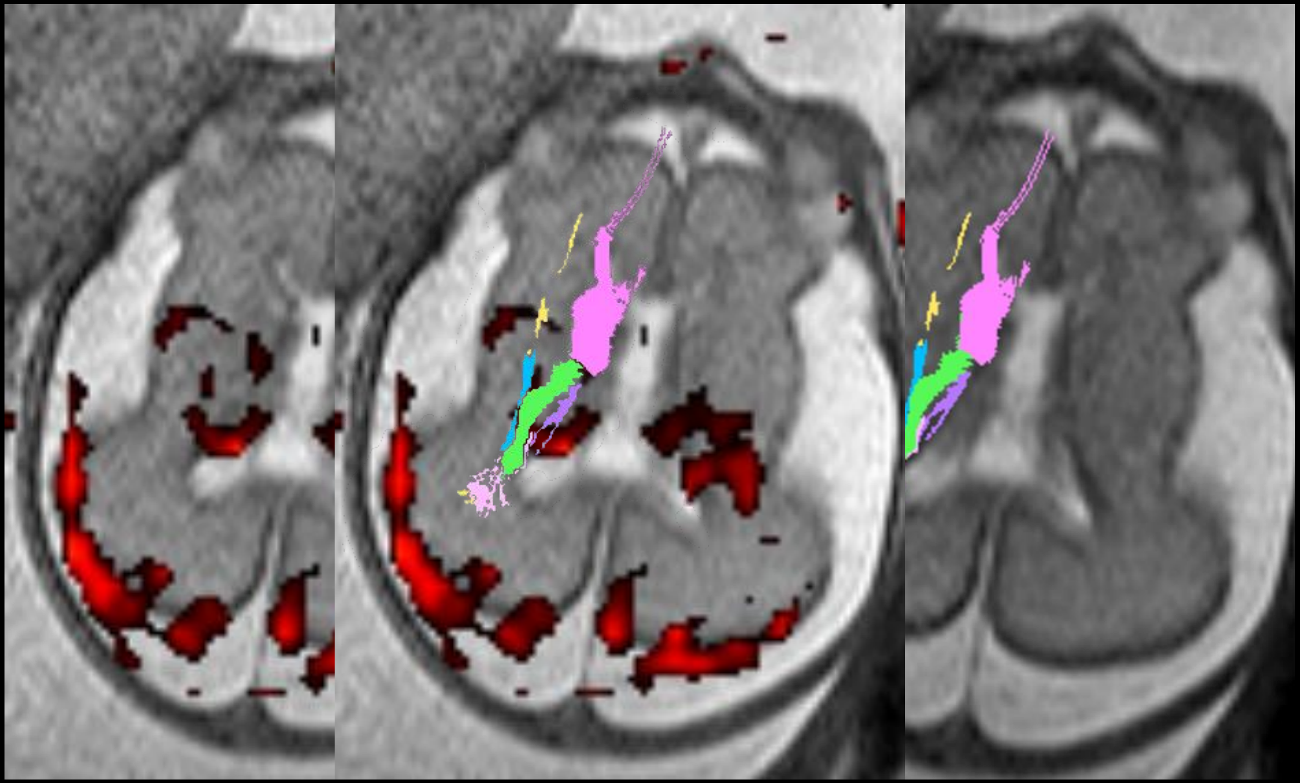

Take home:

T2 – weighted contrast alone is not state of the art any more

Tractography is based on diffusion-weighted sequences

Spectroscopy provides insides into metabolism

Functional MRI may be important in the future

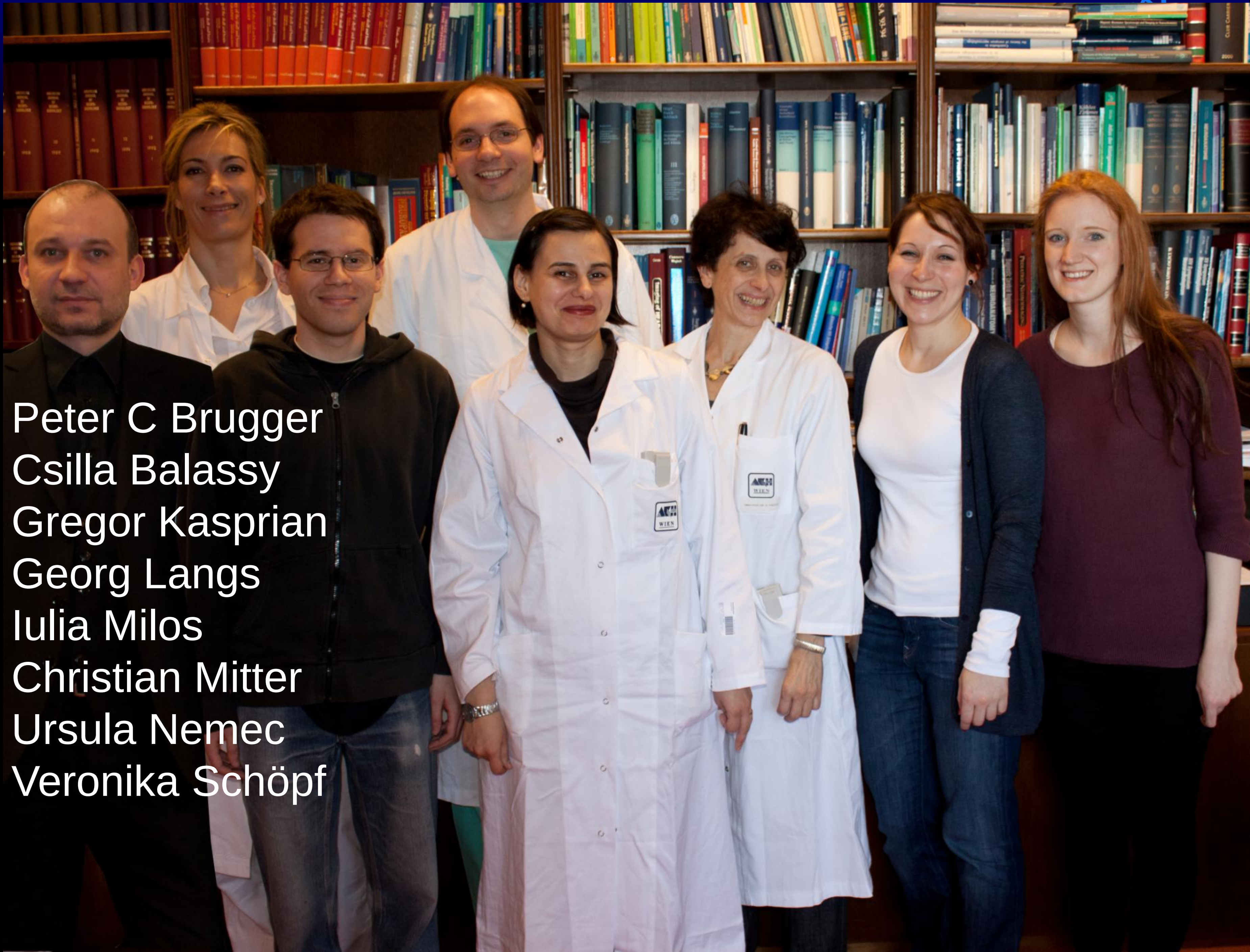

Peter C Brugger
Csilla Balassy
Gregor Kasprian
Georg Langs
Iulia Milos
Christian Mitter
Ursula Nemec
Veronika Schöpf

Ultrasound meets Magnetic Resonance

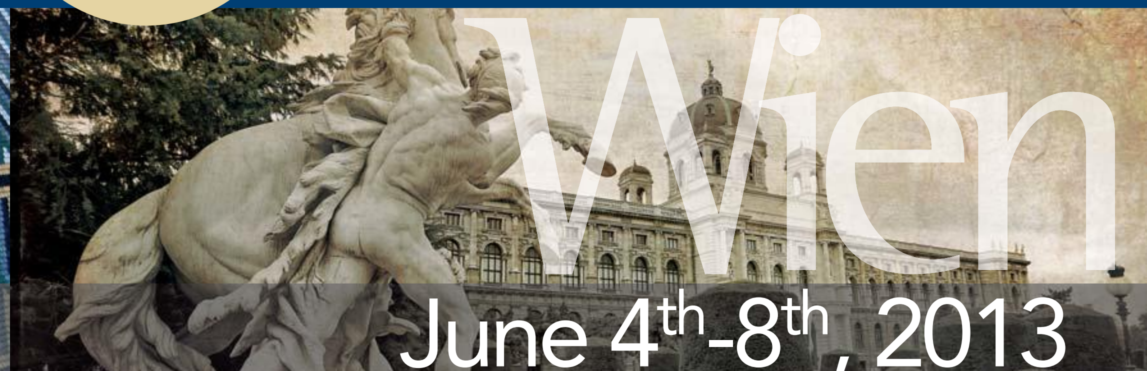

CONGRESS

ESMRN
EUROPEAN SOCIETY OF
MAGNETIC RESONANCE
IN NEUROPEDIATRICS

European Society of Magnetic Resonance in Neuropediatrics

PRESIDENTS OF THE CONGRESS

Prof. Yves Ville and Prof. Daniela Prayer
for Ultrasound meets Magnetic Resonance Congress

Prof. Rainer Seidl and Prof. Daniela Prayer
for ESMRN